



ORKUSTOFNUN

NATIONAL ENERGY AUTHORITY

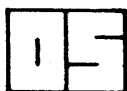
PROGRESS REPORT - 2

**Geophysical logs from
Lopra-1 and Vestmanna-1**

Valgarður Stefánsson
Helga Tulinius

OS-83064/JHD-21 B

July 1983



ORKUSTOFNUN
NATIONAL ENERGY AUTHORITY
GEOTHERMAL DIVISION

GRENSÁSVEGUR 9.
108 REYKJAVÍK ICELAND

PROGRESS REPORT - 2

Geophysical logs from Lopra-1 and Vestmanna-1

Valgarður Stefánsson
Helga Tulinius

OS-83064/JHD-21 B

July 1983



Our date

Our ref.

Your date

Your ref.

The Drilling Committee of the Faeroes Government
c/o Landsverkfröðingur Mikkjal Hemsdal
Tinghúsvegur 5
3800 Tórshavn
Föroyar

The present report is the second progress report on the analyses of the geophysical well log data from Lopra-1 and Vestmanna -1 in the Faeroes. The work is performed in accordance with the proposal from Orkustofnun dated 82.12.09 and the agreement of the Drilling Committee of the Faeroes Government as presented in your letter dated 83.01.06.

Most of the items listed in the proposal of Orkustofnun have already been worked out, either partially or in some cases completely. In general the work is proceeding as scheduled, and in some cases in head of the schedule.

In order to bring this report as close to the final report as possible, we have chosen to collect all available interpretation together here. For the case of overall judgement of the status of this work we feel that this procedure is of benefit.

In our opinion the main results described in this report are:

- a) The statistical behavior of the data indicate that porosity, natural gamma ray, and sonic logs are reliable, whereas some peculiarities seem to be present in the resistivity and gamma-gamma logs.
- b) The 64" normal resistivity log in Lopra-1 and the 16" normal resistivity log in Vestmanna-1 are good estimates of the formation resistivity in respective wells.
- c) The different geological conditions in Lopra-1 and Vestmanna-1 are easily reflected in the porosity and resistivity logs from the wells.

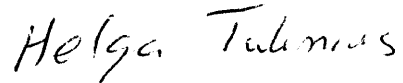
- d) The distribution of porosity in Lopra-1 shows a bimodal form indicating two rock types as is seen by the porosity log. About 74% of the pile is a rock type with a mean porosity of 7.4% whereas the remaining 26% of the pile has a mean porosity of 26+/-5%.
- e) The resistivity logs from Lopra-1 and Vestmanna-1 are textbook examples of the effects of well-size and bed thickness on the resistivity response function.
- f) The distribution of resistivity in Lopra-1 and Vestmanna-1 reflects clearly the different geological composition of the pile penetrated by these wells. A narrow peak of 100 Ωm represent the contact zones in Lopra-1 whereas a narrow peak of 560 Ωm represent the mean value of the thin high resistivity layers in Vestmanna-1.
- g) The resistivity - porosity relationship in Lopra-1 and Vestmanna-1 indicate that fracture porosity is dominating feature of the porosity in the Faeroes.
- h) The mean value of the SiO_2 content in Lopra-1 is 49+/-3% and 46% in Vestmanna-1. These values reflect the pure basaltic nature of the Faeroe pile.
- i) An independent method, based entirely on the geophysical logs have been applied to determine the total thickness of the sediments in Lopra-1 to be approximately 64m.
- j) The basaltic pile of Lopra-1 is proposed to consist of three different basaltic formation series. The uppermost series ranging down to 400m depth is most probably identical to the lower stratigraphic series of Rasmussen and Noe-Nygaard (1970), whereas the other series have not been identified so far. A second series is proposed to range from 400m depth down to 1600m depth. These series are intersected by two doleritic intrusives one at 500 - 600m depth and the other at 750 - 850m depth. Below 1600m depth the pile seems to be of separate chemical composition inferring the third series of the basaltic generation of the Faeroe Islands.

We would appreciate any discussions of the concepts put forward in this report. Please do not hesitate to contact us regarding any subject of this report.

Reykjavík, August 1st. 1983.



Valgarður Stefánsson



Helga Tulinius

LIST OF CONTENT

LIST OF FIGURES	7
LIST OF TABLES	10
1 INTRODUCTION	11
2 ZERO SHIFT OF LOGS	12
3 VARIOGRAMS	14
4 WELL SIZE CORRECTION	24
4.1 Correction of natural gamma ray log	24
4.2 Correction of the neutron-neutron log	26
4.3 Correction of the resistivity logs	26
5 POROSITY	31
5.1 Calibration	31
5.2 Porosity as a function of depth	31
5.3 Distribution of porosity	31
6 DENSITY	41
7 RESISTIVITY	42
7.1 Resistivity as a function of depth	42
7.2 Distribution of resistivity	42
8 RESISTIVITY-POROSITY RELATIONS	58
9 NATURAL GAMMA RAY	71
10 SEDIMENTS	77
11 SONIC VELOCITY	81
12 LARGE SCALE VARIATIONS	83
REFERENCES	95

LIST OF FIGURES

Figure 1.	Variogram for porosity in Lopra-1	16
Figure 2.	Variogram for R16" in Lopra-1	16
Figure 3.	Variogram for R64" in Lopra-1	17
Figure 4.	Variogram for natural gamma ray in Lopra-1	17
Figure 5.	Variogram for gamma-gamma in Lopra-1	18
Figure 6.	Variogram for sonic travel time in Lopra-1	18
Figure 7.	Variogram for sonic amplitude in Lopra-1	19
Figure 8.	Variogram for neutron-neutron in Lopra-1	19
Figure 9.	Variogram for porosity in Vestmanna-1	20
Figure 10.	Variogram for R16" in Vestmanna-1	20
Figure 11.	Variogram for R64" in Vestmanna-1	21
Figure 12.	Absorption function of the borehole fluid used for well size correction of gamma ray log	25
Figure 13.	Borehole correction for 16" normal resistivity log	27
Figure 14.	Borehole correction for 64" normal resistivity log	28
Figure 15.	Empirical relation between R16" and R64" in Lopra-1	29
Figure 16.	Empirical relation between R16" and R64" in Vestmanna-1	29
Figure 17.	Calibration curve for neutron-neutron log	32
Figure 18.	Porosity versus depth in Lopra-1	33
Figure 19.	Porosity versus depth in Vestmanna-1	36

Figure 20. Porosity distribution in Lopra-1	37
Figure 21. Porosity distribution for rock type 2 in Lopra-1	39
Figure 22. Porosity distribution in Vestmanna-1	40
Figure 23. Lopra-1. 16" and 64" normal resistivity versus depth	43
Figure 24. Vestmanna-1. 16" and 64" normal resistivity versus depth	52
Figure 25. Lopra-1. Log distribution of 64" normal resistivity	55
Figure 26. Vestmanna-1. Log distribution of 16" normal resistivity	56
Figure 27. Resistivity-porosity relation for the 190-390m depth interval in Lopra-1	59
Figure 28. Resistivity-porosity relation for the 390-590m depth interval in Lopra-1	59
Figure 29. Resistivity-porosity relation for the 590-790m depth interval in Lopra-1	60
Figure 30. Resistivity-porosity relation for the 790-990m depth interval in Lopra-1	60
Figure 31. Resistivity-porosity relation for the 990-1190m depth interval in Lopra-1	61
Figure 32. Resistivity-porosity relation for the 1190-1390m depth interval in Lopra-1	61
Figure 33. Resistivity-porosity relation for the 1390-1590m depth interval in Lopra-1	62
Figure 34. Resistivity-porosity relation for the 1590-1790m depth interval in Lopra-1	62
Figure 35. Resistivity-porosity relation for the 1790-1990m depth interval in Lopra-1	63

Figure 36.	Resistivity-porosity relation for the 1990-2170m depth interval in Lopra-1	63
Figure 37.	Resistivity-porosity relation for the 190-2170m depth interval in Lopra-1	65
Figure 38.	Resistivity-porosity relation for the 0-200m depth interval in Vestmanna-1	67
Figure 39.	Resistivity-porosity relation for the 200-400m depth interval in Vestmanna-1	68
Figure 40.	Resistivity-porosity relation for the 400-600m depth interval in Vestmanna-1	69
Figure 41.	Resistivity-porosity relation for the 0-600m depth interval in Vestmanna-1	69
Figure 42.	Silica content as a function of depth in Lopra-1	72
Figure 43.	Distribution of silica concentration of the rocks in Lopra-1	75
Figure 44.	Natural gamma ray-porosity cross-plot for Lopra-1	78
Figure 45.	The $(\text{SiO}_2-42)*\phi/2$ as a function of depth for Lopra-1	79
Figure 46.	Upper part of the frequency distribution of $(\text{SiO}_2-42)*\phi/2$ in Lopra-1	80
Figure 47.	Sonic velocity as a function of depth in Lopra-1	82
Figure 48.	100m running average of the natural gamma ray log in Lopra-1	84
Figure 49.	100m running average of the 64" normal resistivity log in Lopra-1	85
Figure 50.	50m running average of the 64" normal resistivity log in Lopra-1	86
Figure 51.	100m running average of the porosity log in Lopra-1	87

Figure 52.	50m running average of the porosity log in Lopra-1	88
Figure 53.	Relation between thorium and zirconium for the lavas of the Faeroe Islands	89
Figure 54.	Long scale variation of natural gamma ray, resistivity and porosity in the Lopra-1 borehole, with the proposed division of the lava pile	91
Figure 55.	Lopra-1. Concentration of Ba, Zr, V, and Cr as a function of depth (Waagstein et al. 1982)	93
Figure 56.	Vestmanna-1. Large scale variations of porosity and resistivity with depth.	94

LIST OF TABLES

Table 1	Depth corrections for the logs in Lopra-1	13
Table 2	Depth corrections for the logs in Vestmanna-1	13
Table 3	Coefficients in Archie's formula for resistivity-porosity relation in Lopra-1	64
Table 4	Coefficients in Archie's formula for resistivity-porosity relation in Vestmanna-1	70

1 INTRODUCTION

In October 1981, the National Energy Authority (NEA) of Iceland carried out geophysical logging in the research wells Lopra-1 and Vestmanna-1 in the Faeroes.

By an agreement between the Drilling Committee of the Faeroes Government and NEA, interpretation of the logs is to be done by NEA in the year 1983. The first progress report on the work was issued on March 30, 1983 (Stefánsson and Tulinius 1983).

The present report is the second progress report, where most of the results obtained so far are summarized. The final report is to be delivered on the 1st of November 1983, and the present progress report is intended to reflect the scope of the final report.

2 ZERO SHIFT OF LOGS

Only one or two parameters were measured with each probe at Lopra and Vestmanna. The probes are of various length and the sensitive parts of the probes are situated at various distances from the cable head. Furthermore, the zero depth for each run is set manually. Consequently a common zero point for all logs is not well defined. However, as much of the analytical work relies on the relationship between various parameters recorded in different runs in the hole, it is of vital importance to have the same depth scale for all logs. The method used here, is to cross-correlate two logs with different offsets in depth. The zero shift between logs is determined by finding a maximum in the cross correlation when the logs correlate. If the logs have inverse correlation a minimum in the cross correlation is used to determine the zero shift.

By using this method, the entire log is used to determine the zero shift and variations in individual depth scales are evened out. The caliper log was chosen as the reference log in Lopra-1, partly because other logs are to be corrected for the well size, and partly because the caliper log has at least one well defined depth point, which is the end of the casing, and could therefore be corrected to an absolute depth value. Neutron-neutron and natural gamma ray logs are measured by the same probe giving a fixed depth offset of 1.58m between them. The same is true for the 16" and 64" resistivity logs which have a fixed depth offset of 0.61m.

Table 1 lists the depth corrections (zero shift) for various logs in Lopra-1. Temperature has been omitted from this table, partly because there is little correlation between temperature and the other logs, and also because this work is not intended to analyze the temperature data.

TABLE 1

Depth corrections for logs in Lopra-1.

Type of log	Zero shift (m)
Caliper	0.0 (reference)
Neutron-neutron	-0.7
Natural gamma	0.9
Resistivity 16"	-0.6
Resistivity 64"	0.0
Gamma-gamma	0.2
Sonic amplitude	-0.3
Sonic travel time	-0.3

The well in Vestmanna was drilled with core-bit and the variance in diameter is negligible. The only logs showing good correlation were resistivity and neutron porosity. Table 2 lists the depth correlations for the logs in Vestmanna-1.

TABLE 2

Depth corrections for the logs in Vestmanna-1.

Type of log	Zero shift (m)
Resistivity 16"	0.0 (reference)
Resistivity 64"	+0.6
Neutron-neutron	-0.4

3 VARIOGRAMS

The concepts of geostatistics are convenient in order to find internal inconsistency in logging data (Czubek 1981 b). The most important relation is the semi-variogram $g(X_1, X_2)$ which is defined as the variance of the increment $Z(X_1) - Z(X_2)$ of some geological realization. By definition we have:

The expected value

$$E(Z(X)) = m(X)$$

The variance

$$D(Z(X)) = E((Z(X) - m(X))^2)$$

The covariance

$$C(X_1, X_2) = E\{[Z(X_1) - m(X_1)] \cdot [Z(X_2) - m(X_2)]\}$$

The variogram

$$\begin{aligned} 2\gamma(X_1, X_2) &= D[Z(X_1) - Z(X_2)] \\ &= E\{[Z(X_1) - Z(X_2)]^2\} \end{aligned}$$

We use the notation;

$$h = |X_1 - X_2|$$

and express the variogram as;

$$\begin{aligned} \gamma(h) &= \frac{1}{2} E\{[Z(X+h) - Z(X)]^2\} \\ &= \frac{1}{2} \lim_{X \rightarrow \infty} \frac{1}{X} \int_0^X [Z(x+h) - Z(x)]^2 dx \end{aligned}$$

In the case of one dimensional space (as for geophysical logging) we calculate the so called experimental variogram

$$\gamma^*(h) = \frac{1}{2N(h)} \sum_{i=1}^{N(h)} [Z(X_i+h) - Z(X_i)]^2$$

where $N(h)$ is the number of pairs $(Z(X_i + h) - Z(X_i))$ available for the distance h equal to the sampling interval in the logging. It has been shown by Matheron (1965) that;

$$E[\gamma^*(h)] = \gamma(h)$$

The experimental variogram $\gamma^*(h)$ is therefore considered to be an estimate of the variogram $\gamma(h)$.

Variograms for eleven runs in the Vestmanna-1 and Lopra-1 holes have been calculated and are shown in figs. 1 - 11. In general, the variograms are as expected monotonic functions. The form and range of the variograms are, however, quite different and each type will be discussed separately.

The variograms for porosity in both wells (figs. 1, 8, and 9) seem to be of spherical form, which for point-like samples can be expressed as;

$$\begin{aligned} \gamma(h) &= C \left[\frac{3}{2} \left| \frac{h}{a} \right| - \frac{1}{2} \left| \frac{h}{a} \right|^3 \right] + C_0 & h < a \\ &= C + C_0 & h \geq a \end{aligned}$$

where;

C_0 = the nugget effect

a = range of the variograms

C = constant (the so called sill of the variogram)

The range of the porosity variogram in Lopra-1 is of the order 10 - 16m whereas the range for the porosity variograms in Vestmanna-1 is approximately 6m. This difference in range is most likely due to the different diameters of the wells.

Statistically this means that "samples" (measurements of porosity) at distances larger than 6m in Vestmanna-1 and 16m in Lopra-1 are independant of each other.

Spacings in the neutron-neutron logs are in the order of 0.5m and will therefore not influence the range of the variograms (figs. 1, 8, and 9) the nugget effect is negligible, and the sill of the variograms are

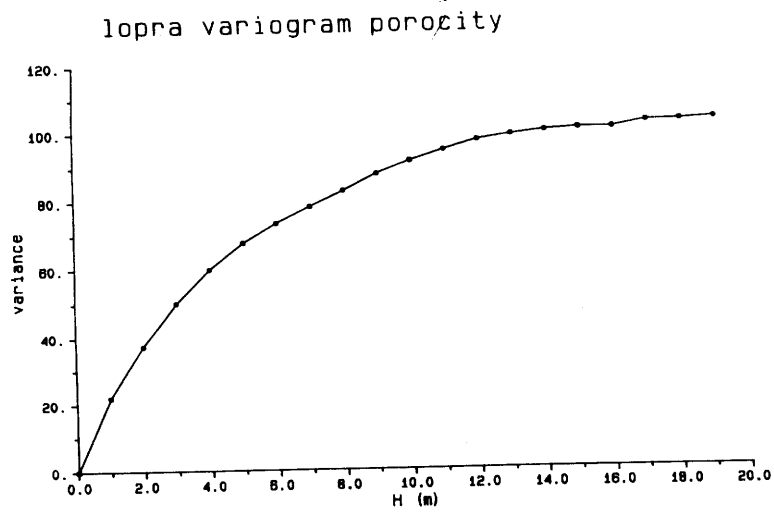


Figure 1. Variogram for porosity in Lopra-1

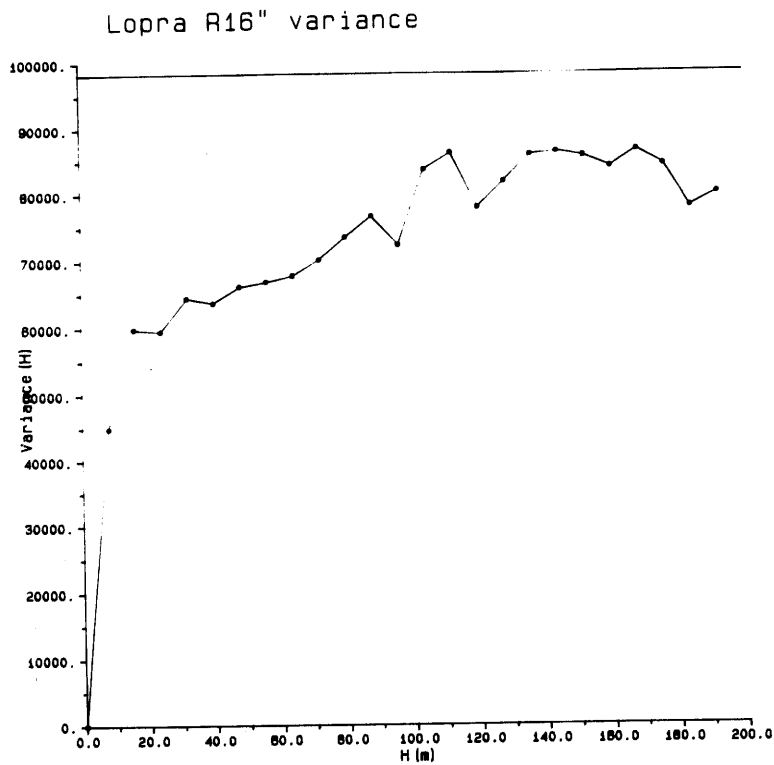


Figure 2. Variogram for R16" in Lopra-1

LOPRA R 64" VARIANCE 190M-

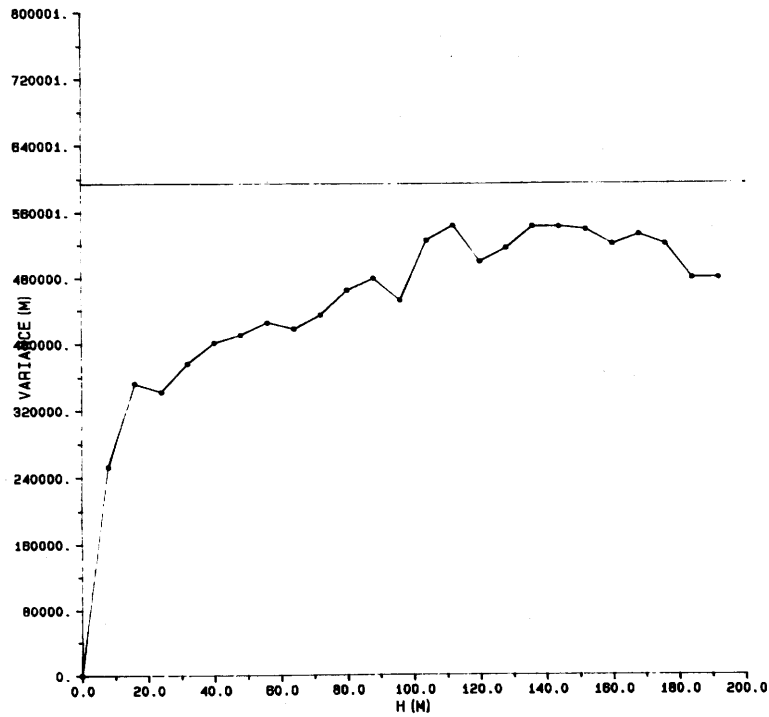


Figure 3. Variogram for R64" in Lopra-1

LOPRA VARIANCE SI02

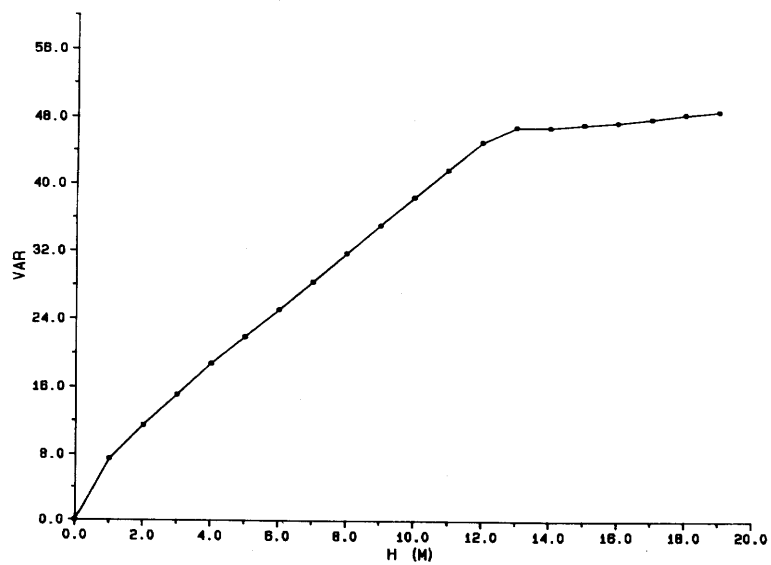


Figure 4. Variogram for natural gamma ray in Lopra-1

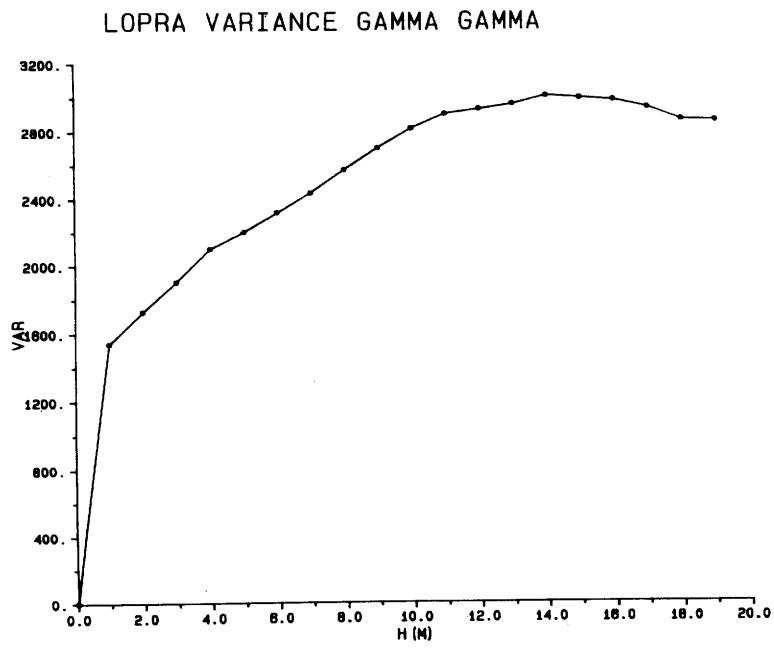


Figure 5. Variogram for gamma-gamma in Lopra-1

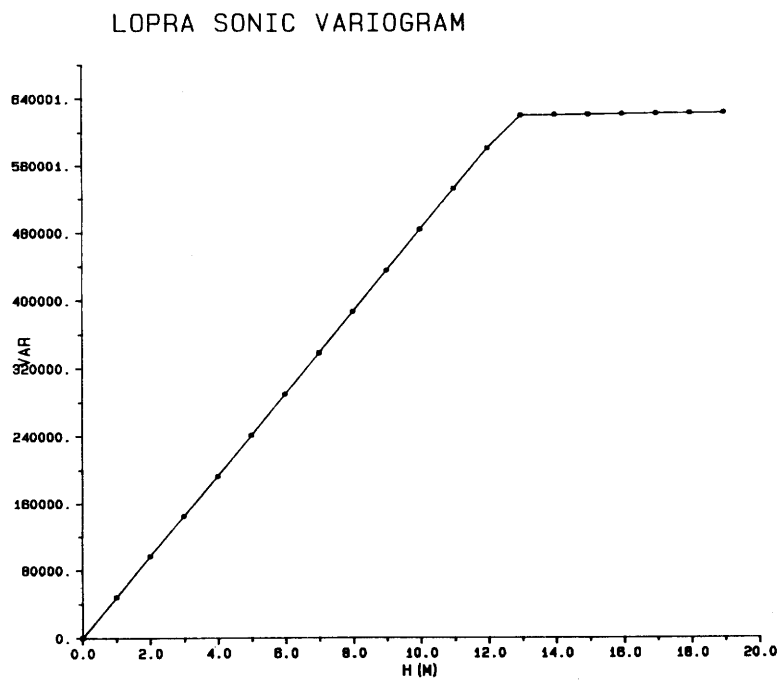


Figure 6. Variogram for sonic travel time in Lopra-1

LOPRA VARIOGRAM SONIC AMPLITUDE

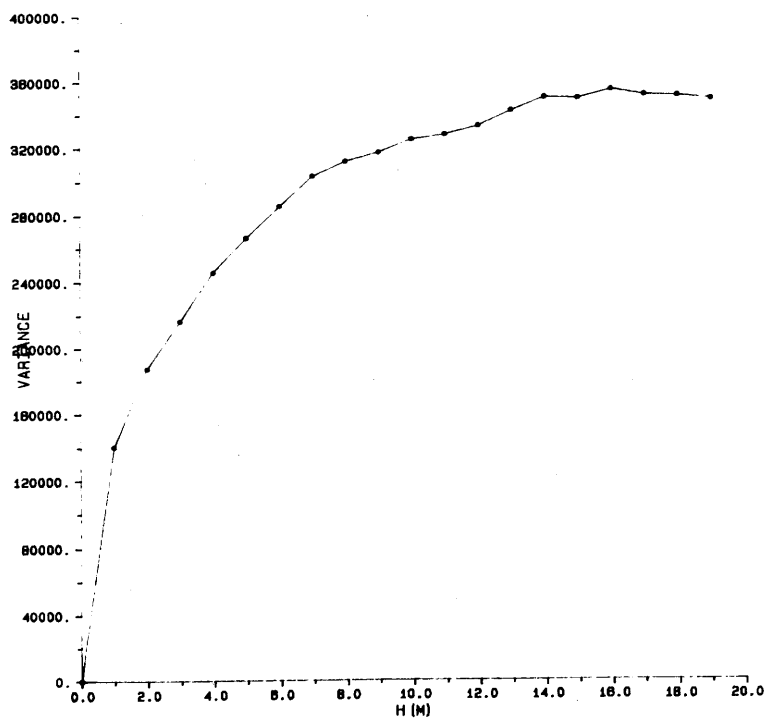


Figure 7. Variogram for sonic amplitude in Lopra-1

VESTMANNA N-N VARIANCE

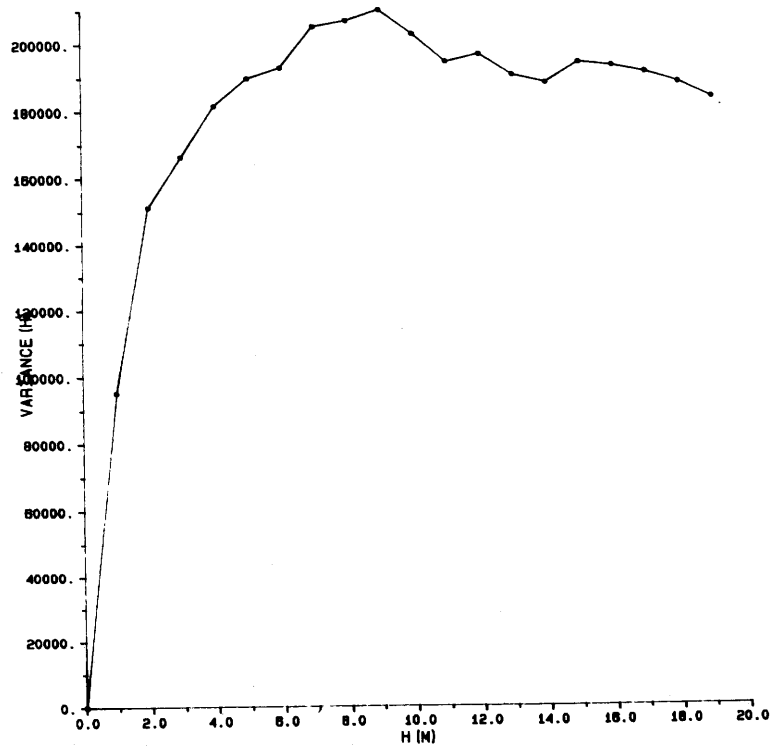


Figure 8. Variogram for neutron-neutron in Lopra-1

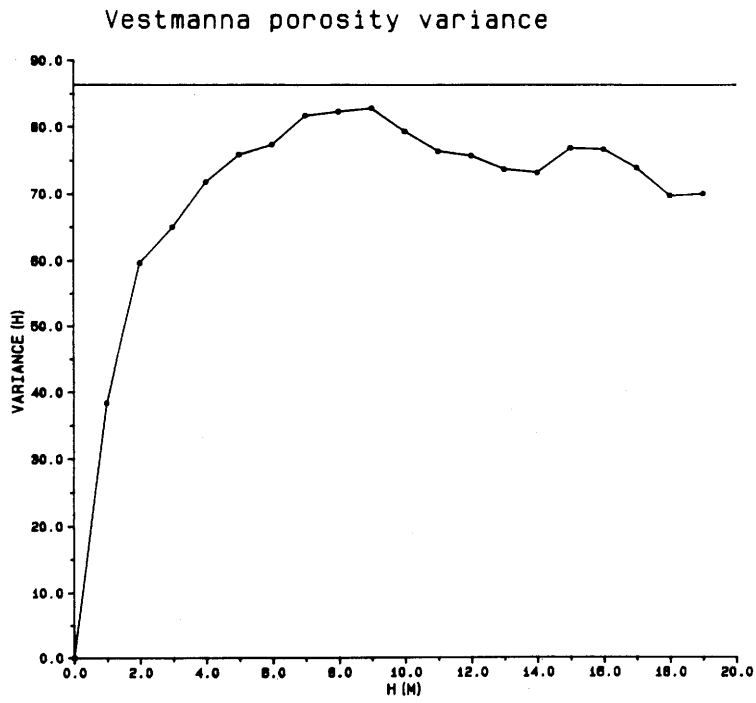


Figure 9. Variogram for porosity in Vestmanna-1

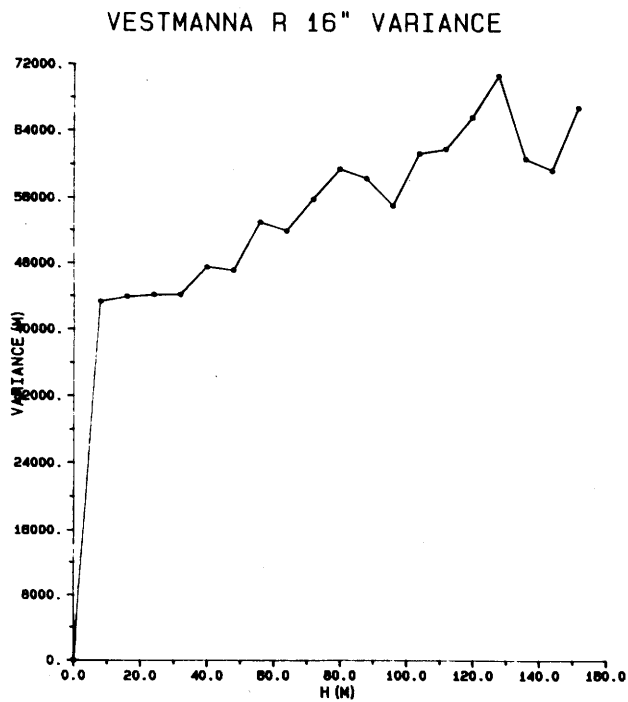


Figure 10. Variogram for R16" in Vestmanna-1

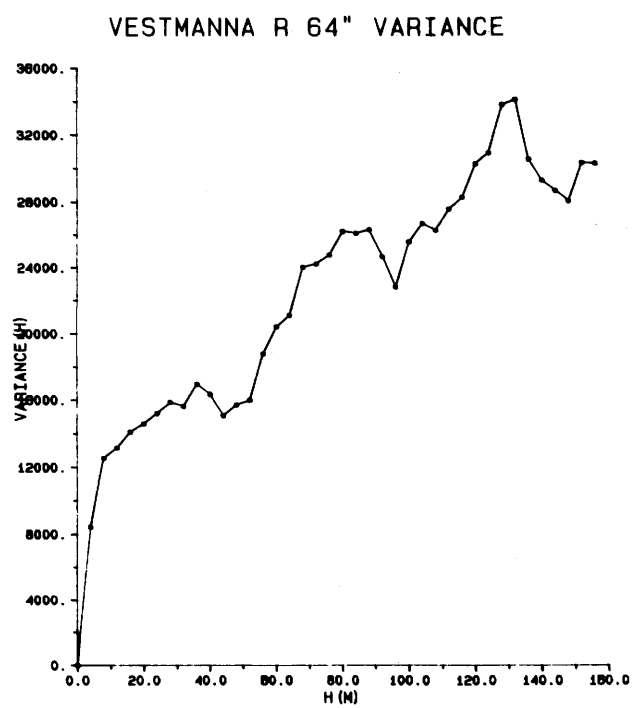


Figure 11. Variogram for R64" in Vestmanna-1

close to the experimental variance $S^2(\phi)$. The variograms for porosity are therefore found to follow normal statistical behaviour.

The variograms for resistivity (figs. 2, 3, 10, and 11) show rather peculiar behaviour. Even though the variograms have been calculated for an increment of up to 160 - 200m the variograms are still increasing. For the Lopra-1 data the variograms for R16" and R64" are considerably less than the experimental variance $S^2(R)$, whereas the resistivity variograms in Vestmanna-1 exceed the experimental variance for these large values of the increment h . These circumstances might indicate that on extended depth intervals the resistivity data contains some drift. However, the beginning of the resistivity variograms shows that for the range of 10 - 20m the data shows good correlation. The assumptions for variograms might therefore be valid locally (in the range of 10 - 20m increments), but not on a long range (100 - 200m). It might be possible to interpret the form of the resistivity variograms as due to very large nugget effects. Due to the spacings in the resistivity logs (0.4 - 1.6m), this possibility looks improbable.

The variograms for natural gamma ray in Lopra-1 (fig. 4) seems to be of spherical form with a small nugget effect (ca. 4%). The range of the variogram is approximately 13m which is in agreement with the value found for porosity in the same well. The sill of the natural gamma ray variogram is close to the experimental variance $S^2(\text{SiO}_2)$.

The variogram for gamma-gamma log in Lopra-1 shows relatively large nugget effect, and the experimental variance S^2 is considerably larger than the values in the variogram. As will be described later, quite large systematic errors in the gamma-gamma data from Lopra-1 have been found. The shape of the variogram for the gamma-gamma data only reflects these circumstances.

Variograms for sonic travel time and sonic amplitude for Lopra-1 are shown in figs. 6 and 7. The travel time variogram has a sill which is exactly the same as for the experimental variance $S^2(t)$. For small values of h the variogram seems to be a straight line and no nugget effect can be seen. The range of the variogram is 13m which is approximately the same as for porosity and natural gamma ray logs.

The experimental variance for the sonic amplitude is considerably larger than the values in the variogram on fig. 7, and it is not

obvious what the range is for this variogram. As this data is hardly used in the present interpretation, further elaboration of this variogram will not be performed here.

In summary it can be concluded that the data of porosity, natural gamma ray and sonic travel time do not show any sign of systematic error or drift. The data on resistivity is not satisfactory on a long range scale, but are probably usable on a short scale. The data on gamma-gamma contains most likely some systematic error or drift.

4 WELL SIZE CORRECTION

Most of the geophysical parameters measured in the wells Lopra-1 and Vestmanna-1 are sensitive for the well diameter. In some cases like the gamma-gamma and sonic logs, different well diameters influence the log response quite heavily, and may in some cases destroy the information on the surrounding rocks. In other cases like the neutron-neutron, resistivity 64" and temperature the influence of different well size is little or moderate resulting in quite reliable records for the entire depth range. This chapter is devoted to the well size corrections for different types of logs.

4.1 Correction of natural gamma ray log

The drilling fluid (water or mud) acts as an extra absorbant for the natural gamma ray intensity surrounding the probe. We call the true gamma intensity I_0 , and the recorded intensity I . The relationship between these intensities is:

$$I_0 = CF * I$$

where the correction factor CF is a function of the borehole radius R , the radius of the probe R_s , the density of the drilling fluid r , and the effective mass absorption coefficient of the fluid μ_p . Here the absorption function $A_p(\mu_p R)$ as calculated by Czubek (1981) is used to obtain the correction coefficient CF . We get:

$$CF = 1 / (1 - A_p(\mu_p R))$$

Figure 12 shows $A_p(\mu_p R)$ as function of R_s/R . In our case R_s , μ_p , and r are constants and furthermore we assume $\mu_p = 0.03 * r$. This means that CF is a function of R alone. By using the functions shown on fig. 12 the following expression for CF can be obtained:

$$CF = \frac{1}{1.192 - 0.3937 \log R} + \frac{0.32}{R * R}$$

This expression has been used for well size correction of the natural gamma ray logs.

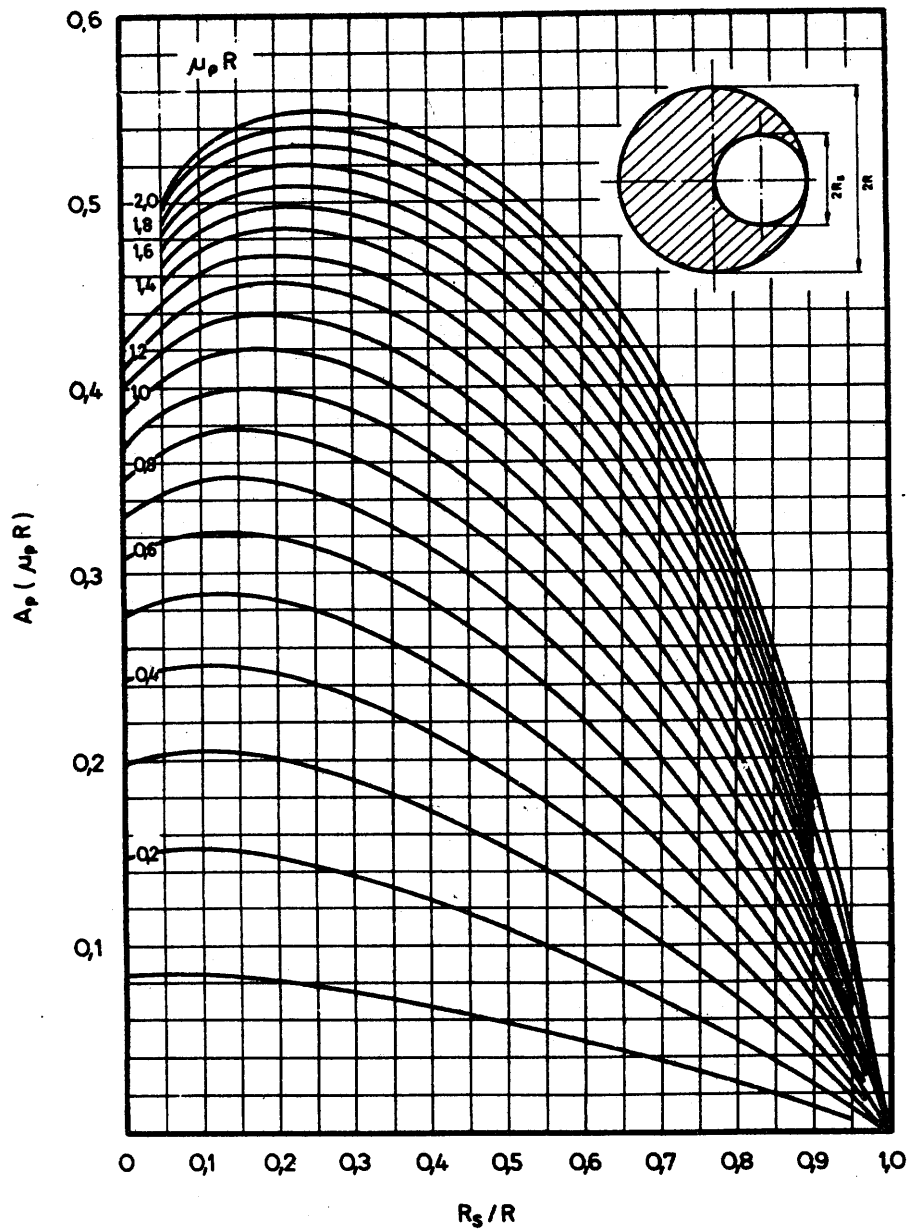


Figure 12. Absorption function of the borehole fluid used for well size correction of gamma ray log

R - borehole radius
 R_s - probe radius
 μ_p - $0.03 * r$
 ρ - fluid density

4.2 Correction of the neutron-neutron log

In general, the effect of the well size on the counting rate in the neutron-neutron log is that the logarithm of the counting rate is a linear function of the well diameter. If I_{nn} is the neutron intensity and D is the diameter of the well we can write:

$$\log I_{nn} = a * D + b$$

where a and b are particular constants for a given probe construction. The neutron-neutron probe used in Lopra-1 and Vestmanna-1 has been used for many years in Iceland and an empirical value :

$$a = -0.0015 / \text{mm}$$

has been deduced from numerous investigations in wells in the Krafla Geothermal Field (Stefánsson et al., 1983). This value is also in reasonable agreement with calibration curves published by the manufacturer of the probe (GO 1976). For a fixed diameter D_0 of the well we can write:

$$\log I_{nn}(D_0) = a * D_0 + b$$

and by dividing $I_{nn}(D_0)$ by I_{nn} we obtain:

$$I_{nn}(D_0) = X * I_{nn}$$

where:

$$X = 10^{a(D_0 - D)}$$

In this work $D_0 = 9" = 228.6\text{mm}$ is chosen as reference and all values of the neutron-neutron logs have been corrected to that diameter.

4.3 Correction of the resistivity logs

The response function of 16" and 64" normal resistivity logs are known, and figs. 13 and 14 show the correction curves published by Gearhaft Owen Inc. (now Gearhart Inc.). As can be seen in fig. 14, the influence of well-size on 64" normal resistivity is very small

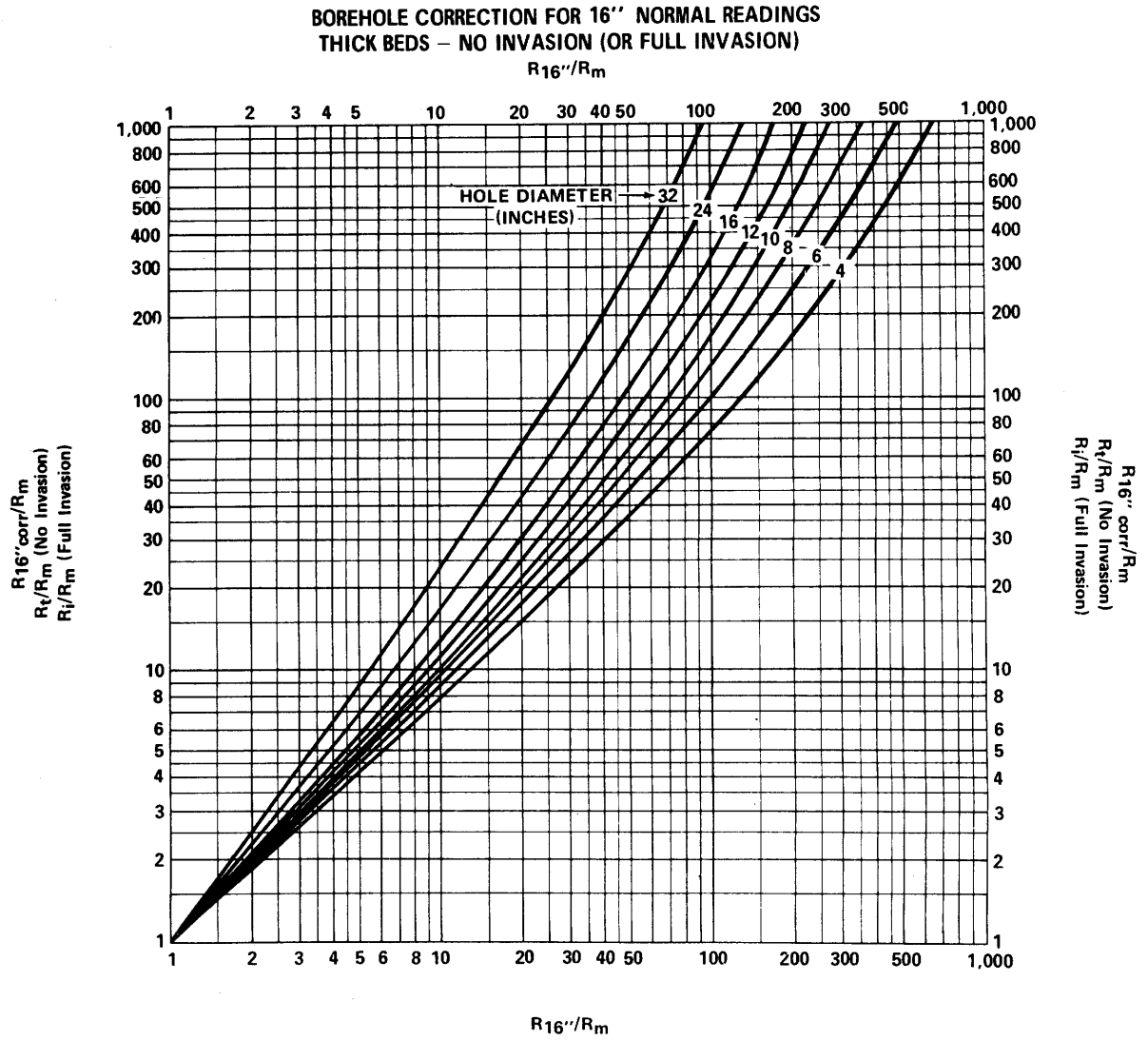


Figure 13. Borehole correction for 16" normal resistivity log

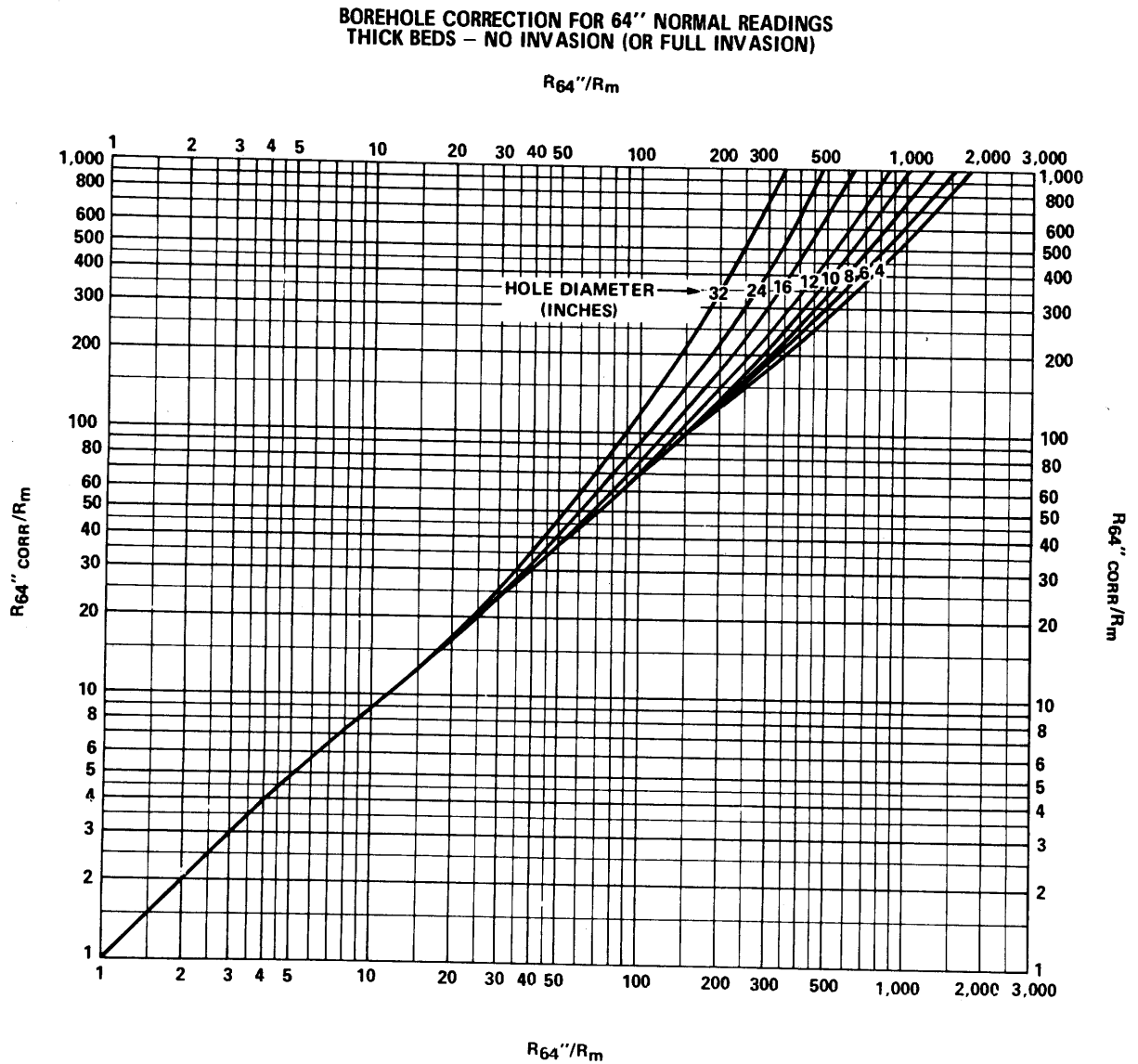


Figure 14. Borehole correction for 64" normal resistivity log

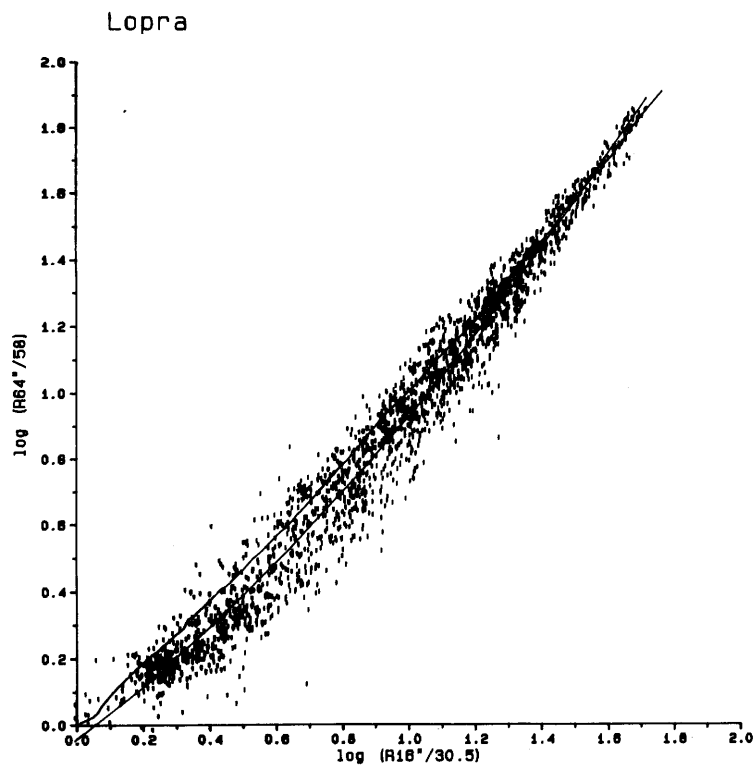


Figure 15. Empirical relation between R16" and R64" in Lopra-1

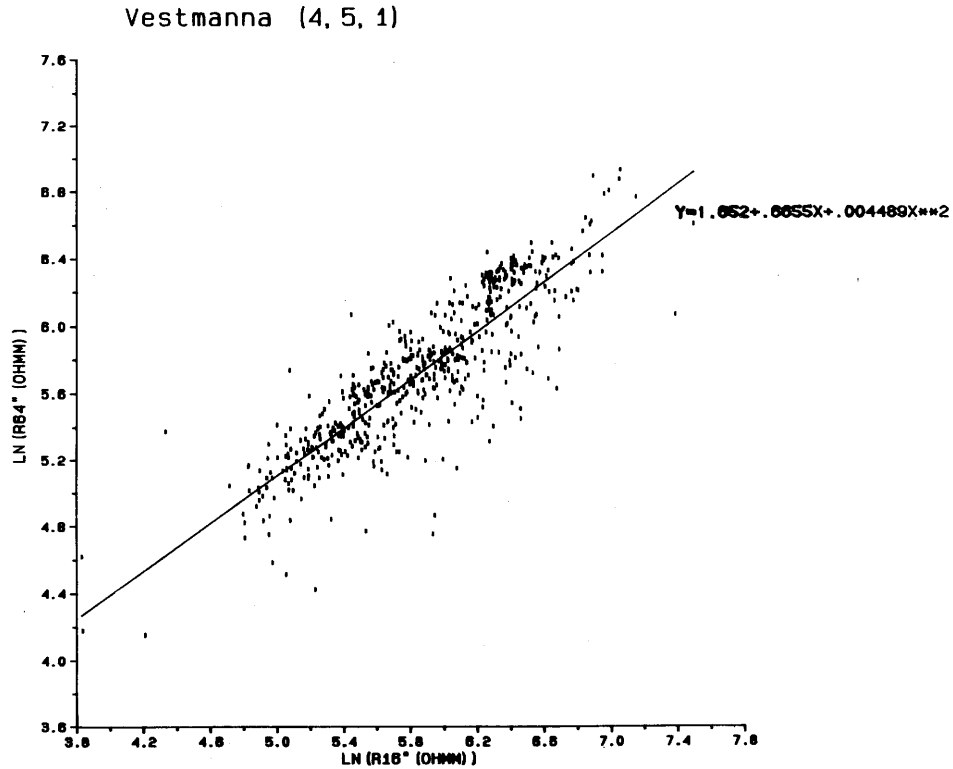


Figure 16. Empirical relation between R16" and R64" in Vestmanna-1

for moderate well diameter and $R_f/R_w < 500$. For comparison of resistivity with other logs the 64" normal resistivity was therefore used without well size correction. This approach is justified in the following way: Figure 15 shows the empirical relation between the 16" and 64" normal resistivities in Lopra-1, and fig. 16 shows similar relation between the 16" and 64" normal resistivities in Vestmanna-1. The expected relation as deduced from fig. 13 is also shown on fig. 15. Since these two curves agree quite well it is concluded that the 64" normal resistivity is a good estimate of the formation resistivity without well size correction.

5 POROSITY

5.1 Calibration

When all the neutron-neutron data has been corrected to 9" well diameter, calibration curves from the manufacturer of the probe are used to obtain real porosity. The curve for 9" diameter is shown in fig. 17 is reproduced from Stefánsson (1979). This calibration curve is actually only valid for limestone but, as shown by Czubek (1981), the difference between limestone porosity and the porosity of igneous rock should not be larger than 3% in this respect. The calibration curve in fig. 17 should therefore give a reasonable estimate of the porosity of the rocks in the Faeroe Islands.

It should also be noted here that the neutron-neutron method is sensitive for the total amount of water in the rock, which means that both water in pores and fissures as well as bounded water will influence the neutron-neutron response. The term "porostiy" as used in this report actually means the total water content of the rock.

5.2 Porosity as a function of depth

Calculated porosity values as a function of depth is shown for Lopra-1 in fig. 18 and for Vestmanna-1 in fig. 19. As can be seen in fig. 18 some of the porosity values are actually zero, which means that the influence of bounded water is negligible at least for rocks with low porosity.

Comparison of figs. 18 and 19 shows clearly the difference in the thicknesses of the basalt units in these two wells. The succession at Vestmanna-1 consists of thin (1 - 2m) flow units, whereas the units in Lopra-1 are of an order of magnitude thicker.

5.3 Distribution of porosity

The average porosity for the whole pile in Lopra-1 is found to be 12 +/- 10% (standard deviation). The porosity distribution is shown in fig. 20. This distribution shows a clear bimodal form, indicating two rock types as seen by the neutron-neutron log. In fact this

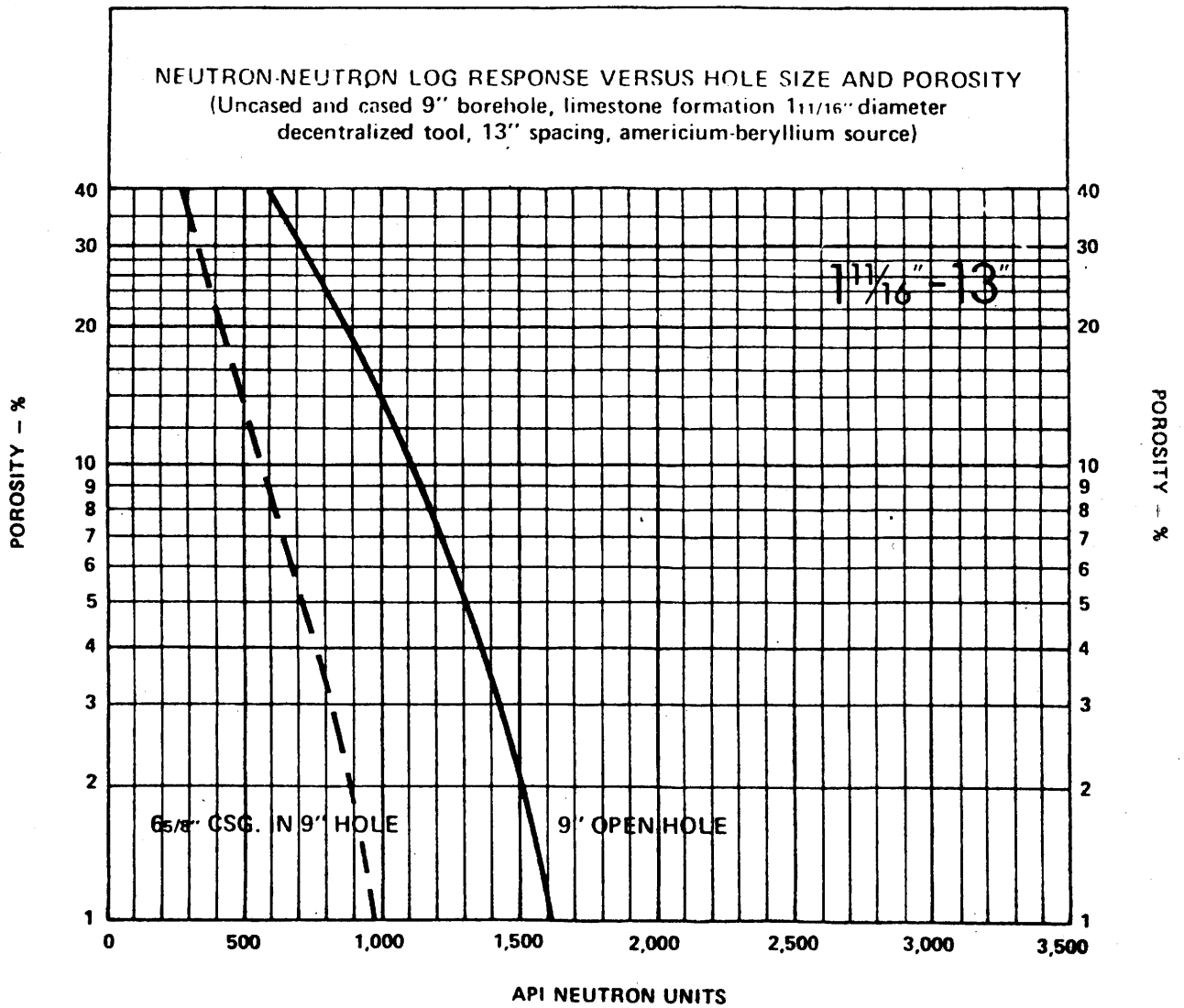


Figure 17. Calibration curve for neutron-neutron log

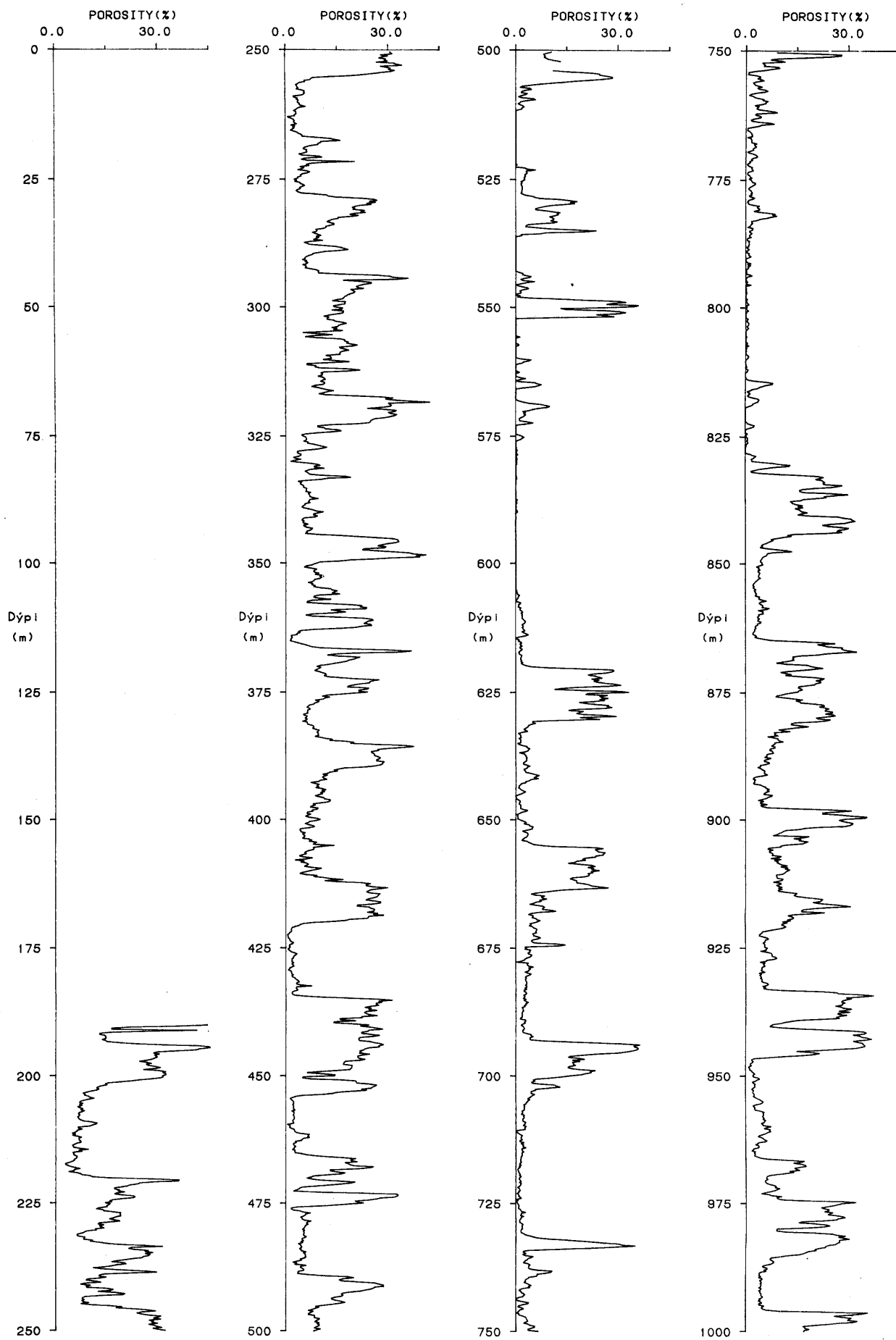


Figure 18. Porosity versus depth in Lopra-1

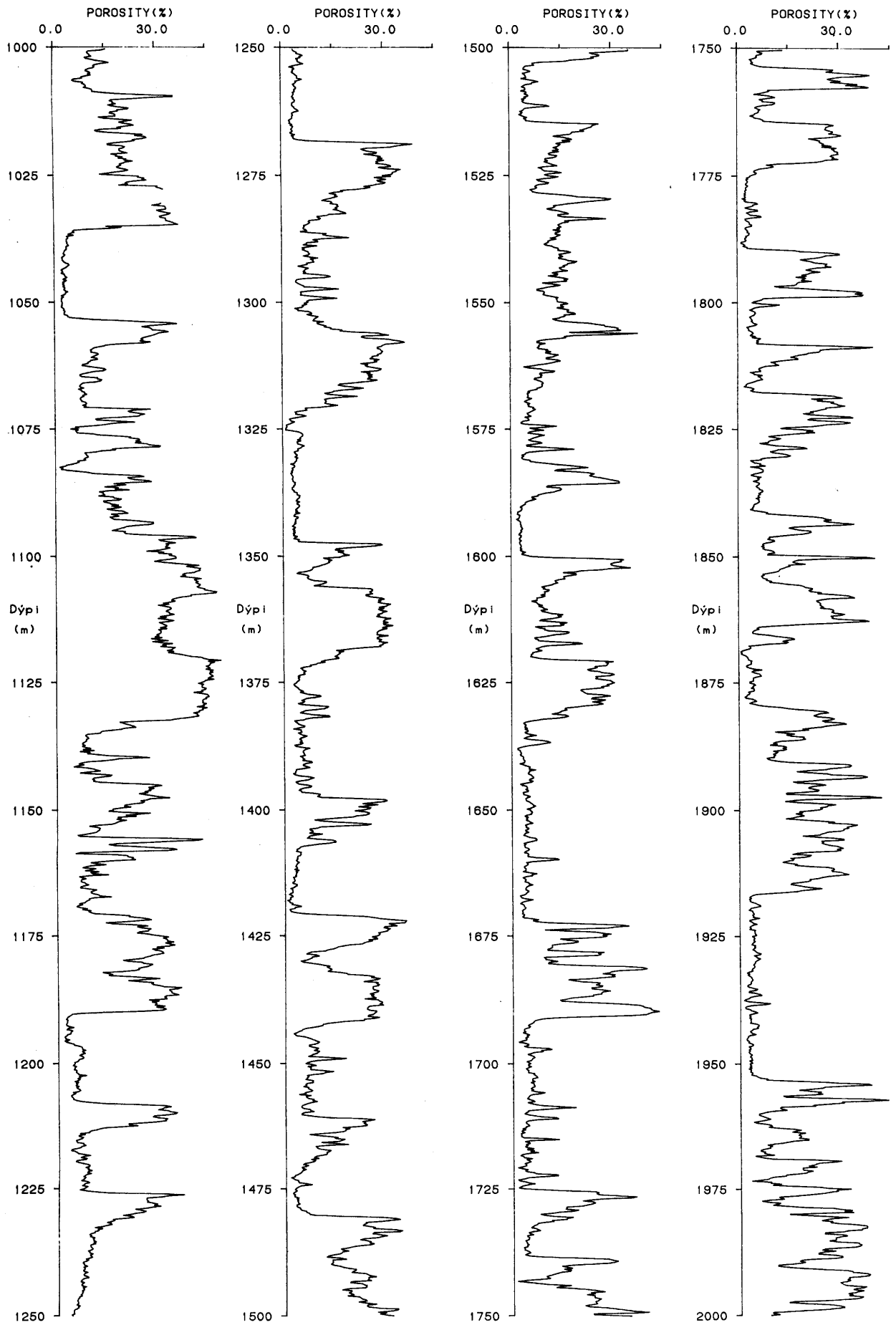


Figure 18. Continue.

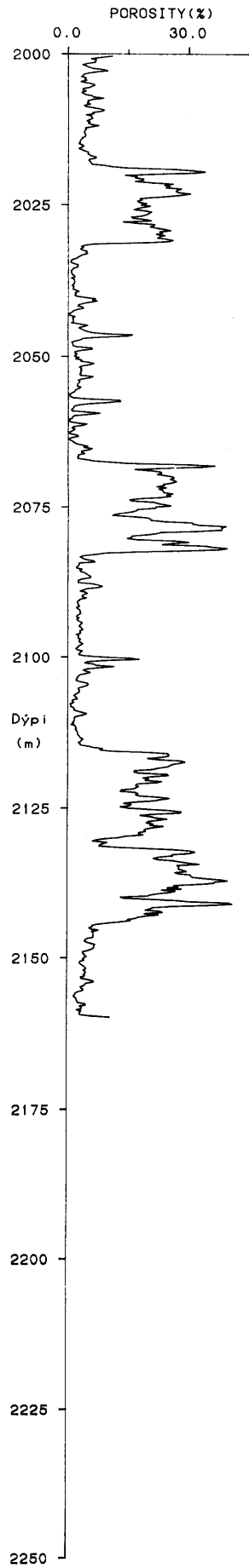


Figure 18. Continue.

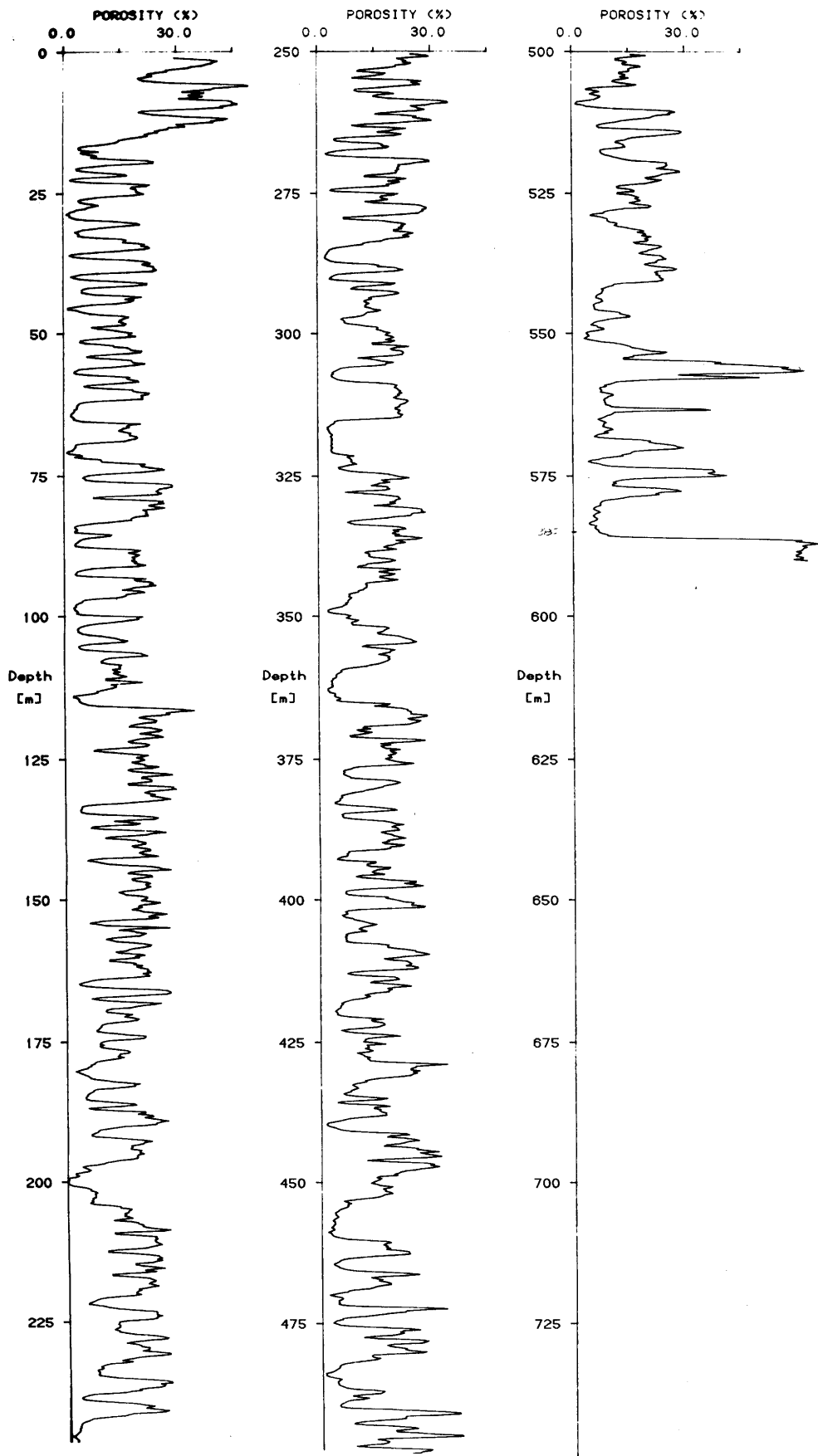


Figure 19. Porosity versus depth in Vestmanna-1



Lopra I Porosity distribution

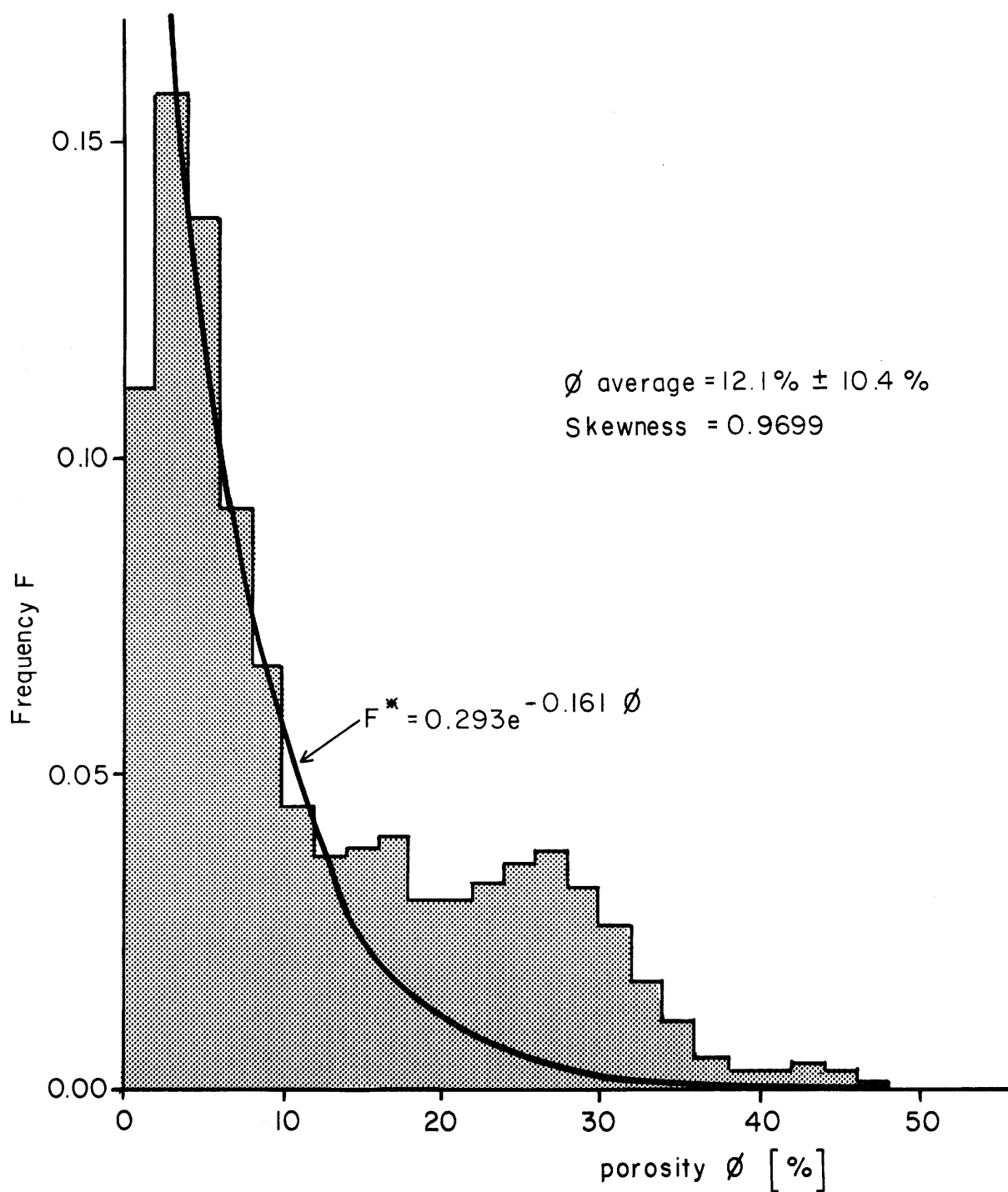


Figure 20. Porosity distribution in Lopra-1

behaviour can also be seen in fig. 18 as the porosity values appear to be either high or low.

In order to separate the two peaks in fig. 20, an exponential function was fitted to the right flank of the first peak and subtracted from the total. The second distribution is shown on fig. 21.

The first peak in the porosity distribution has an average porosity of $(7.4 \pm 1.5)\%$, with a maximum occurrence at 2-4%. This rock type represents about 74% of the total pile penetrated by the Lopra-1 well. The second peak in the porosity distribution has an average porosity of $(26 \pm 5)\%$ and the maximum occurrence at 26-28%. This rock type is about 26% of the total rock pile penetrated.

The distribution of porosity in Vestmanna-1 is shown in fig. 22. The distribution is bimodal as in the case for Lopra-1. The mean value of the porosity is $(15 \pm 9\%)$ (standard deviation). The peaks of the distribution are at 6% and 20% respectively. There is almost equal occurrence of the low porosity and high porosity rocks in the sequence penetrated by Vestmanna-1 whereas the distribution in Lopra-1 shows an uneven distribution. These circumstances reflect the difference in thickness of basaltic flows at Lopra and Vestmanna.

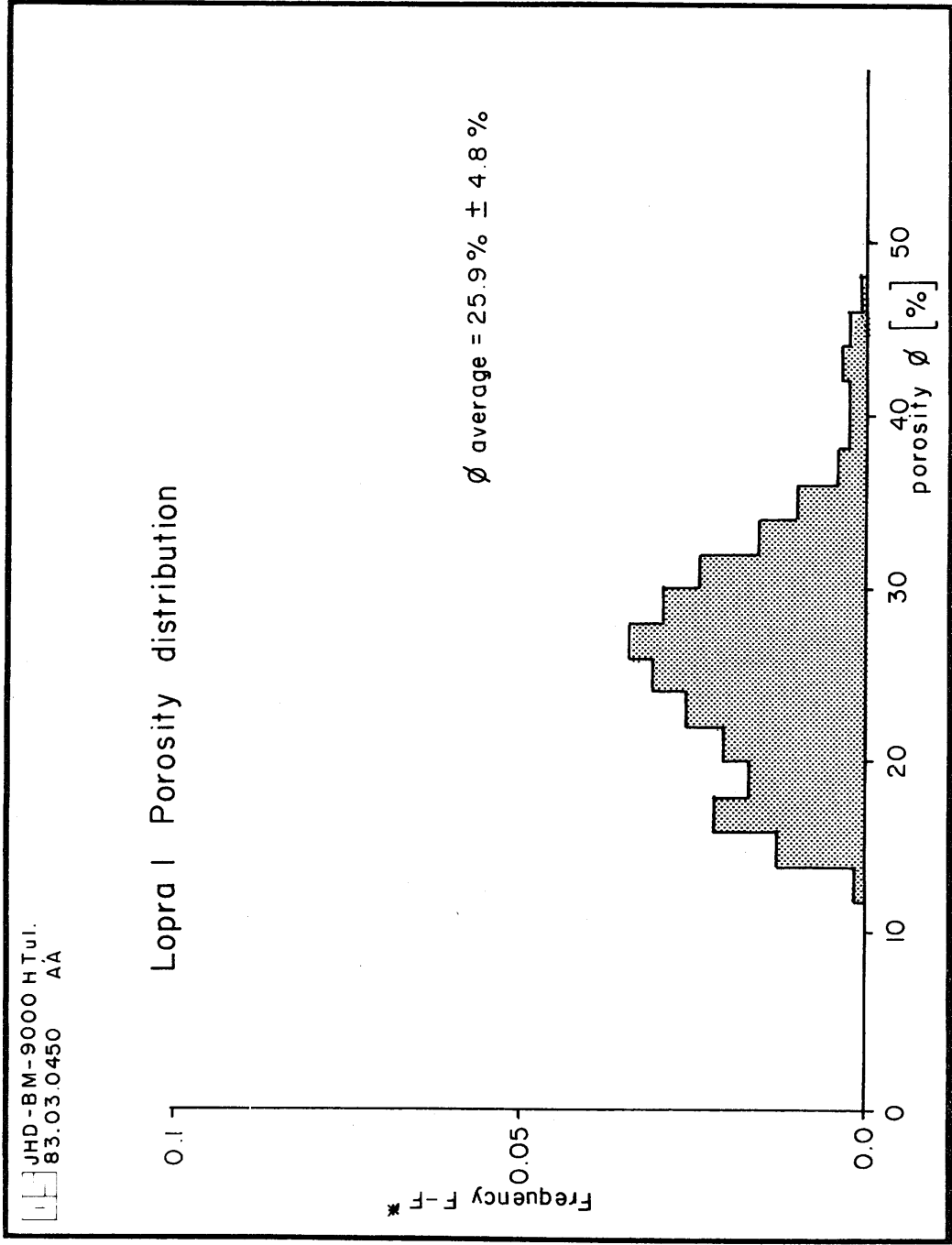


Figure 21. Porosity distribution for rock type 2 in Lopra-1

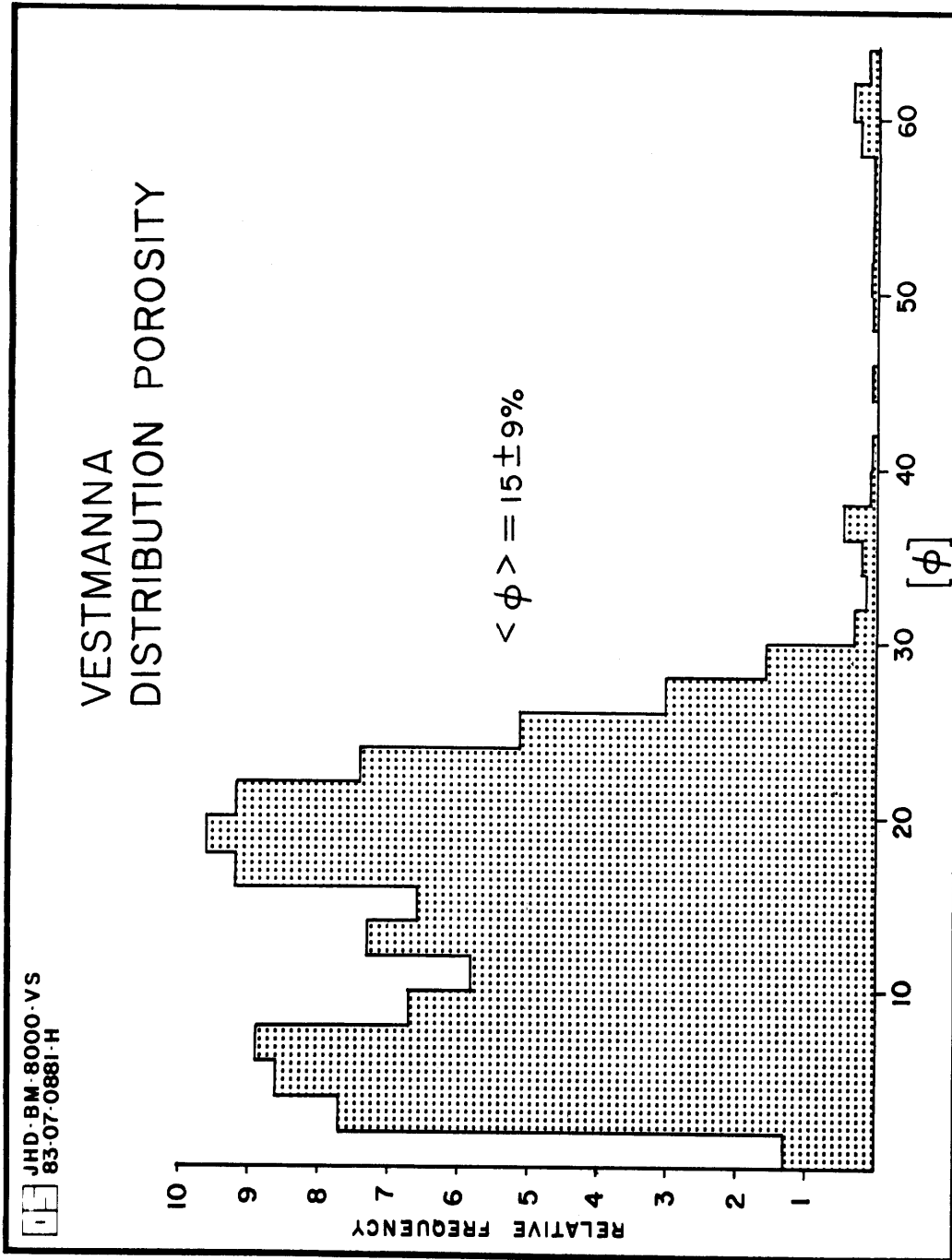


Figure 22. Porosity distribution in Vestmanna-1

6 DENSITY

Considerable effort has been put on the calibration and corrections of the gamma-gamma log from Lopra-1. Several difficulties have been during the work, mainly due to large effect of the well diameter on the registered data. At present, it seems that approximately 80% of the signal registered is due to variations in the well size but only 20% is due to variations in density. These are quite unfavorable conditions, and it has not been possible to separate these two effects in the registered data. We hope that it will be possible to extract some information on the density from the data, but it seems that the uncertainties in this log is larger than in other logs in Lopra-1. As the results obtained so far are not satisfactory, we prefer to wait with the presentation of the results.

7 RESISTIVITY

7.1 Resistivity as a function of depth

Resistivity in the wells Lopra-1 and Vestmanna-1 was measured by a conventional 16" and 64" normal electrode configuration. Normal resistivity in Lopra-1 as a function of depth is shown in fig. 23 for both 16" and 64", and in fig. 24 for Vestmanna-1. Two main differences are in the resistivity logs from the two wells. In the case of Lopra-1 the resistivity values for R64" are larger than corresponding values for R16". In Vestmanna-1 the situation is reversed i.e. the values for R16" are usually larger than the ones for R64". This effect is especially pronounced for thin, high resistivity beds. This difference in behaviour for the resistivity logs is a fine textbook example of the effect of well-size and bed thickness on the resistivity response function. The bed thickness in Lopra is relatively large (of the order of 10 - 20m), which means that it is mainly the well size effect that reduces the response for R16", whereas the values for R64" are close to the formation resistivity as described in chapter 4.3. In Vestmanna the average bed thickness is of the order of 1 - 2m which is similar to the electrode spacing for R64". Thin beds that have high resistivity are therefore not registered by the R64" configuration as can clearly be seen in fig. 24. The well diameter in Vestmanna-1 is small as compared with the R16" electrode spacing, and the well size attenuation is therefore almost negligible. In general it can be concluded that;

- . R64" is a good estimate of the formation resistivity in Lopra-1.
- . R16" is a good estimate for the formation resistivity in Vestmanna-1

7.2 Distribution of resistivity

The mean value for R64" in Lopra-1 is 715 Ω m and the standard deviation of the distribution is 755 Ω m. The corresponding value for R16" in Vestmanna-1 is 405 Ω m for the mean value and 230 Ω m for the standard deviation. Since the range of the resistivity values is rather large, it is more convenient to present the distribution in a logarithmic scale. Figures 25 and 26 show the logarithmic distribution for the resistivity in Lopra-1 and Vestmanna-1

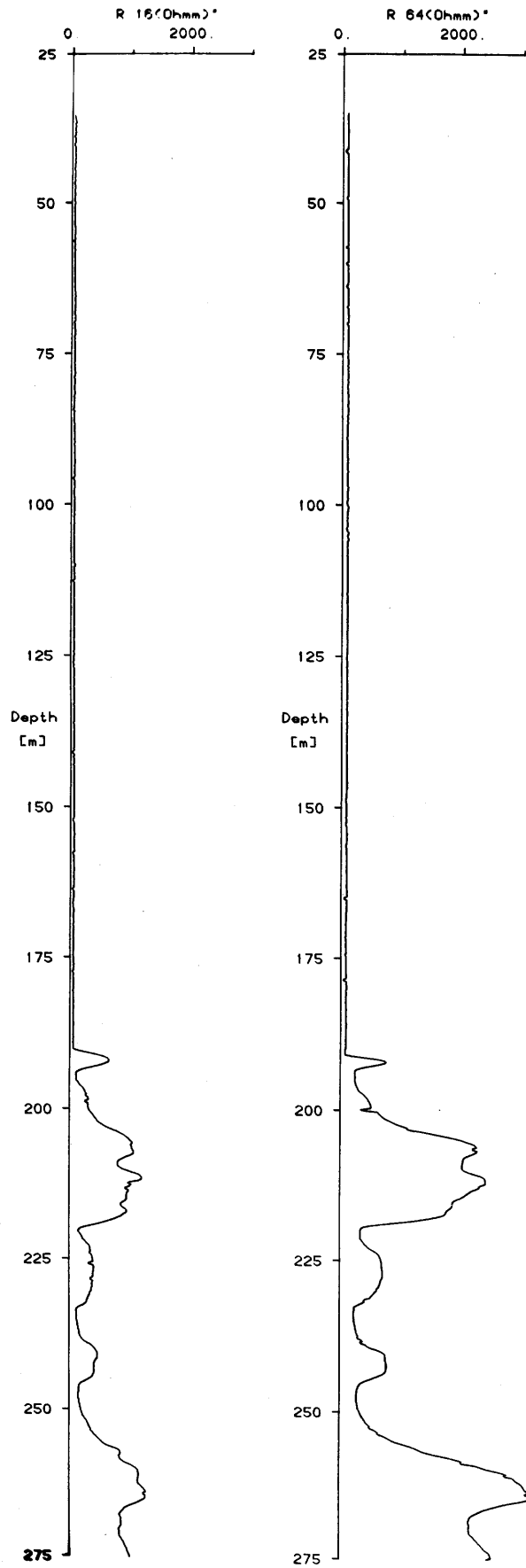


Figure 23. Lopra-1. 16" and 64" normal resistivity versus depth

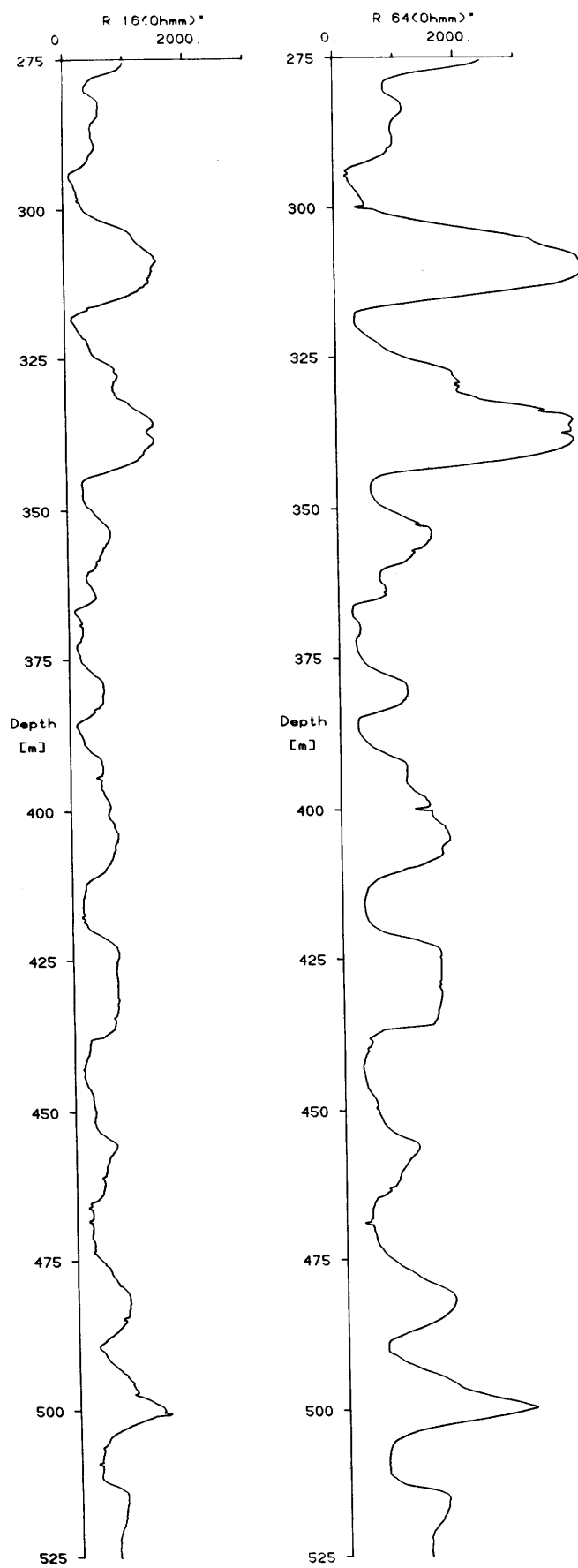


Figure 23. Continue.

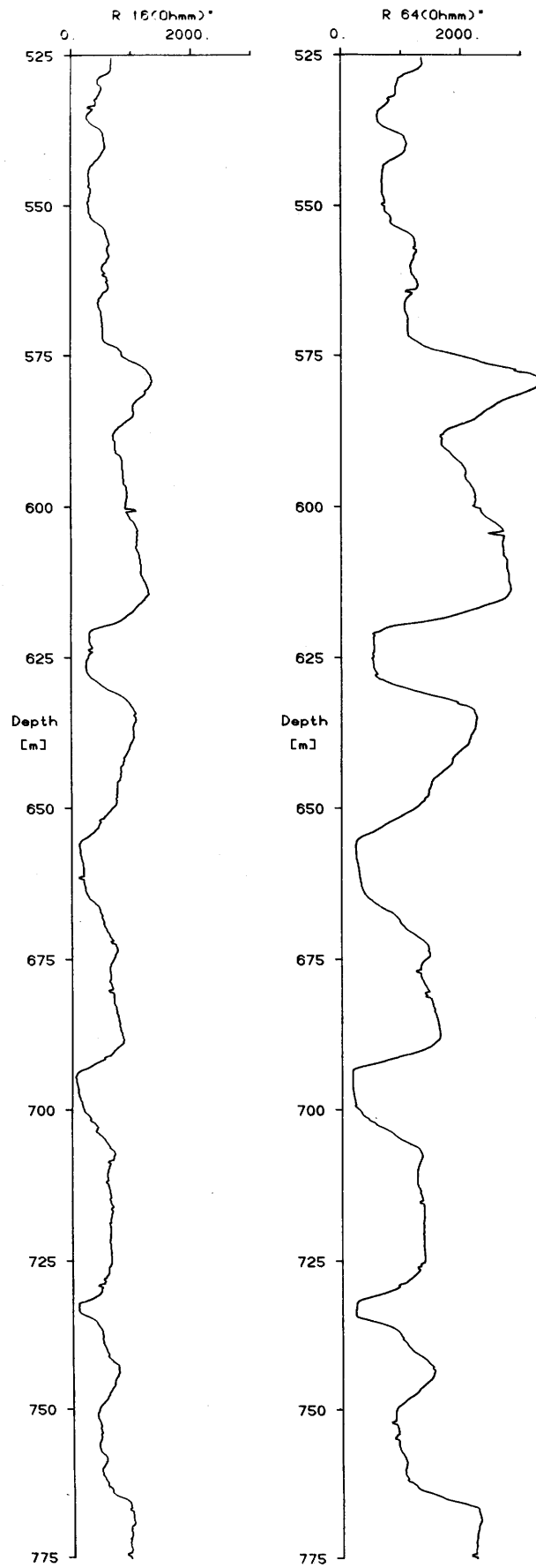


Figure 23. Continue.

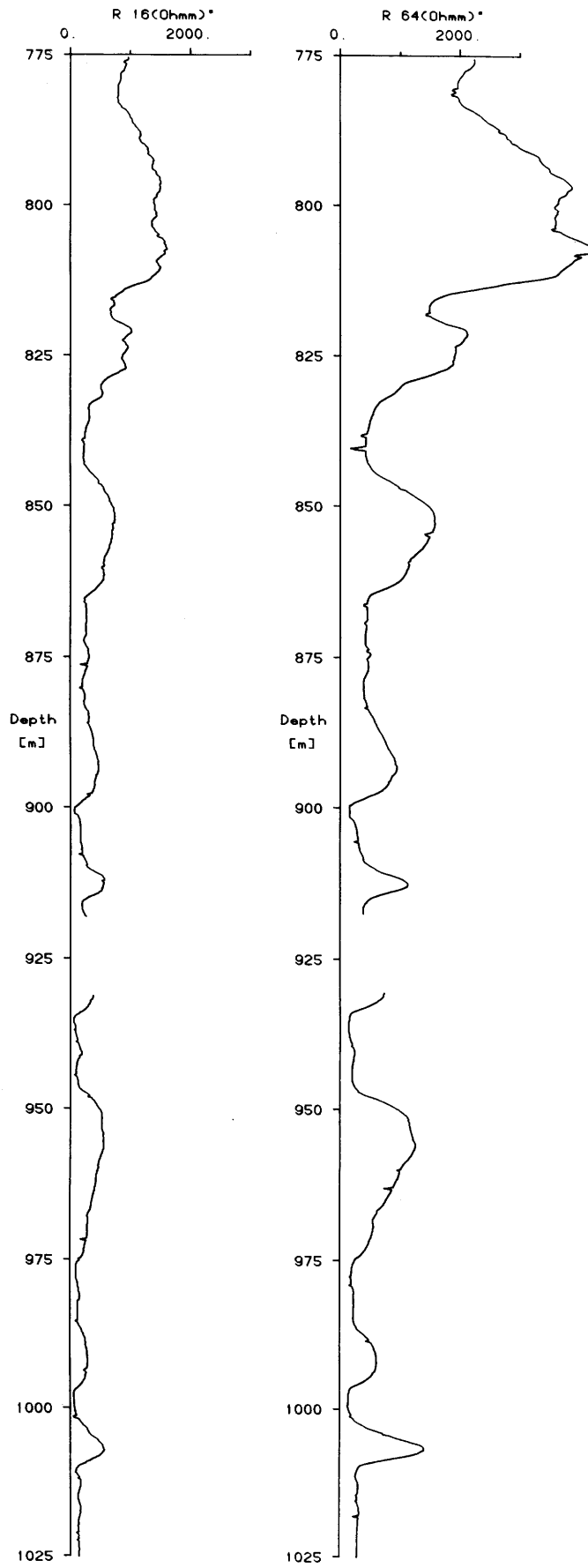


Figure 23. Continue.

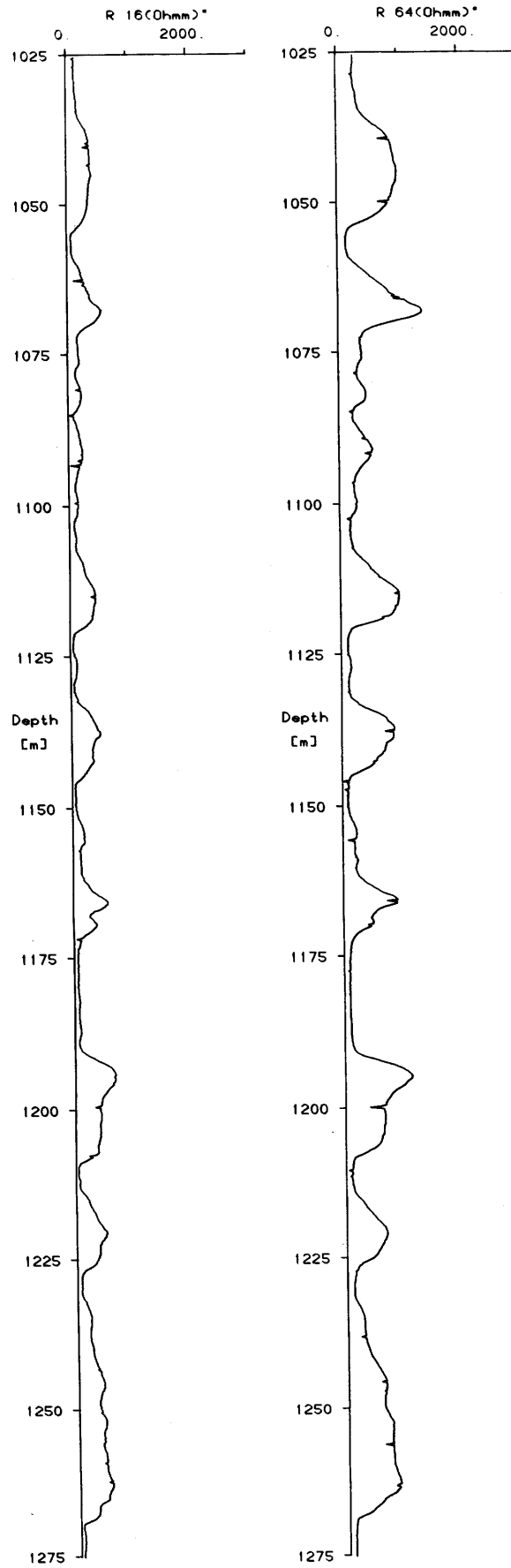


Figure 23. Continue.

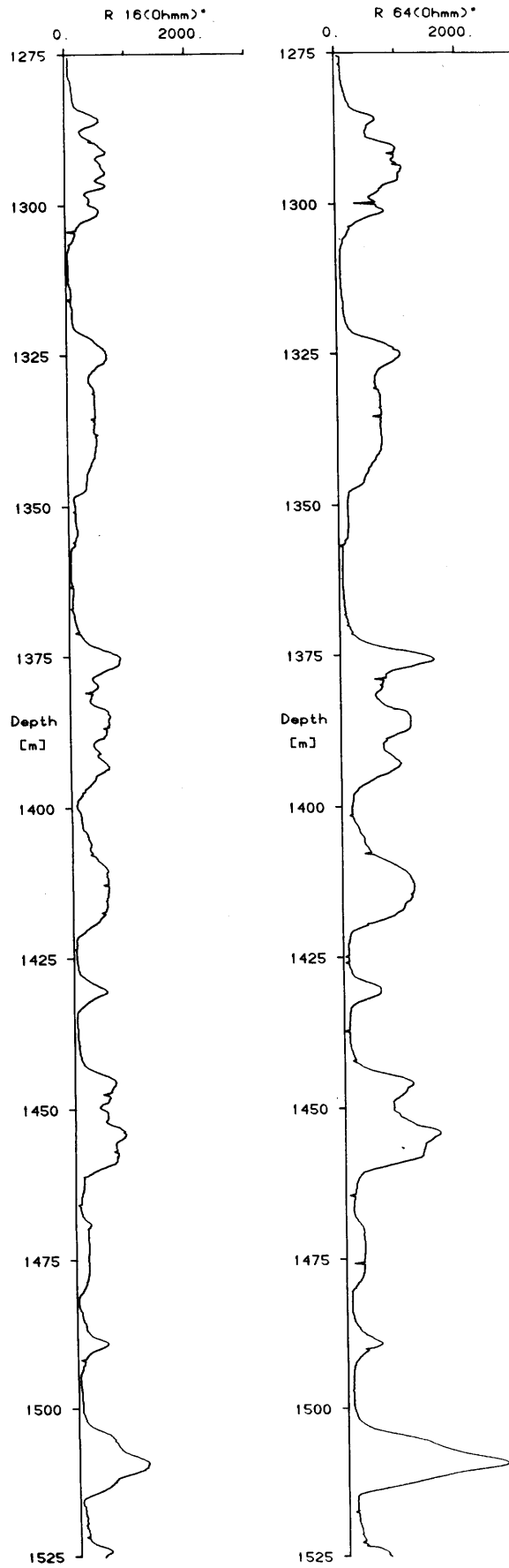


Figure 23. Continue.

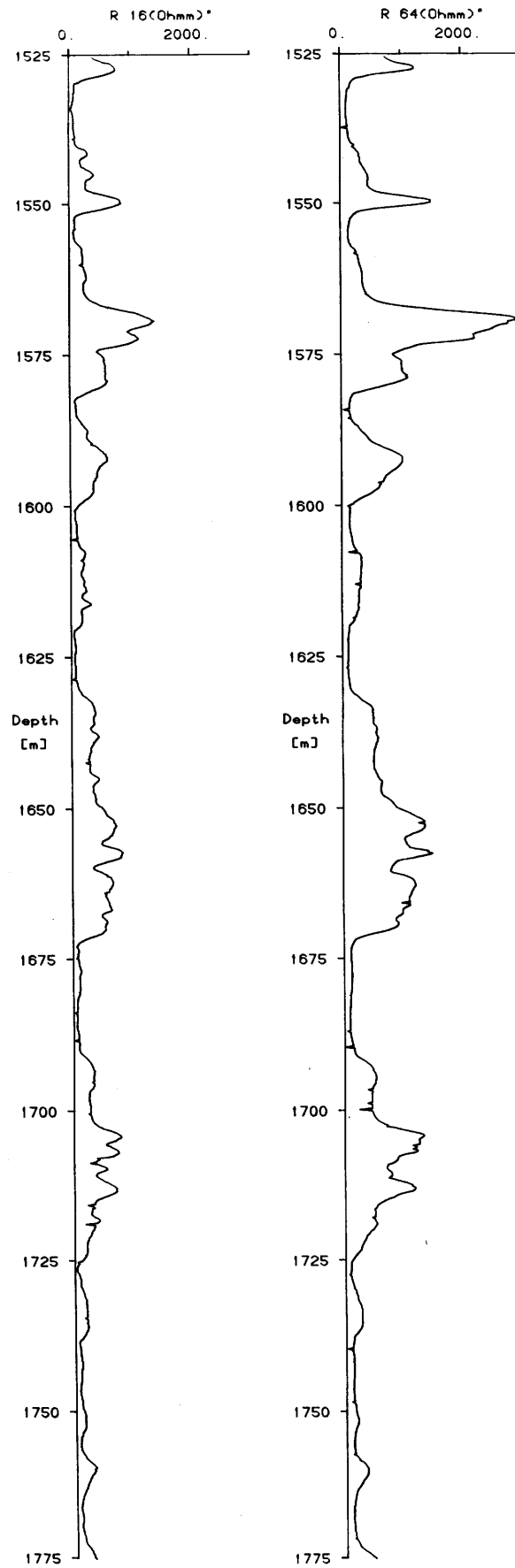


Figure 23. Continue.

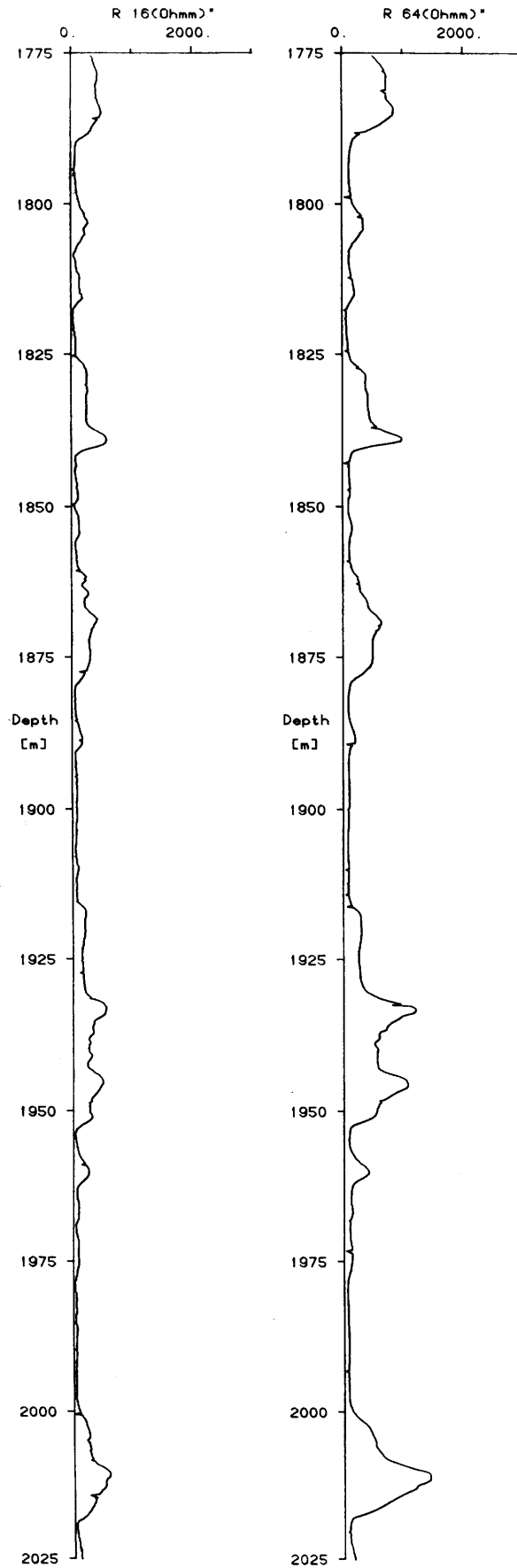


Figure 23. Continue.

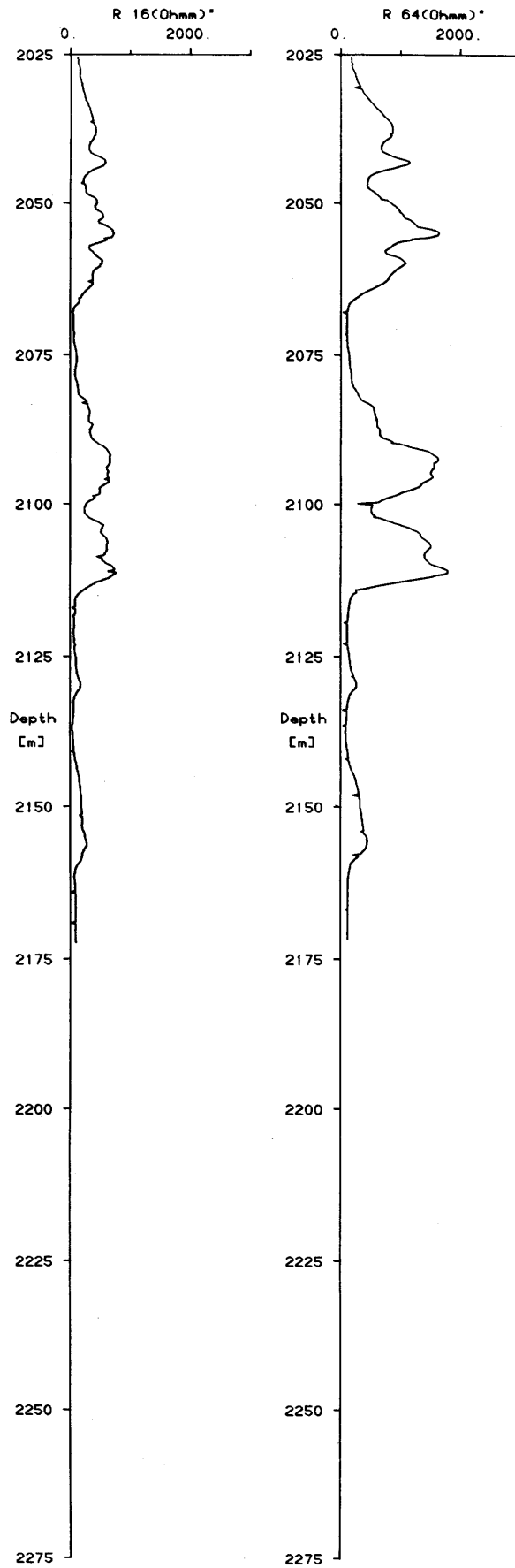


Figure 23. Continue.

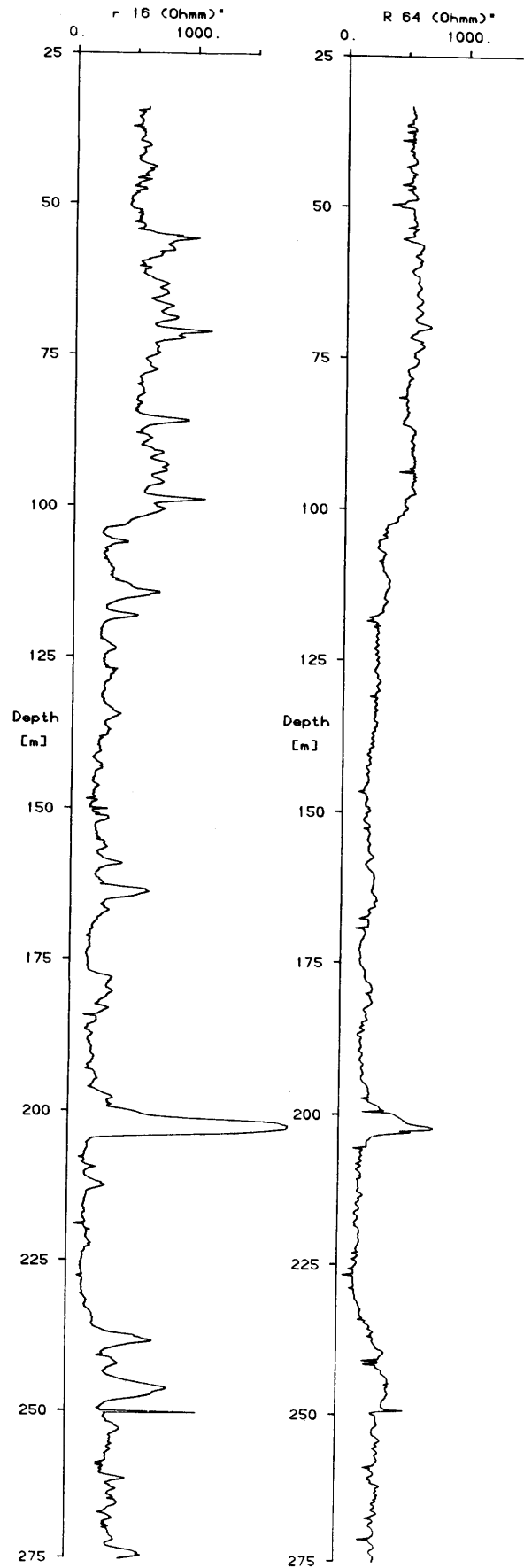


Figure 24. Vestmanna-1. 16" and 64" normal resistivity versus depth

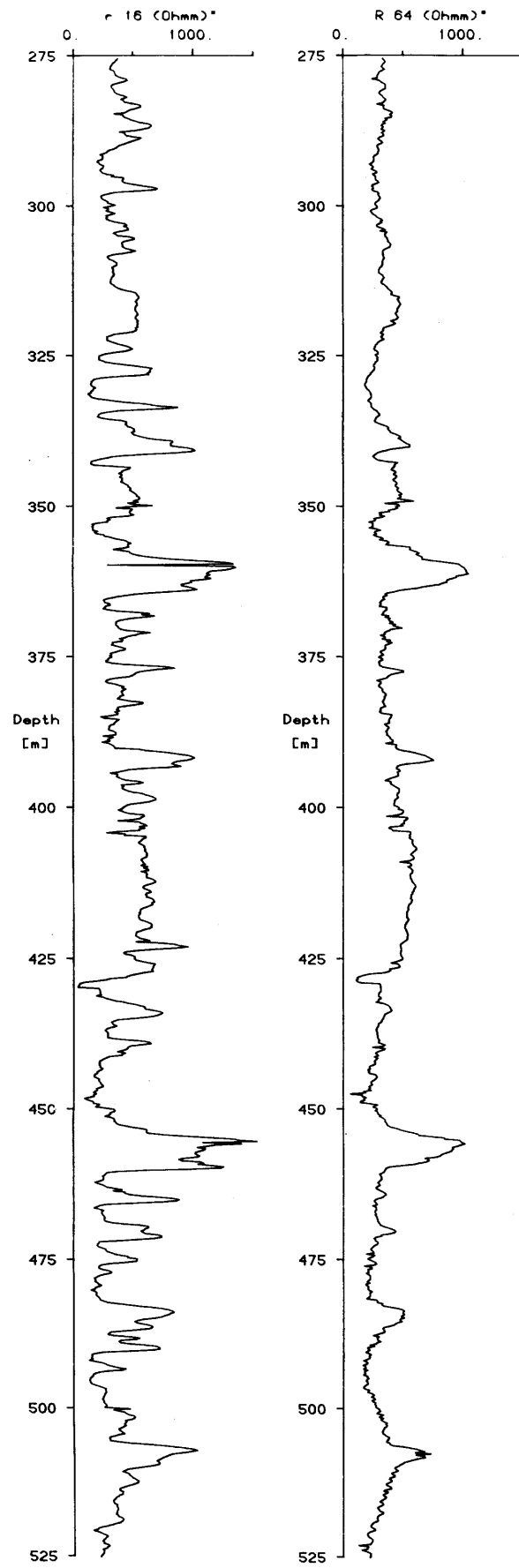


Figure 24. Continue.

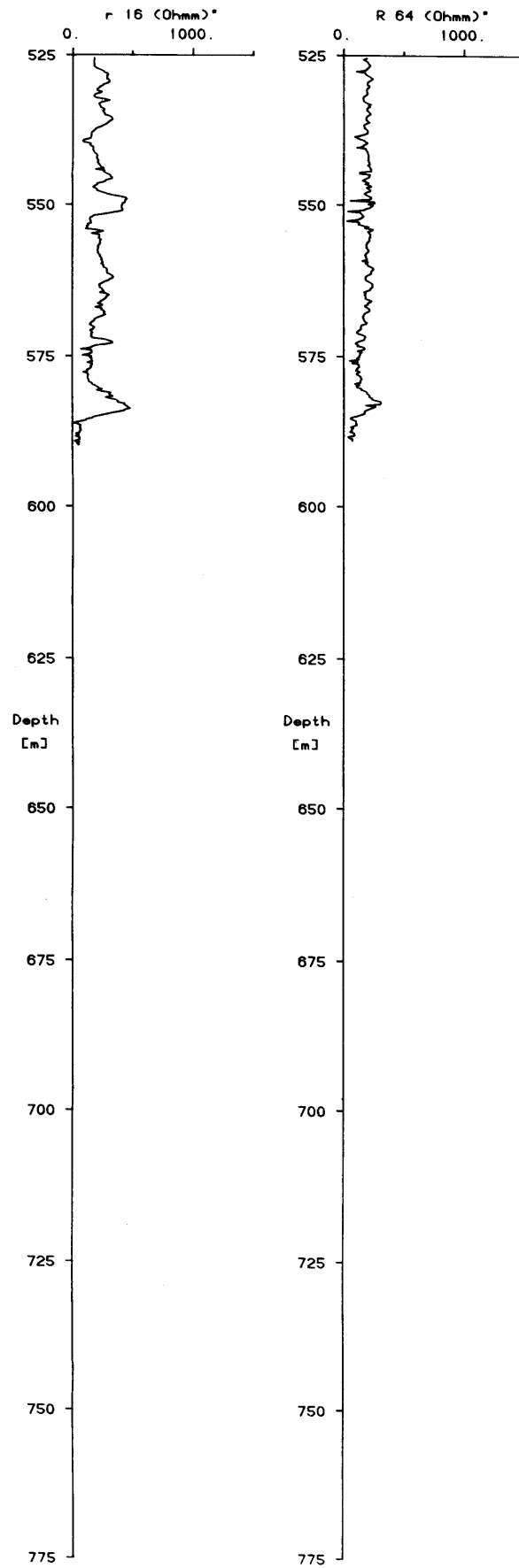


Figure 24. Continue.

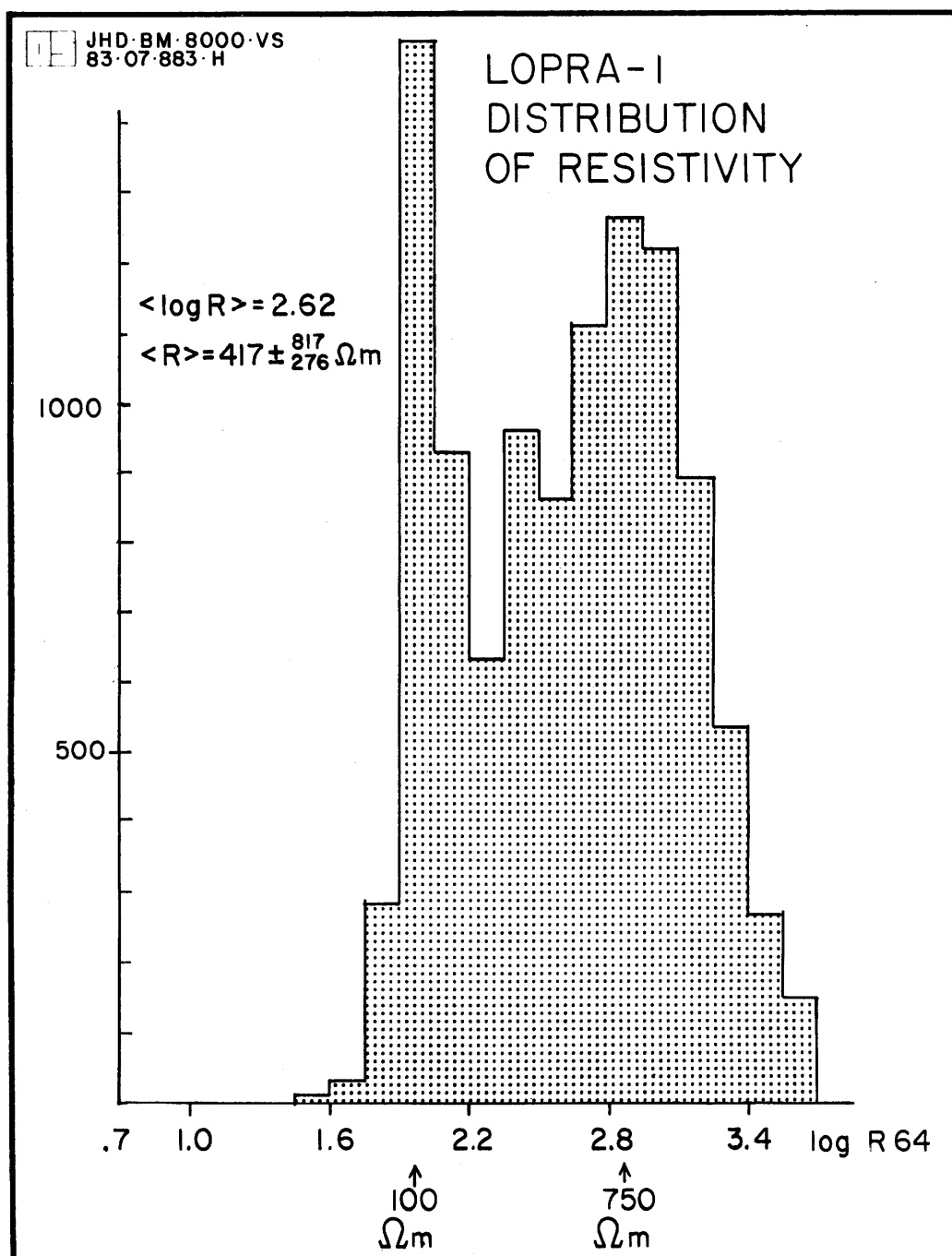


Figure 25. Lopra-1. Log distribution of 64" normal resistivity

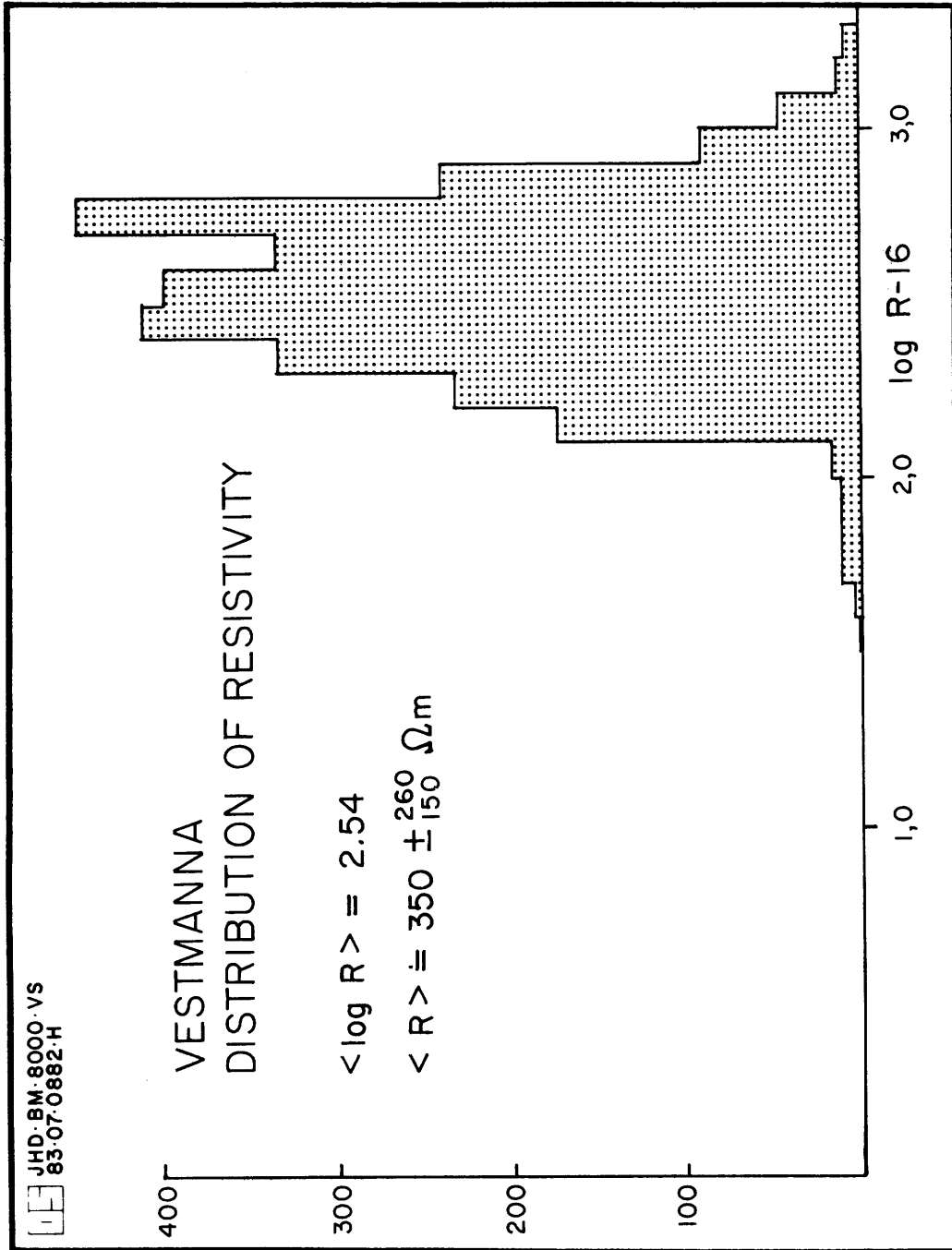


Figure 26. Vestmanna-1. Log distribution of 16" normal resistivity

respectively. R64" is used for Lopra-1 and R16" for Vestmanna-1 as mentioned earlier. In both cases the distributions have two maxima, and reflect the different conditions in the two wells. The narrower peak in fig. 25 represents the low resistivity zones at the contact between the basalt units, whereas the broader high resistivity peak represents the thick flow units at Lopra-1. In the case of Vestmanna-1, however, the thin high resistivity layers form a narrow peak at the upper part of the distribution whereas the bulk of the values is of lower resistivity.

8 RESISTIVITY-POROSITY RELATION

The relation between resistivity and formation porosity has been a subject of interest for many decades. The pioneer work on this subject was done by Archie (1942) who suggested the well-known empirical formula correlating the formation factor and porosity. Archie's formula can be written in the following form;

$$F = \frac{R_f}{R_w} = a \cdot \phi^{-m}$$

where:

F = formation factor

R_f = formation resistivity

R_w = resistivity of fluid

a = constant (usually equal to 1 in sedimentary rocks)

m = cementation factor.

The exponent m (cementation factor) is usually close to 2 for intergranular rocks, but values in the range of 1 - 4 have been reported. It was shown by Brace and Orange (1968) that the exponent m in Archie's formula seems to be 1.0 in the case of fractured crystalline rocks, whereas the value 2.0 seems to be valid for non-fractured rocks (Brace et al. 1965). Results from resistivity and porosity logs in Icelandic basalts have revolved values of m close to 1.0 and Stefánsson et al. (1982) have used a simple lumped double porosity model to estimate the effects of fractures on the resistivity-porosity relationship. The resistivity-porosity relationship in the wells Lopra-1 and Vestmanna-1 have been studied in order to estimate the ratio between fracture porosity to porosity of the formations.

The scatter in the data is considerable, and it was decided to consider 200m sections of the logs separately in order to see the consistency in the data. Figures 27 to 36 show the relation between resistivity and porosity for 200m intervals in the Lopra-1 well. In each 200m interval the exponent m in Archie's formula has been determined and the values are listed in Table 3.

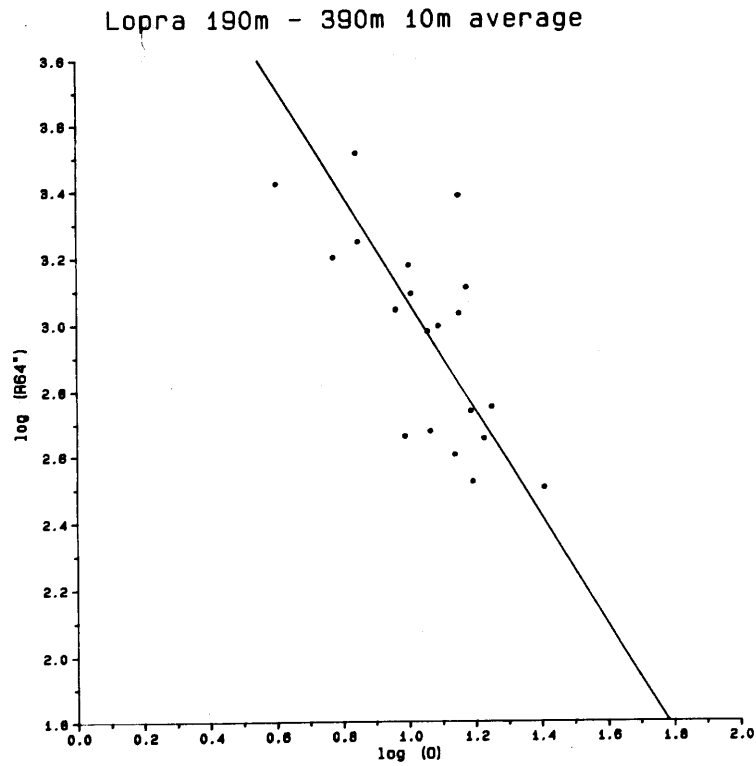


Figure 27. Resistivity-porosity relation for the 190-390m depth interval in Lopra-1

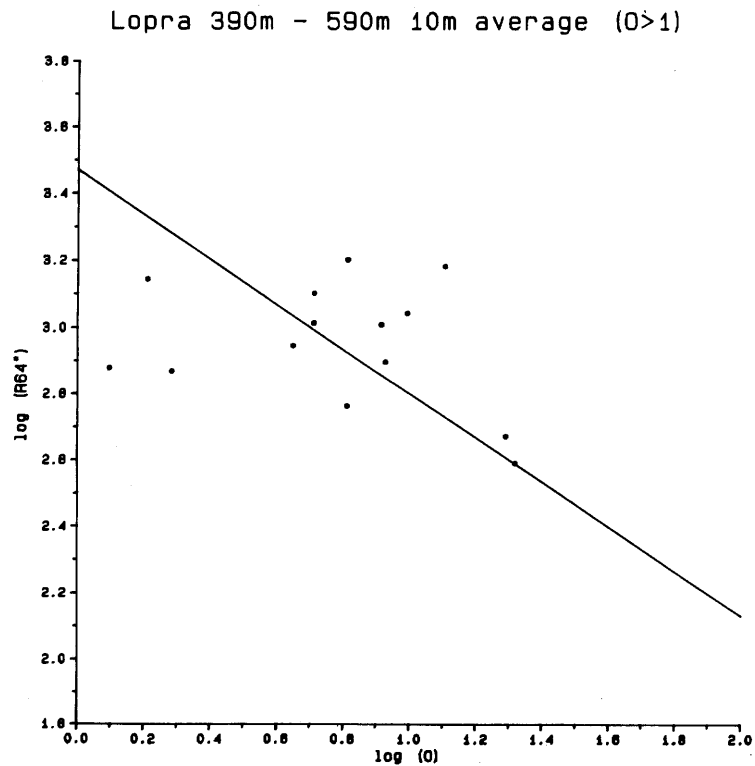


Figure 28. Resistivity-porosity relation for the 390-590m depth interval in Lopra-1

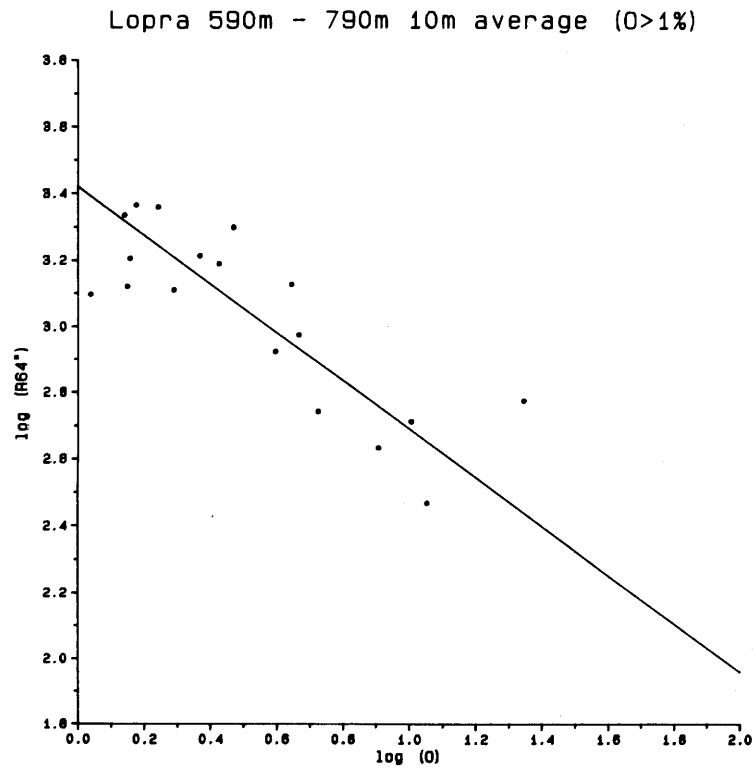


Figure 29. Resistivity-porosity relation for the 590-790m depth interval in Lopra-1

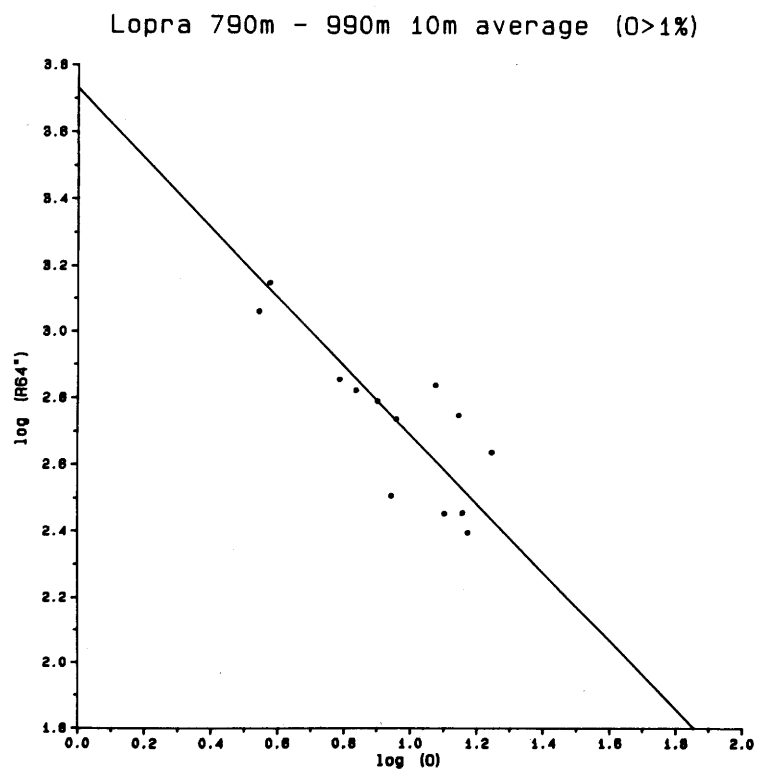


Figure 30. Resistivity-porosity relation for the 790-990m depth interval in Lopra-1

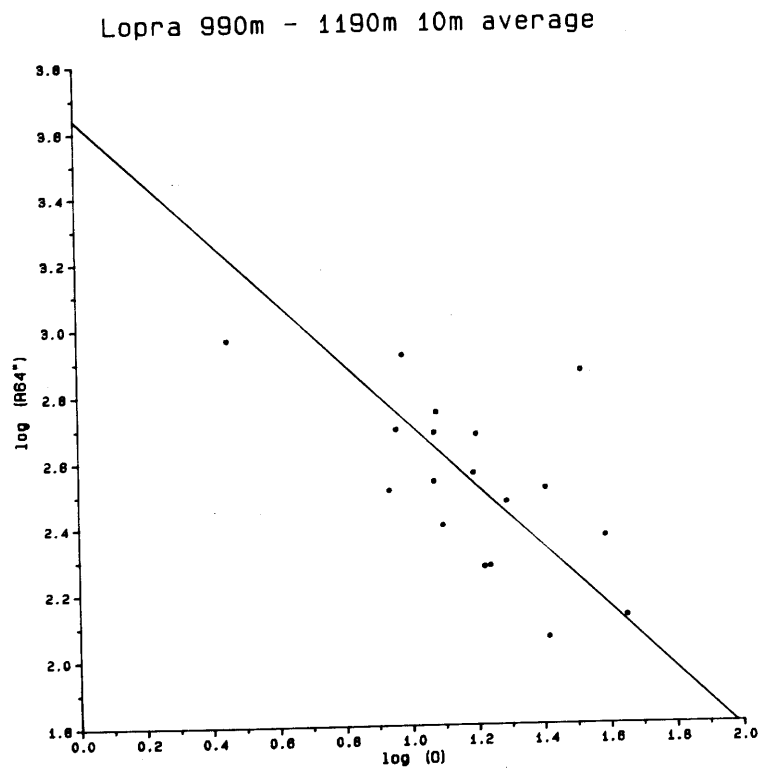


Figure 31. Resistivity-porosity relation for the 990-1190m depth interval in Lopra-1

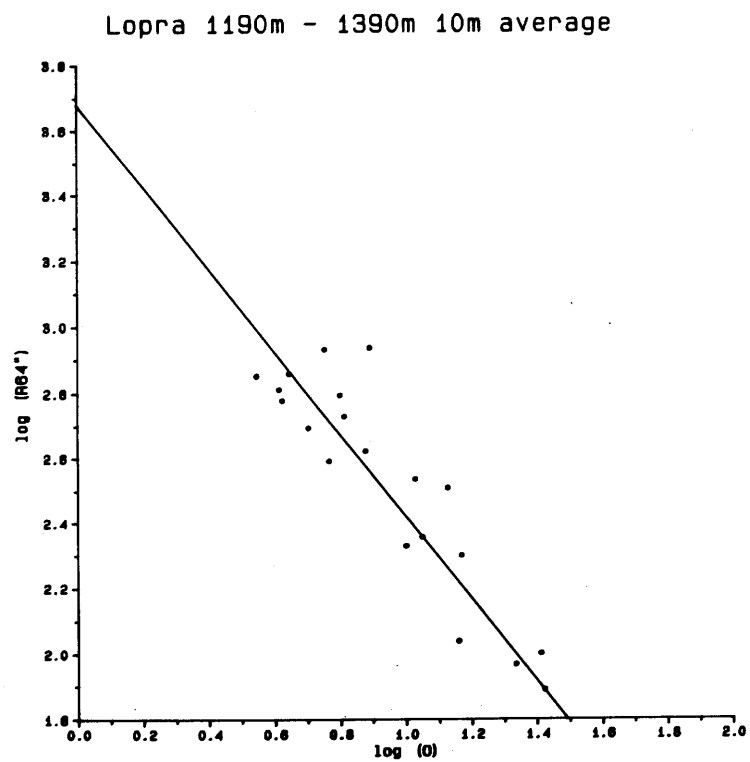


Figure 32. Resistivity-porosity relation for the 1190-1390m depth interval in Lopra-1

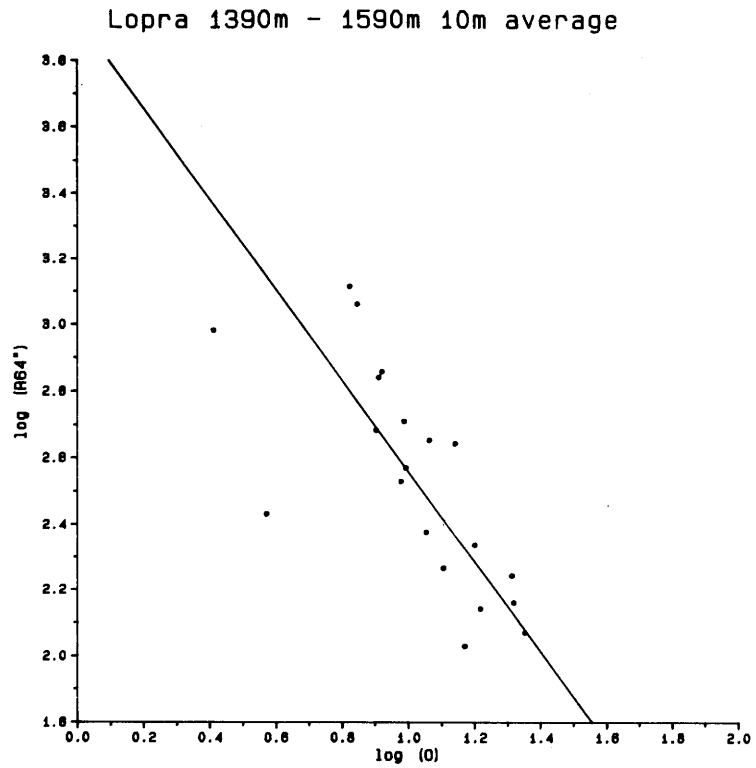


Figure 33. Resistivity-porosity relation for the 1390-1590m depth interval in Lopra-1

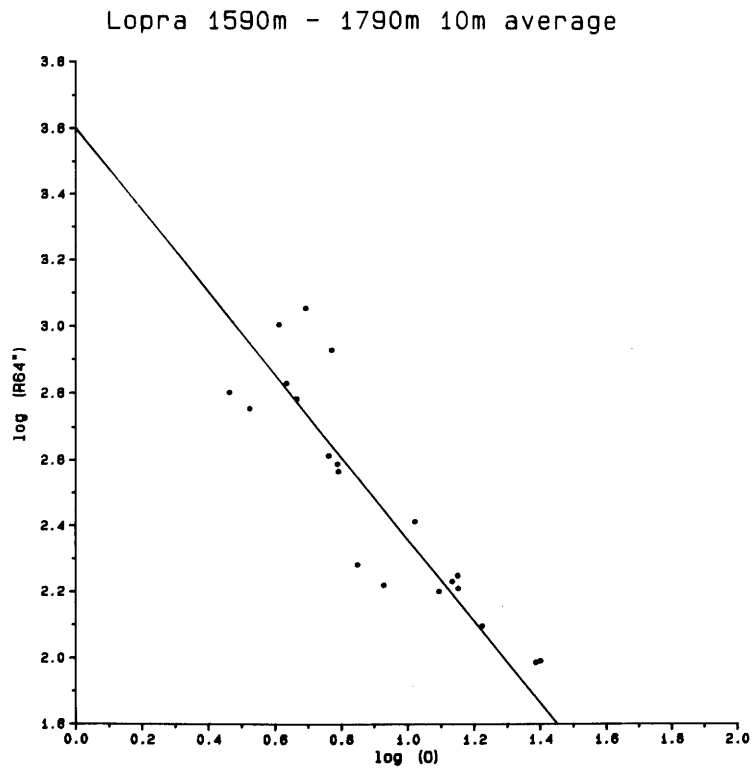


Figure 34. Resistivity-porosity relation for the 1590-1790m depth interval in Lopra-1

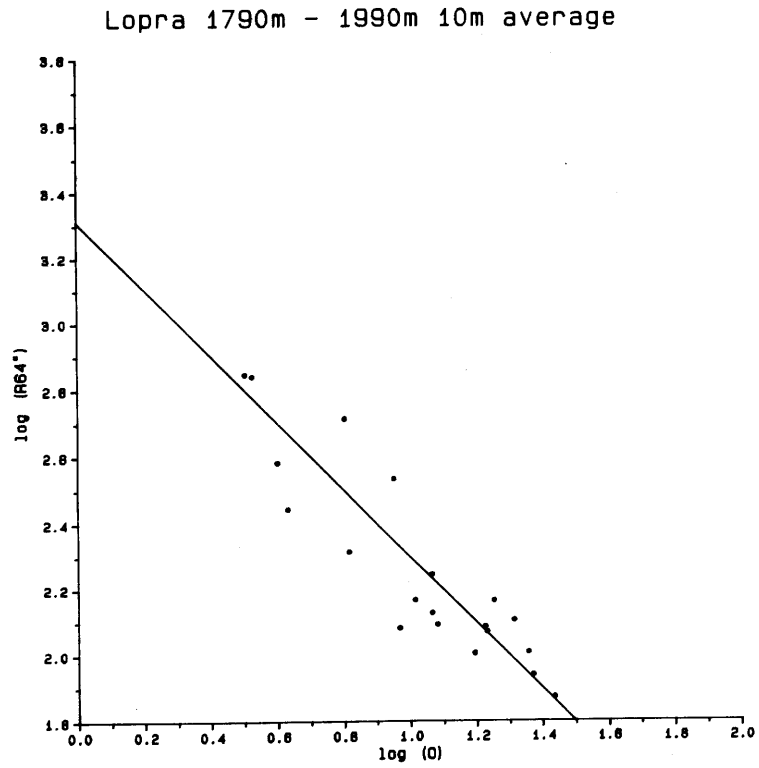


Figure 35. Resistivity-porosity relation for the 1790-1990m depth interval in Lopra-1

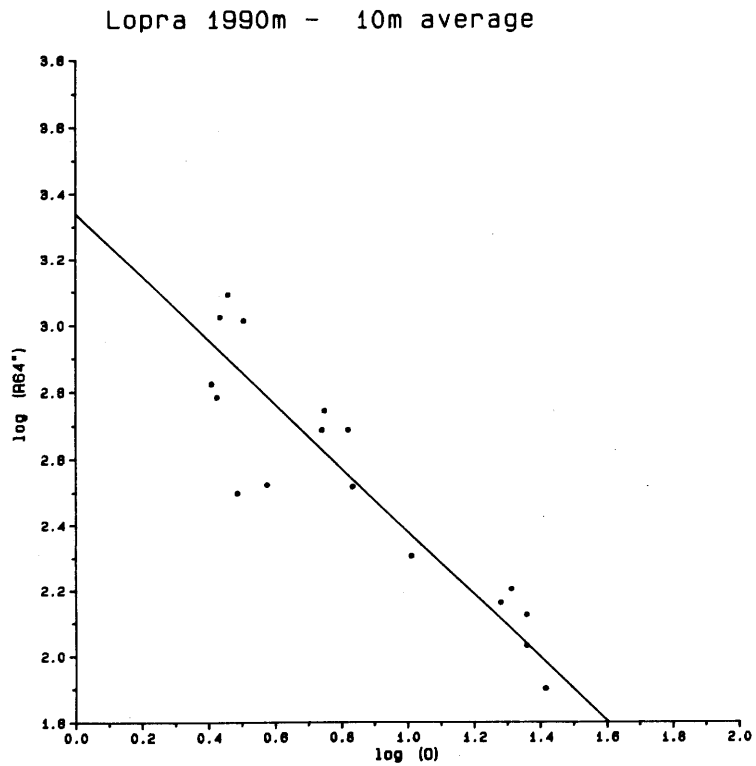


Figure 36. Resistivity-porosity relation for the 1990-2170m depth interval in Lopra-1

TABLE 3

Coefficients in Archie's formula for resistivity-porosity
cross-plots for Lopra-1

Depth Interval (m)	Exponent	a*R _w (Ω m)	Correlation Coefficient
190-390	(-1.62)	(490)	-0.70
390-590	-0.67	29.5	-0.30
590-790	-0.73	26.3	-0.82
790-990	-1.04	53.7	-0.81
990-1190	-0.93	43.6	-0.60
1190-1390	-1.26	47.8	-0.91
1390-1590	-1.37	85.1	-0.71
1590-1790	-1.24	39.8	-0.90
1790-1990	-1.01	20.4	-0.90
1990-2170	-0.96	21.9	-0.91
190-2170	-1.16	51.3	-0.67
Average			
190-2170	-1.02	41	-0.76
	+/-0.24	+/-21	

Figure 37 shows the resistivity-porosity relation for the whole well at Lopra. The average value for the exponent $\langle m \rangle$ is found to be;

$$\langle m \rangle = -1.02 \pm 0.24$$

and the average value for a*R_w is;

$$\langle a \cdot R_w \rangle = (41 \pm 21) \text{ m}$$

According to recent determination of the resistivity of the fluid in the Lopra-1 well (Peder Hedeboel Nielsen personal communication) the resistivity is;

$$R_w = 6.25 \text{ } \Omega\text{m}$$

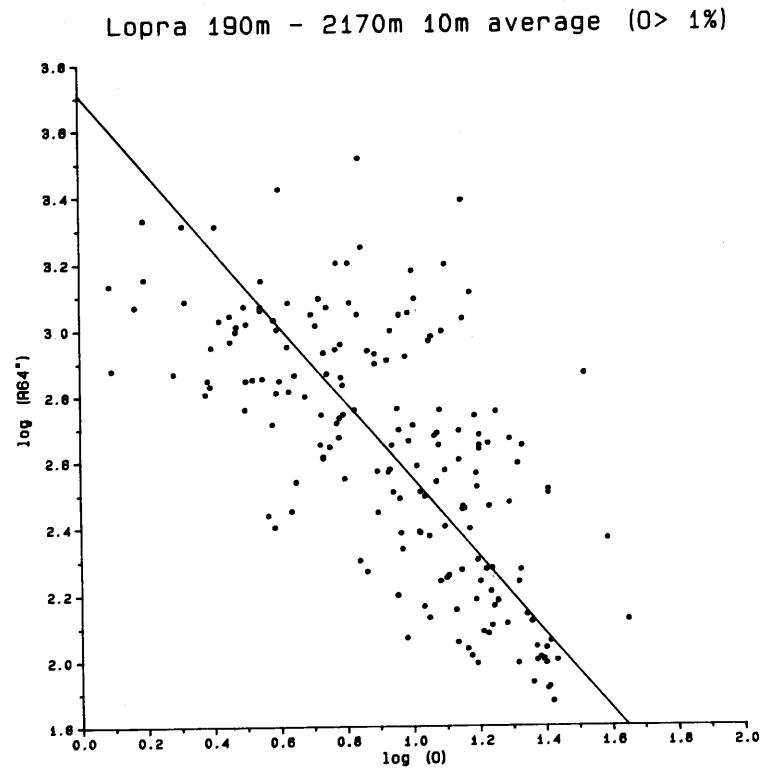


Figure 37. Resistivity-porosity relation for the 190-2170m depth interval in Lopra-1

This value gives the constant a in Archie's formula as;

$$a = 6.6 \pm 3.4$$

In order to calculate the expected ratio between fracture porosity and total porosity, the formation factor is needed. Time did not allow recalculation of the resistivity data after the information on R_w was obtained. That work is scheduled for the final report. From the average value for $\langle m \rangle = (1.02 \pm 0.24)$ it can be concluded at this stage that fracture porosity is of considerable importance in the lava pile penetrated by the Lopra-1 well.

The resistivity-porosity relation in the Vestmanna-1 is treated in a similar way. Figures 38 to 40 show the resistivity-porosity relation for 200m intervals in Vestmanna-1. The coefficients in Archie's formula as determined in figs. 38 to 40 are listed in Table 4. All the data is plotted on fig. 41 and the average values for the whole well are found to be;

$$\langle m \rangle = -1.13 \pm 0.17$$

$$\langle a \cdot R_w \rangle = (56 \pm 23) \text{ m}$$

According to recent determination the resistivity of the fluid in the well is (Peder Hedebol Nielsen personal communication);

$$R_w = 32 \Omega m$$

this implies that the constant a in Archie's formula;

$$a = 1.6 \pm 0.7$$

The presentation of the ratio between fracture porosity and total porosity for Lopra-1 has to wait for recalculation of the resistivity data where the knowledge of R_w is taken into consideration. The values obtained so far, especially the value for $\langle m \rangle$ indicate clearly that fracture porosity is of considerable importance.

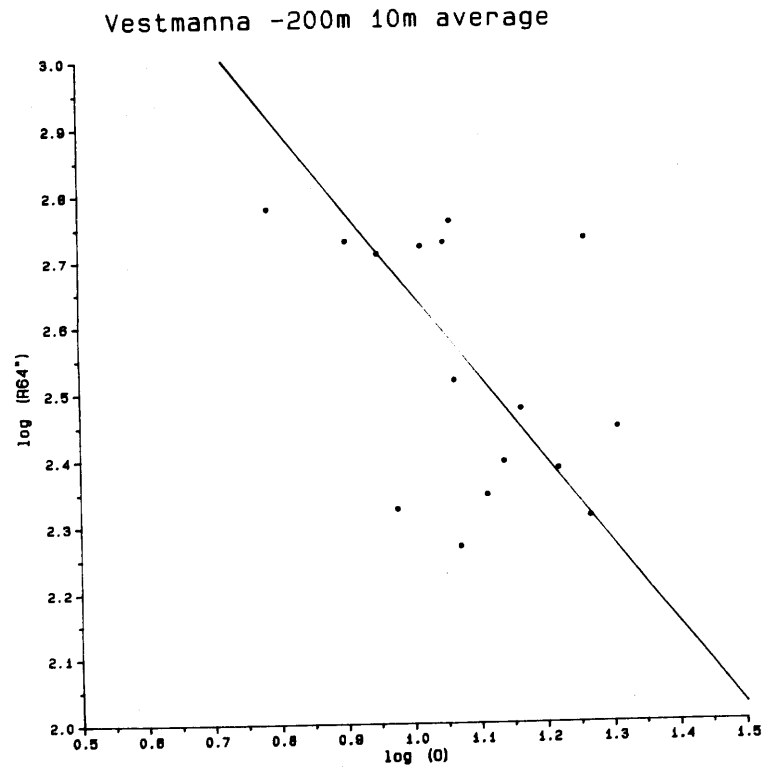


Figure 38. Resistivity-porosity relation for the 0-200m depth interval in Vestmanna-1

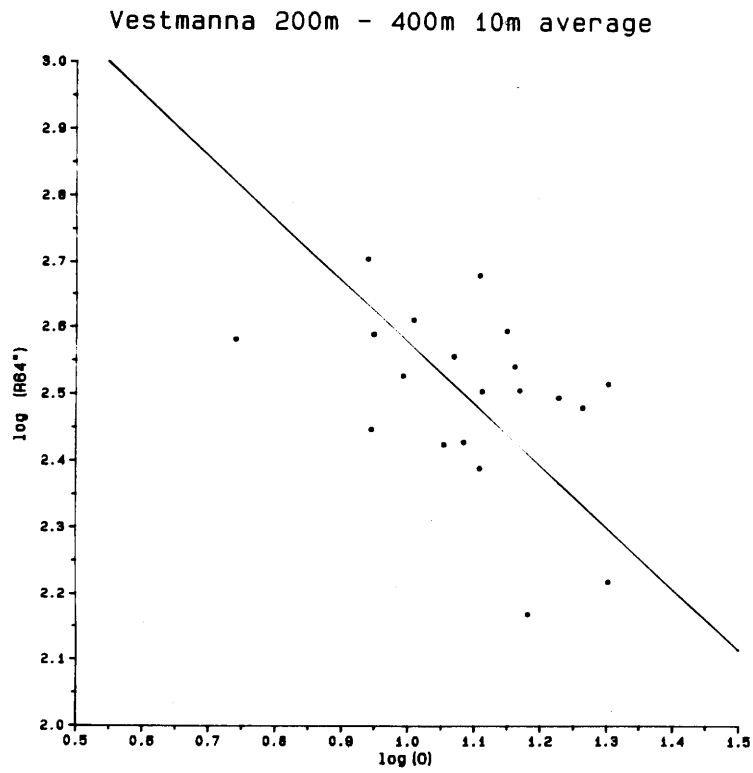


Figure 39. Resistivity-porosity relation for the 200-400m depth interval in Vestmanna-1

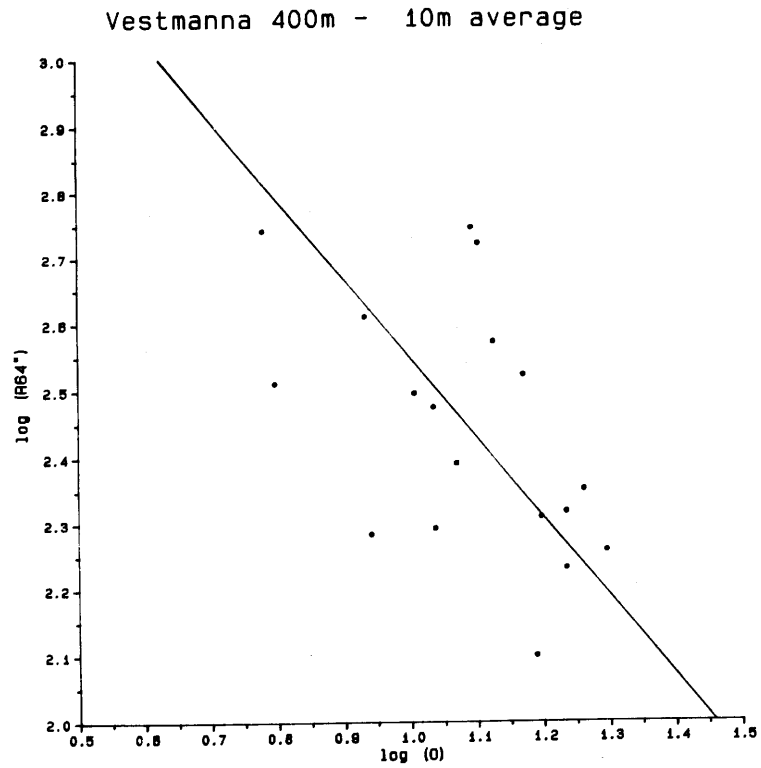


Figure 40. Resistivity-porosity relation for the 400-600m depth interval in Vestmanna-1

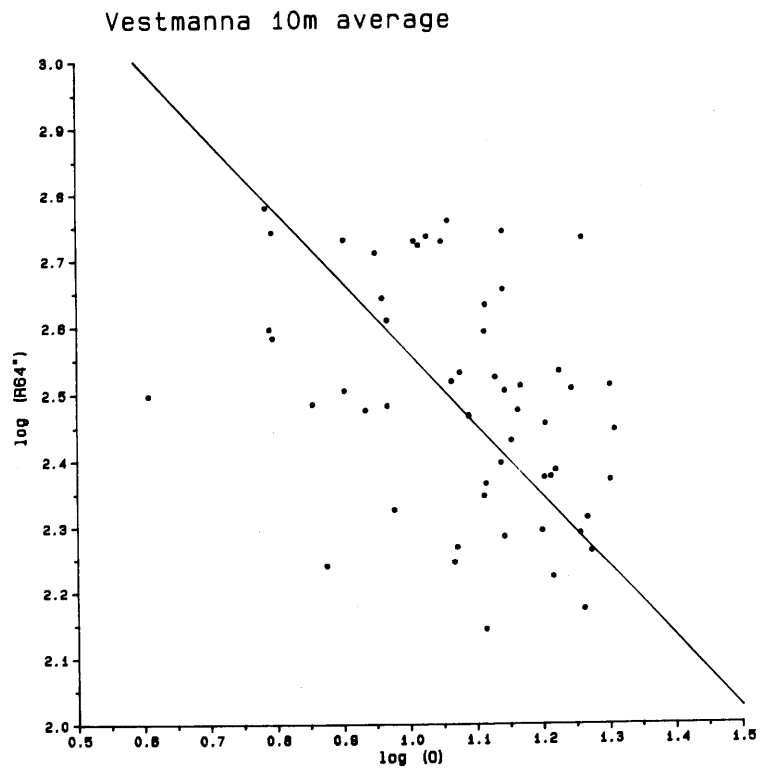


Figure 41. Resistivity-porosity relation for the 0-600m depth interval in Vestmanna-1

TABLE 4

Coefficients in Archie's formula for resistivity-porosity
cross-plots in Vestmanna-1.

Depth interval (m)	Exponent	$a \cdot R_w$ (Ωm)	Correlation Coefficients
0-200	-1.25	79	-0.48
200-400	-0.93	32	-0.44
400-600	-1.20	56	-0.51
Average			
0-600	-1.13	56	-0.47
	+/-0.17	+/-23	

9 NATURAL GAMMA RAY

The relation between the gamma ray intensity and the SiO_2 content of Icelandic rocks has been studied by Stefánsson and Emmerman (1980) and by Stefánsson et al. (1982). It is found that for the tholeiitic trend there is a linear relation between the gamma ray intensity and the SiO_2 content of the rocks. For crystalline rocks, the empirical relation:

$$\text{SiO}_2 = 0.264 * I_o + 40.6\%$$

has been found applicable in many locations in Iceland. Here SiO_2 is in per cent and I_o is the gamma ray intensity in API gamma ray units corrected for the well diameter.

Local variations as well as a shift between tholeiite and mild alkalic trend is observed in the relation between SiO_2 and the gamma ray intensity in Iceland. However, as the variation in the gamma ray intensity in the wells in the Faeroes is very small, and the rocks there are known to be tholeiite it was considered worthwhile to apply the Icelandic calibration curve for tholeiite on the gamma ray logs in Lopra-1 and Vestmanna-1.

The result from Lopra-1 is shown in fig. 42, where the SiO_2 in per cent is drawn versus depth. The small narrow peaks in this log are all associated with thin sedimentary layers between the lava flows. The increased gamma ray intensity in the sediments is partly caused by induced gamma activity from the neutron source. One of the major objectives for the drilling in Lopra was the investigation of deep sediments. The procedure of logging in the downward direction and therefore inducing gamma ray activity in the sediments was therefore appropriate in order to use the gamma ray log for pinpointing the sediments. The distribution of the SiO_2 content in Lopra-1 is shown in fig. 43. The distribution is rather narrow and shows only one peak. The average SiO_2 content is $(49 \pm 3)\%$ and reflects the basaltic nature of the rocks at Lopra.

Laboratory measurements of the SiO_2 contents of lavas and intrusions at Lopra-1 give results in the range from 46.99% to 48.43% (Waagstein et al., 1982) which is in good agreement with the results of the gamma ray log.

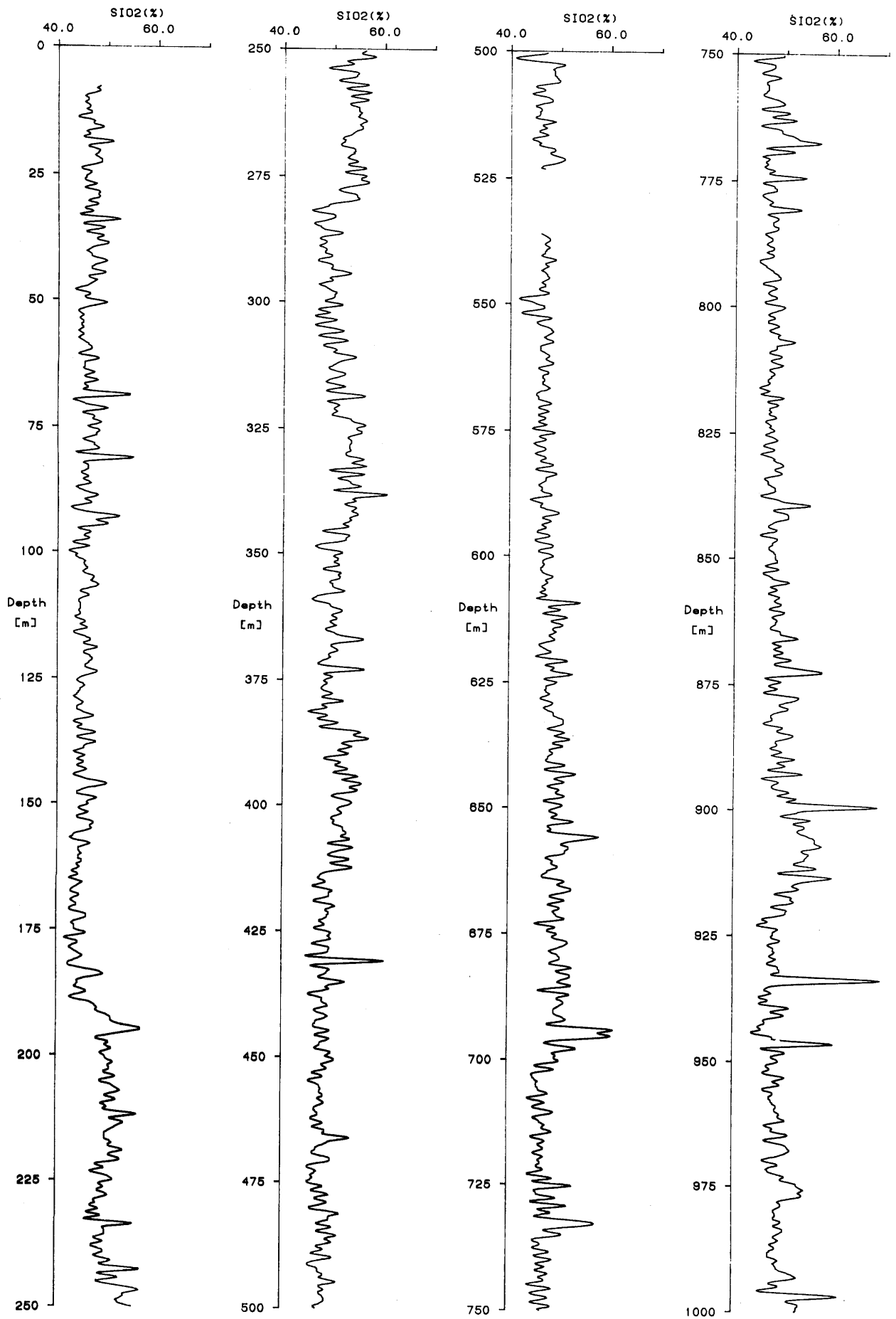


Figure 42. Silica content as a function of depth in Lopra-1

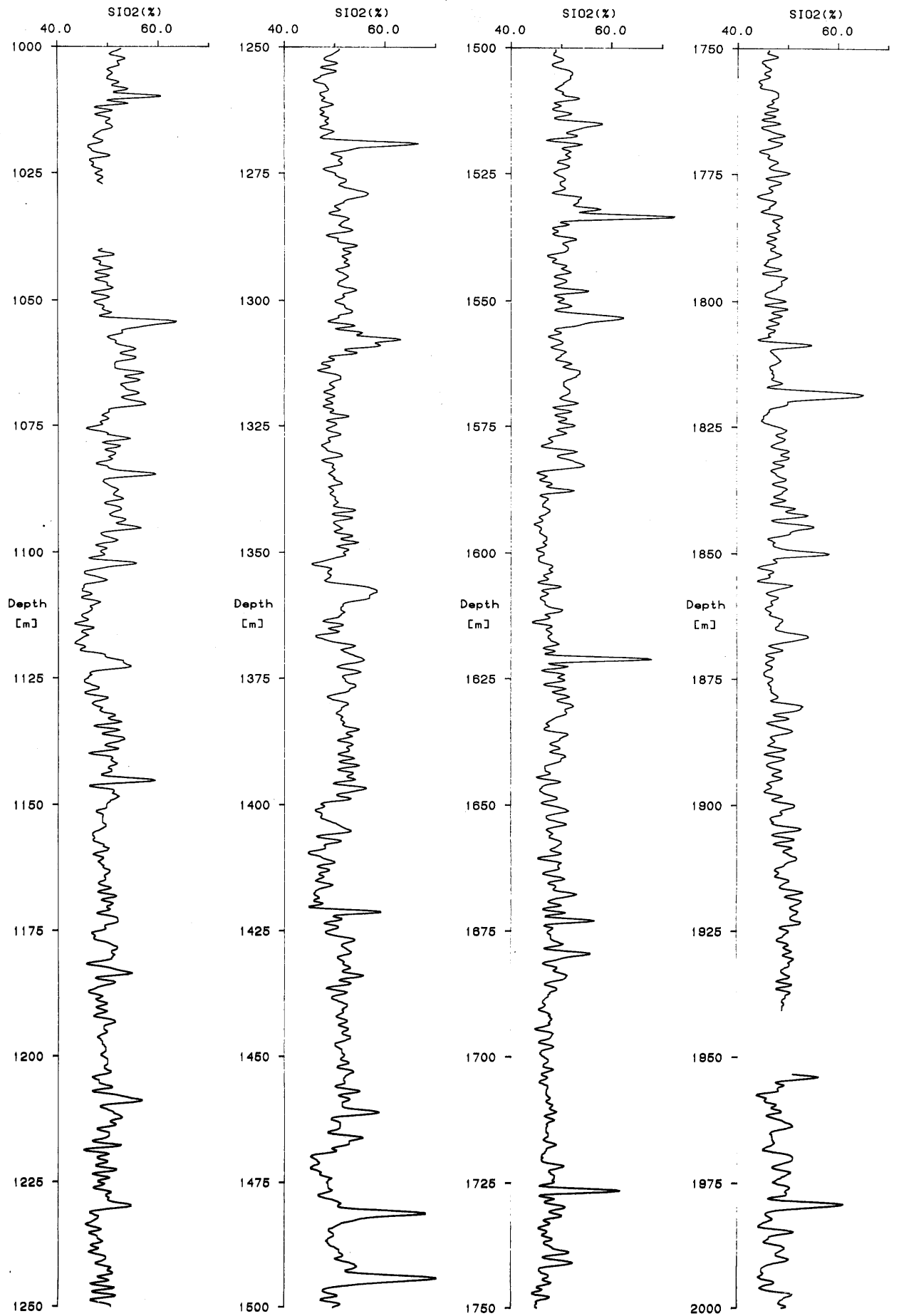


Figure 42. Continue.

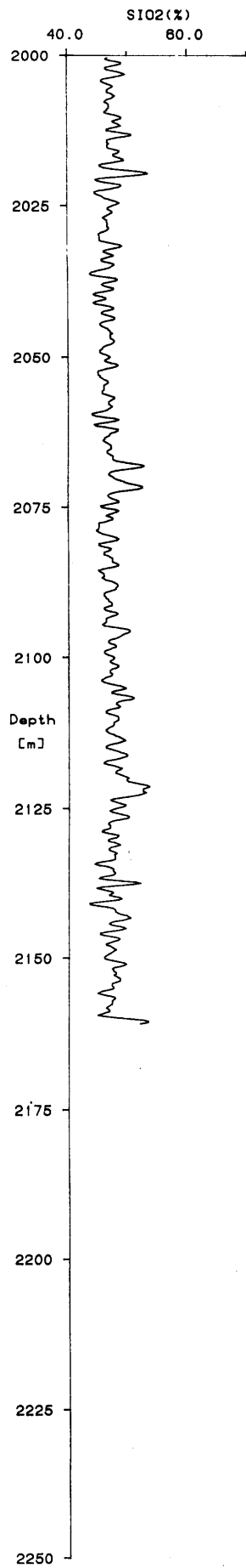


Figure 42. Continue.

Lopra I SiO₂ content distribution

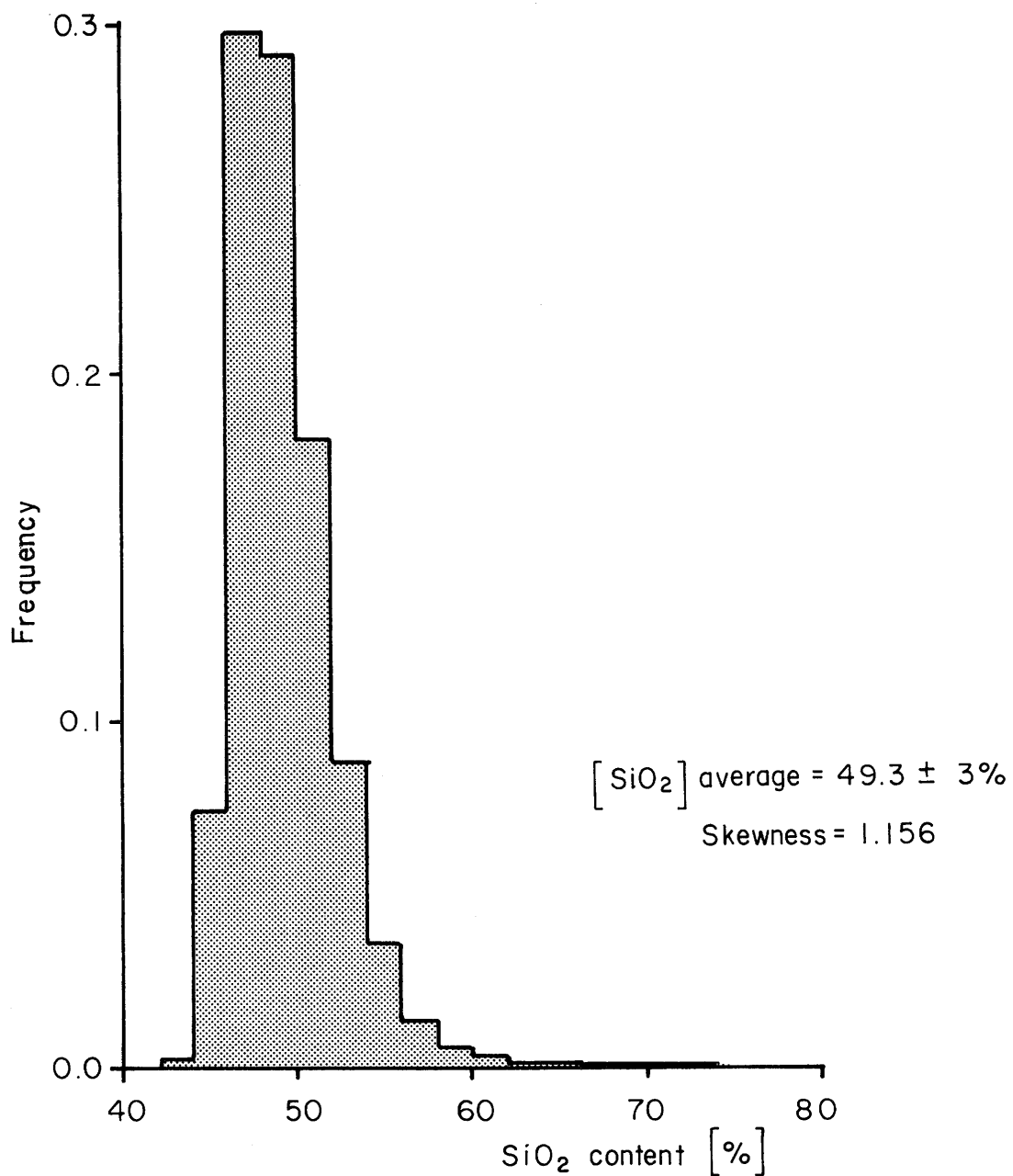


Figure 43. Distribution of silica concentration of the rocks in Lopra-1

Digital registration of natural gamma ray log in Vestmanna-1 was not successful, but analog registration is available. Almost no changes in the natural gamma ray is observed, so digitization of the analog data is not considered worthwhile. From the analog data we obtained a mean value for Vestmanna-1 to be;

$$\langle \text{GR} \rangle = 19 \text{ API GU}$$

and with well-size correction;

$$\langle \text{GR} \rangle = 20.3 \text{ API GU}$$

Applying the empirical formula from Iceland we obtained the value;

$$\langle \text{SiO}_2 \rangle = 46\%$$

as a mean value for the silica concentration of the basaltic pile in Vestmanna-1.

Finally, it should be noted that the method of using calibration curves obtained from Icelandic rocks on rocks in Lopra could easily cause some shift in the absolute value of the SiO_2 content, but the relative distribution should not be much affected. The good agreement between laboratory data and the logs indicate, however, that the results shown in figs. 42 and 43 are reasonably reliable.

10 SEDIMENTS

Considerable effort has been made in order to identify the sediments from the geophysical logs in Lopra-1. The parameters used for this purpose are porosity and natural gamma. The small induced peaks in the gamma ray log were intended to map the locations of sediments in Lopra-1 as mentioned earlier. In order to suppress the noise in the gamma ray log an attempt was made to correlate the porosity log with the SiO_2 log. Figure 44 shows a conventional cross-plot of natural gamma ray versus porosity. No unambiguous separation of sediments can be deduced from this figure. Therefore, another method was applied. The quantity $(\text{SiO}_2 - 42) * \phi / 2$ was calculated as a function of depth. This log is shown in fig. 45. By using this expression the weight of the porosity and natural gamma ray becomes approximately the same in the product. The aim of this method is to amplify the zones in the well where porosity is high and where the gamma ray intensity is simultaneously high. Pronounced peaks are seen in fig. 45 but it is not obvious where the limit between sediments and other rock is. In order to determine this limit the frequency distribution of the product $(\text{SiO}_2 - 42) * \phi / 2$ is studied. Figure 46 shows the upper part of this distribution. A pronounced tail is observed in this distribution. By assuming that this tail represents the sediments in the pile, a limit can be introduced in fig. 45 in order to select the sediments from the remaining part of the pile. The limit of 160 is shown in fig. 45 and the location and thickness of the interpreted "sediments" can be read directly from fig. 45. The total thickness of the sediments as determined by this method is 46 m, which is slightly higher than the value of 35-40m reported by Waagstein et al. (1982). In this connection we like to point out that the determination of sediment thickness reported here is an independent method, based entirely on the data from the geophysical logs.

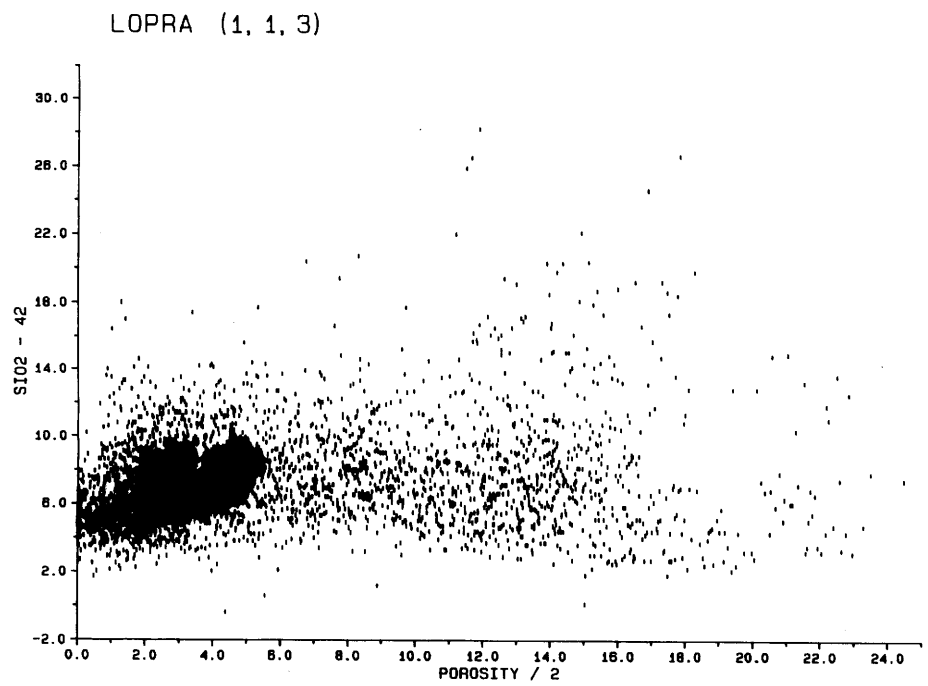


Figure 44. Natural gamma ray-porosity cross-plot for Lopra-1

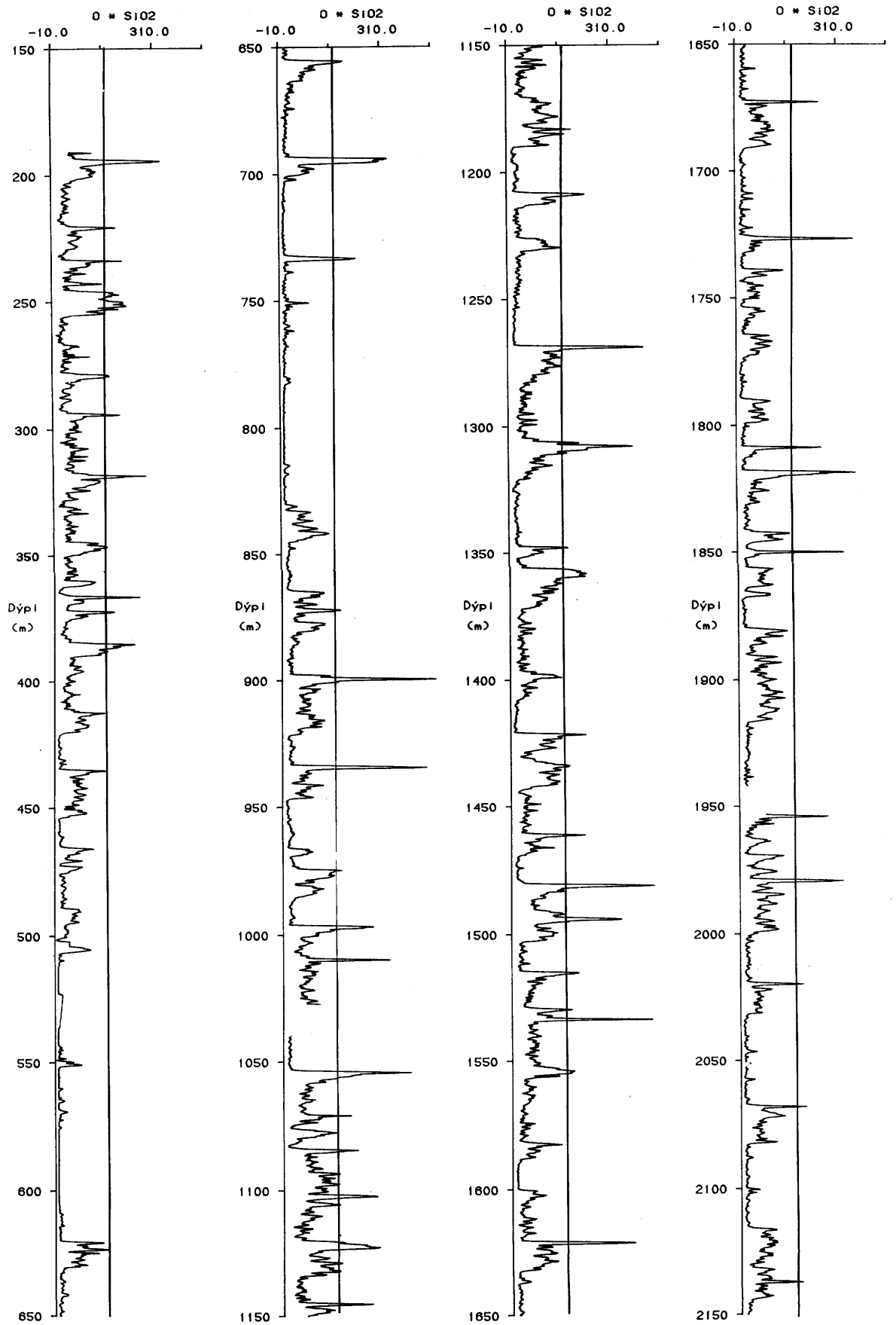


Figure 45. The quantity $(\text{SiO}_2-42) \cdot 0/2$ as a function of depth for Lopra-1



JHD-JED-9000 VS
83.08.0904AA

PART OF THE $\left[\frac{\phi}{2}\right] * [\text{SiO}_2 - 42]$
FREQUENCY DISTRIBUTION IN LOPRA-1

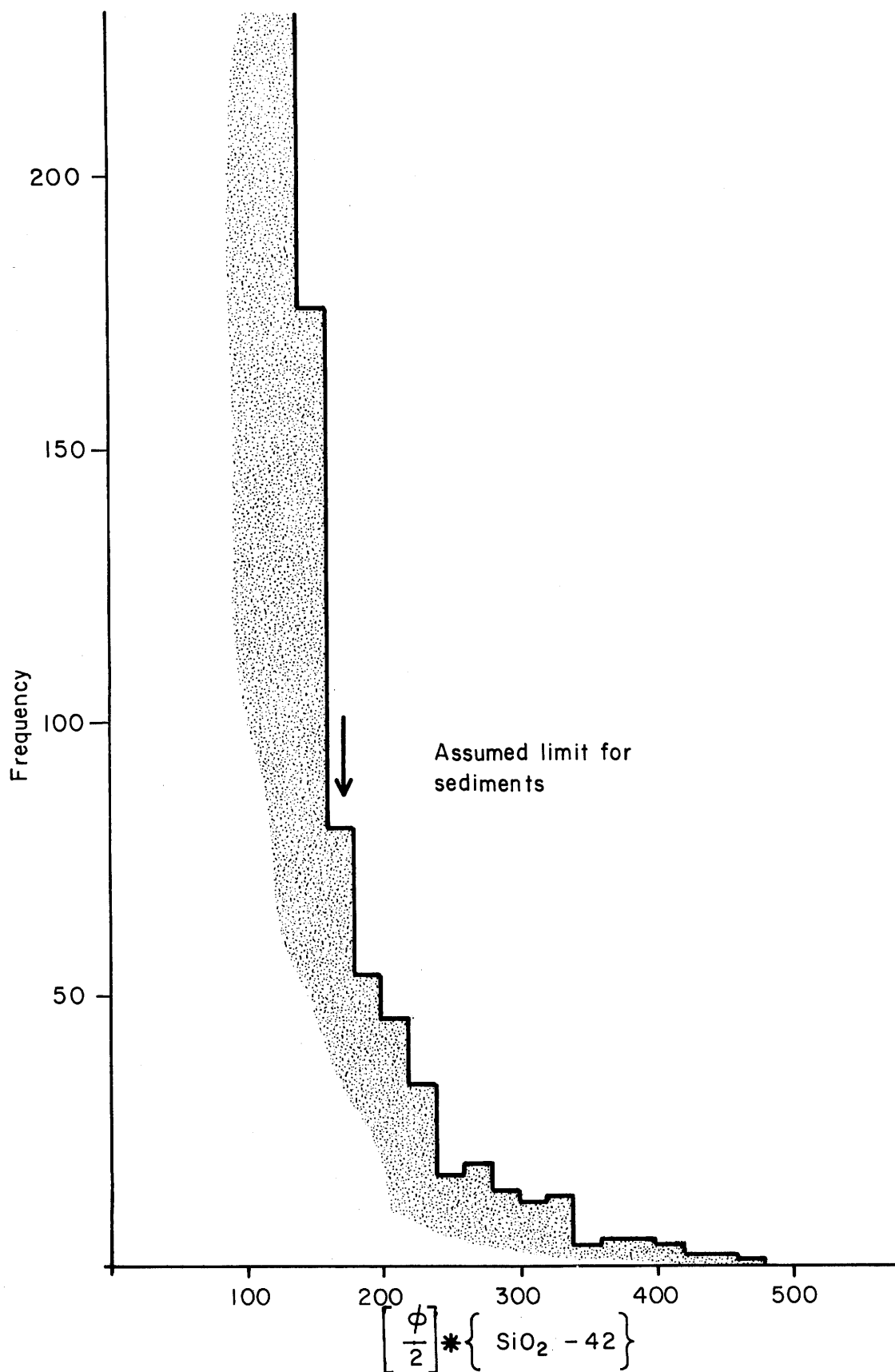


Figure 46. Upper part of the frequency distribution of $(\text{SiO}_2 - 42) * 0/2$ in Lopra-1

11 SONIC VELOCITY

Several difficulties have been encountered in the treatment of the sonic data from Lopra-1. At present there are several problems, which have not been solved satisfactorily. These obstacles include;

- . well size correction
- . calibration
- . cycle skipping.

The reason for these difficulties is partly due to the fact that the logging tool used is a cement bond tool which is not primarily designed for measurements of sonic velocity. The sonic log in Lopra-1 is therefore more considered as an experiment in order to see if useful information on sonic velocity can be deduced from the records of such a tool. The most likely velocity distribution at this time is presented as a function of depth in fig. 47. In this picture a new calibration has been applied and those zones have been omitted where cycle skipping disturbed the records. Further work will be devoted to this subject in order to obtain more satisfactory picture of the sonic velocity in Lopra-1.

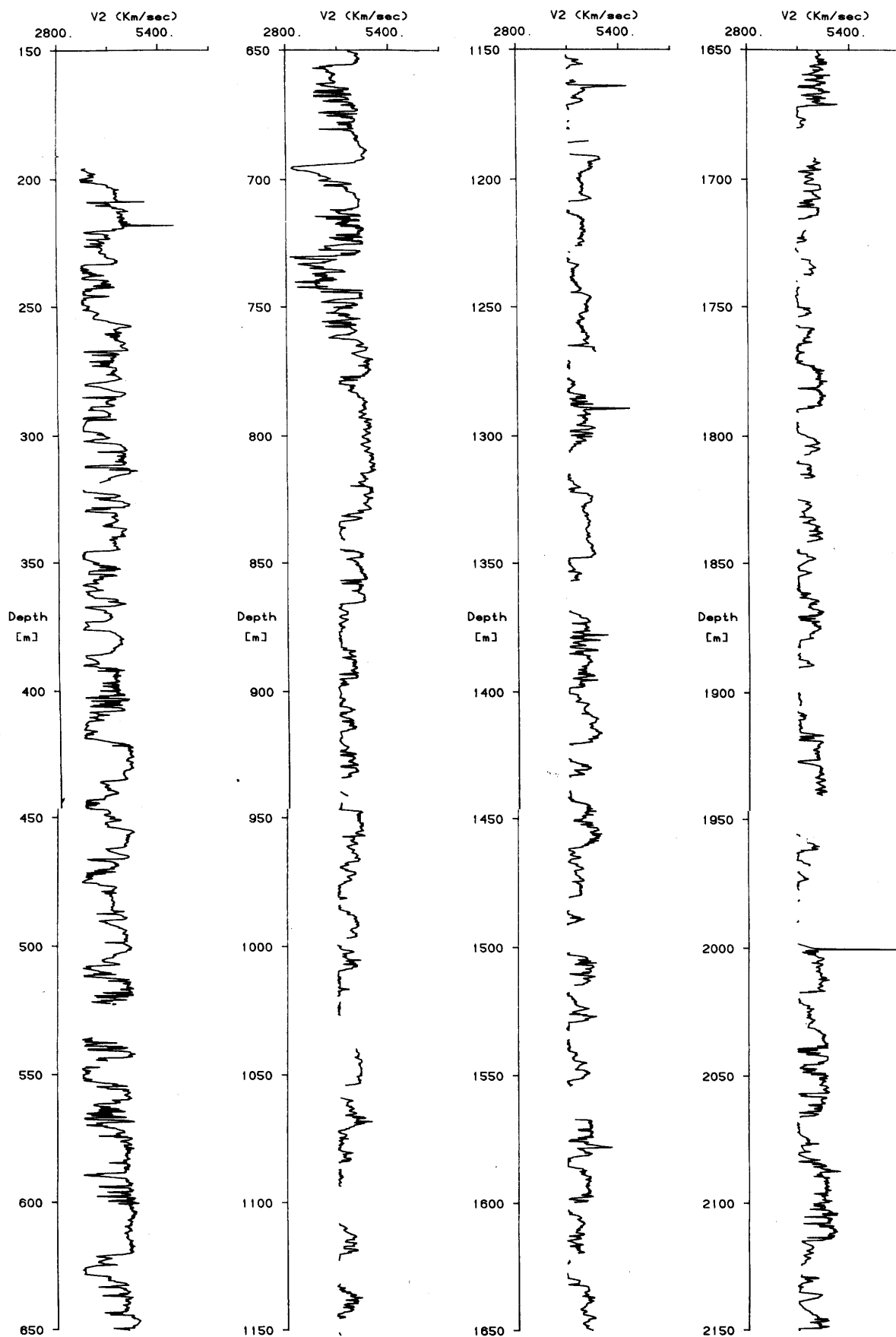


Figure 47. Sonic velocity as a function of depth in Lopra-1

12 LARGE SCALE VARIATIONS

Geophysical logs are a convenient investigation method to detect detailed changes in the lithological stratigraphy. They can, however, also be used to map large scale structure of the formation pile penetrated by the borehole.

In order to visualize the large scale structure of the geological pile, the logs can be filtered by low pass filters or other similar statistical treatments. Figure 48 shows the 100m running average of the natural gamma ray log in Lopra-1. Quite pronounced zones of the gamma ray intensity can be seen in this figure.

In figs. 49 and 50 are similar 100m and 50m running averages for the 64" normal resistivity logs in Lopra-1. The most pronounced zones in these figures are the dolerite intrusions at 500-600m and 750-850m depths. A third zone with high resistivity is found approximately between the depth of 250 to 350m. Analysis of cuttings from these depths (Waagstein et al. 1982) do not indicate intrusions. The 100m and 50m running average of the porosity log in Lopra-1 are shown in figs. 51 and 52. The main zonation of these figures are the low porosity zones at the intrusions (500-600m and 750-850m) as well as a high porosity zone at approximately 1050-1150m depth. Furthermore, the high resistivity zone at 250-350m depth does not show up in the porosity log which is in agreement with that the basalt at this depth being lava flows.

The 3km thick basaltic pile of the Faeroe Islands can be divided into three stratigraphic series (Rasmussen and Noe-Nygaard 1969, 1970). In this pile exposed on the surface two definite geochemical groups are distinguished (Garepy et al. 1983).

It is noteworthy that even if the lower and middle basaltic series can not be distinguished chemically by the REE, some interesting correlation between these elements are obvious. Figure 53 shows the relation between thorium and zirconium as reported by Garepy et al. (1983). A clear positive correlation is found.

The large scale variation in the natural gamma ray intensity can reflect the changes in the chemical composition of the pile (Jonsson and Stefánsson, 1982, Stefánsson, 1982). By comparing the long scale

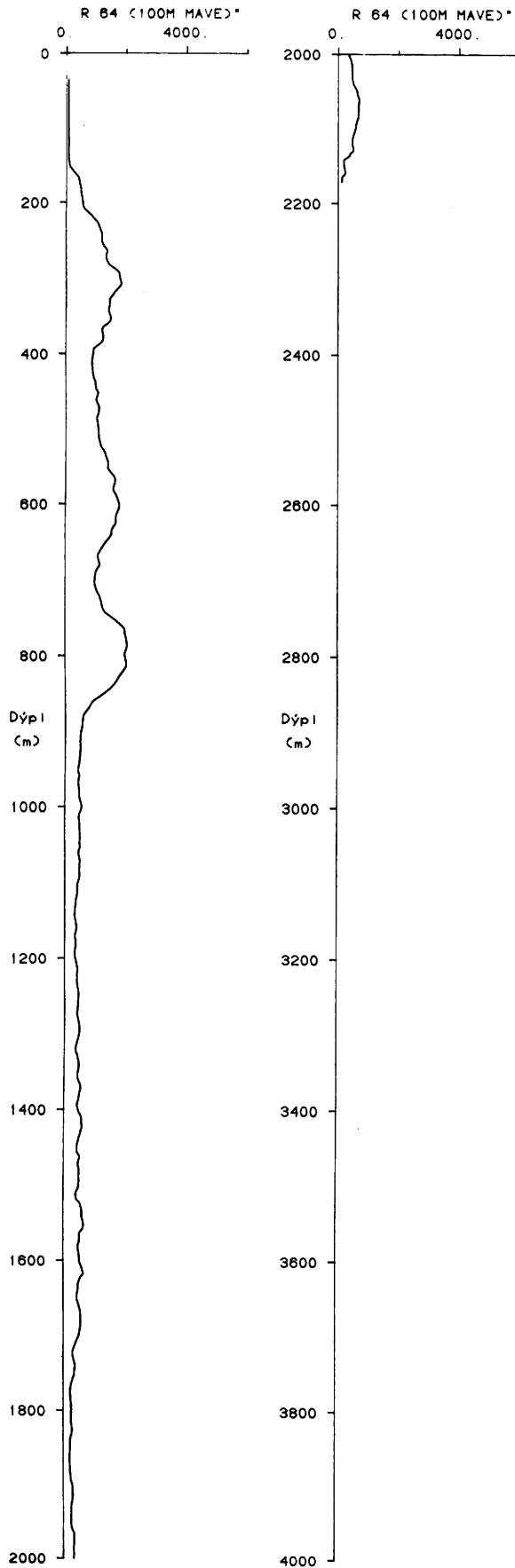


Figure 49. 100m running average of the 64" normal resistivity log in Lopra-1

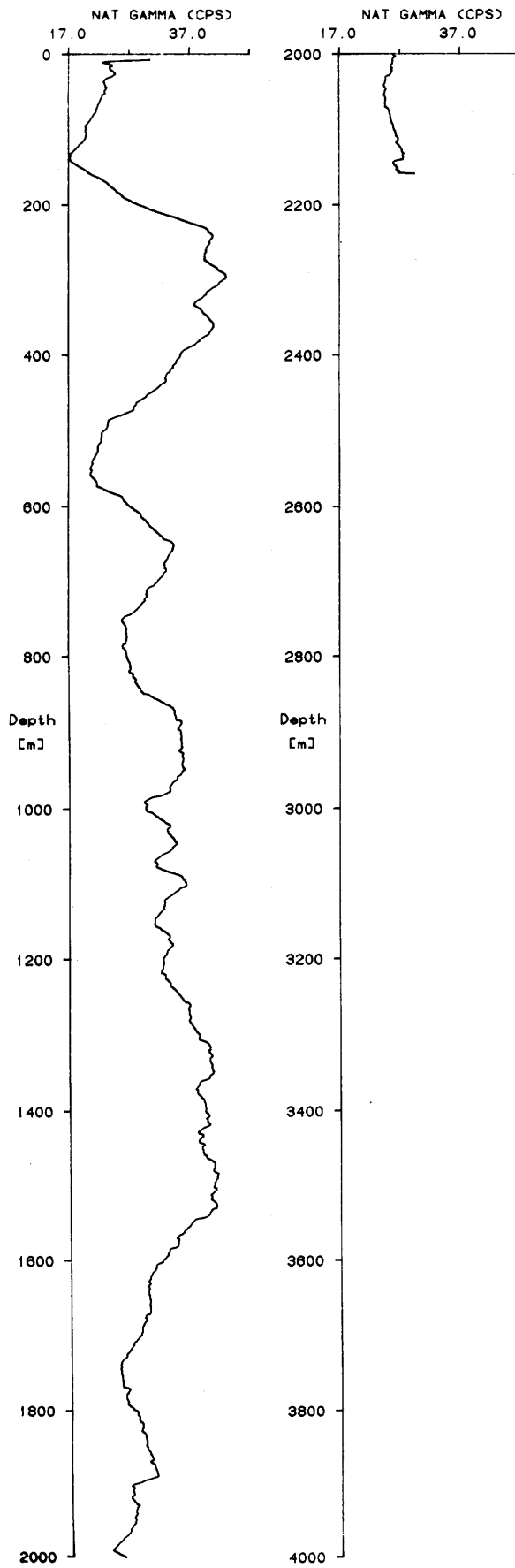


Figure 48. 100m running average of the natural gamma ray log in Lopra-1

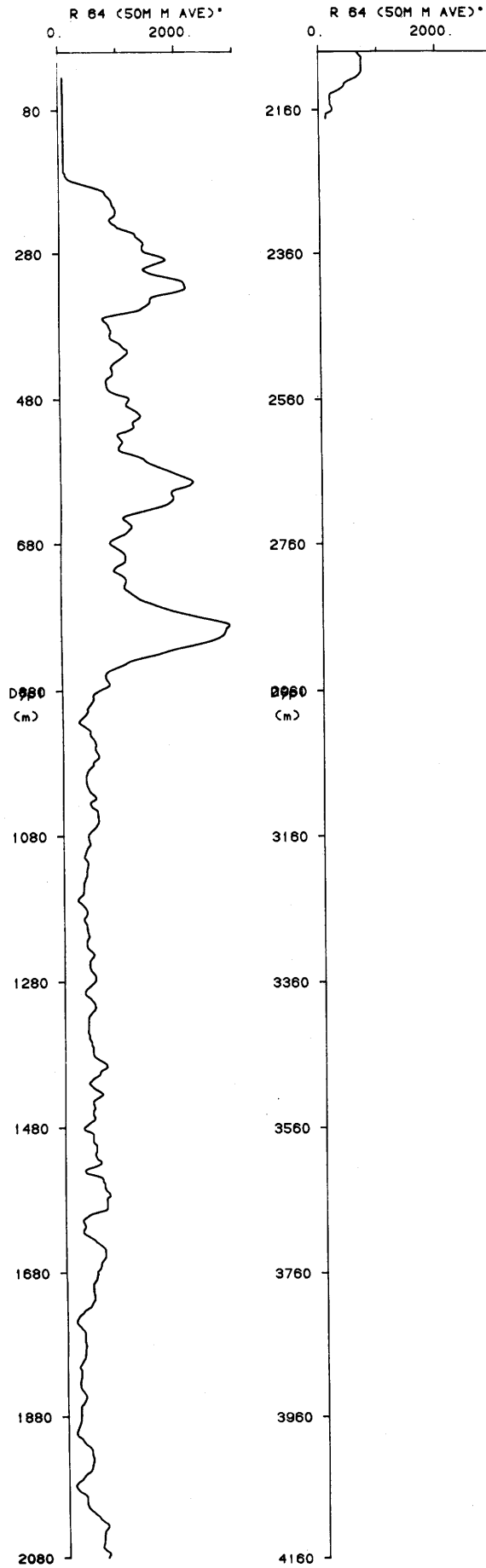


Figure 50. 50m running average of the 64" normal resistivity log in Lopra-1

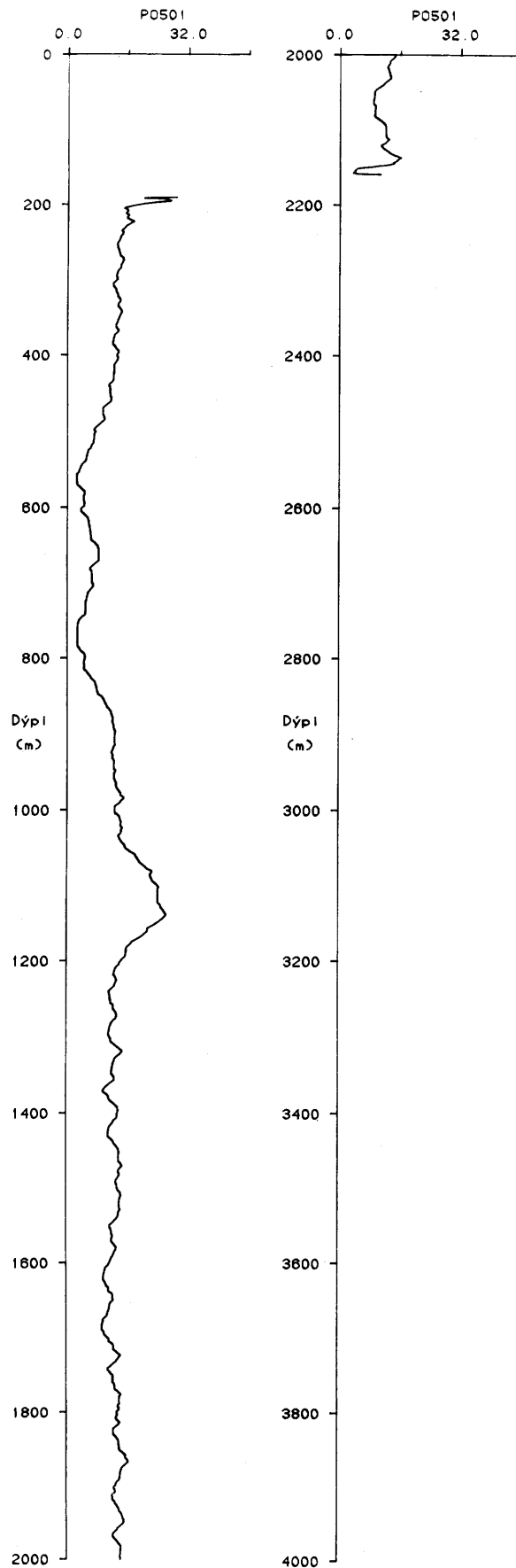


Figure 51. 100m running average of the porosity log in Lopra-1

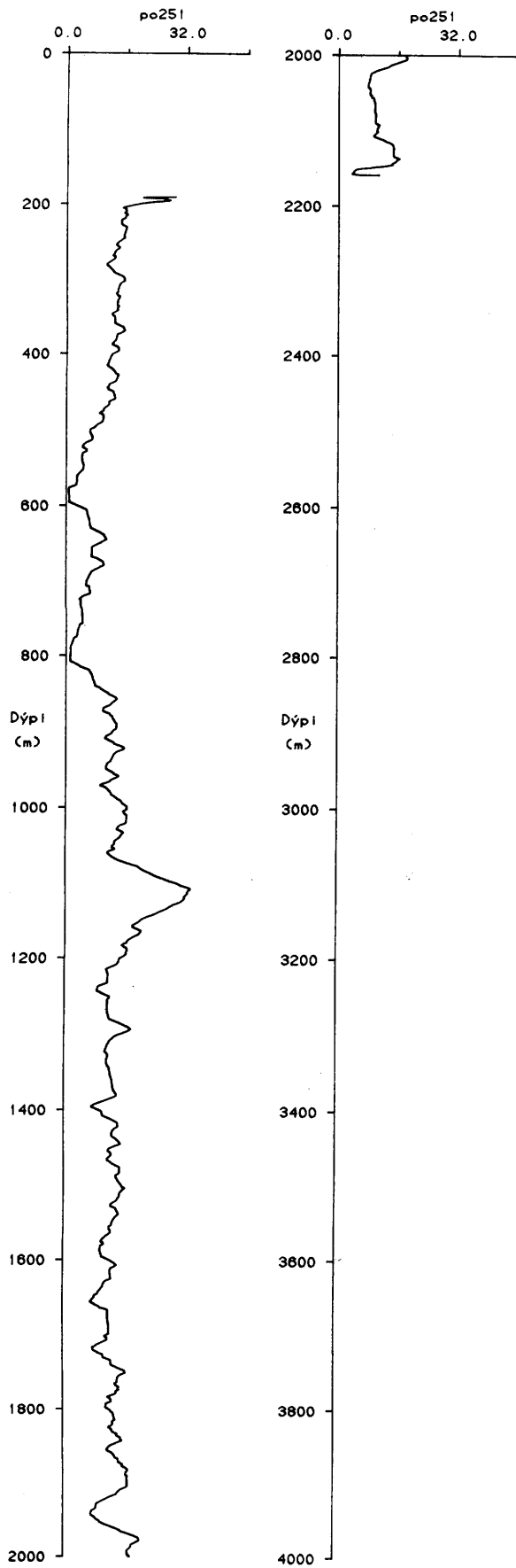
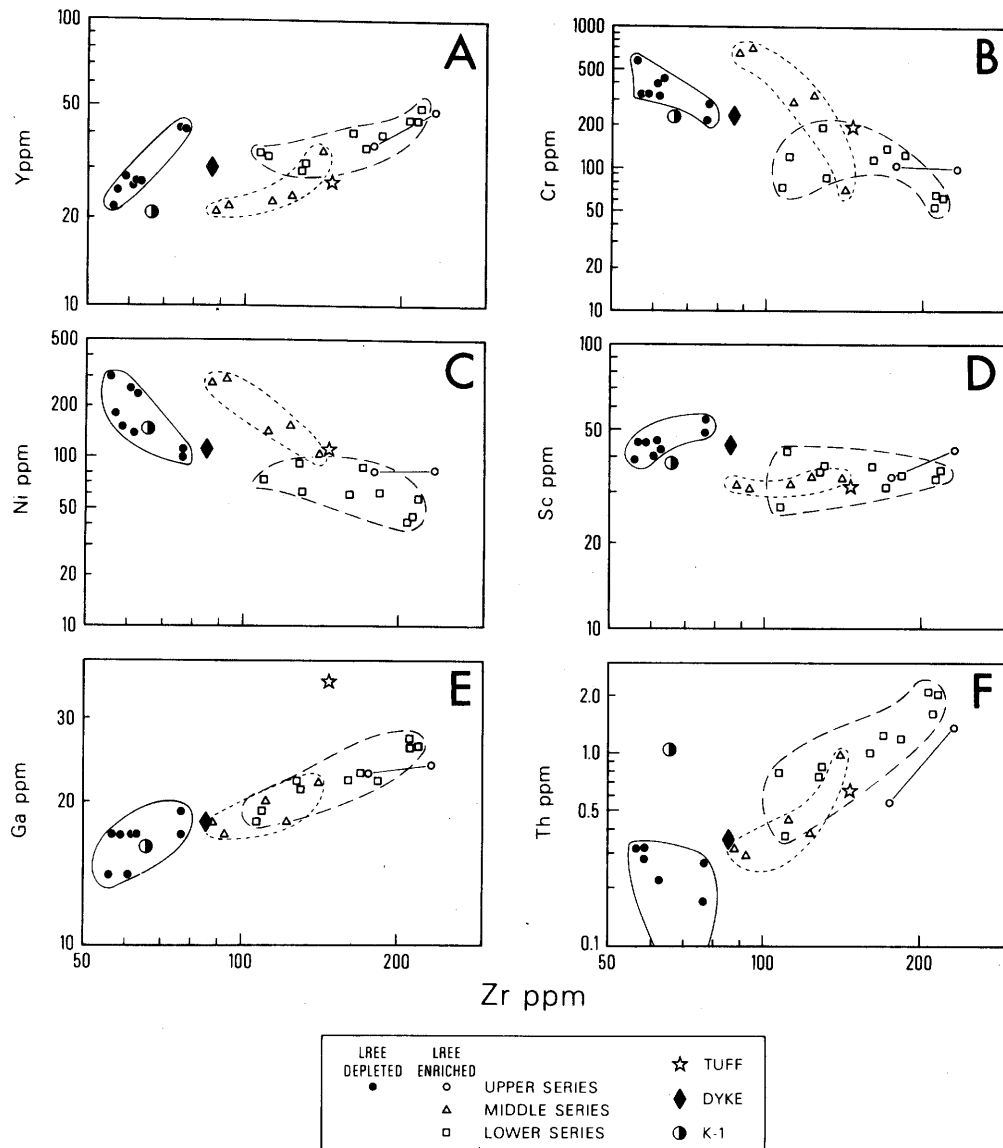


Figure 52. 50m running average of the porosity log in Lopra-1



Log-normal trace element plots for the lavas of the Faeroe Islands. Open symbols: LREE-enriched rocks; filled symbols: LREE-depleted rocks. Squares = lower series, triangles = middle series, circles = upper series. Diamond = dyke sample V-4; star = tuff sample K-3 and half-filled circle = sample K-1.

Figure 53. Relation between thorium and zirconium for the lavas of the Faeroe Islands

changes in natural gamma ray, resistivity and porosity, an attempt has been made to divide the 2km thick pile penetrated by the borehole in Lopra into series (fig. 54). It is proposed here that the lava pile can be divided into three distinct series, and these series are intruded by two intrusions.

Series I This group extends down to approximately 400m depth. The characteristics are seen in fig. 54 in the interval 200-400m, but the interval down to 200m is screened off by the casing. This series extends most likely from the surface down to ca 400m depth. The main characteristics of this series are;

- high intensity in natural gamma ray
- high resistivity
- medium porosity.

Series I is most likely the continuation of the "lower series" of Rasmussen and Noe-Nygaard.

Series II extends approximately from 400m depth down to 1600m depth. Characteristics of this series are;

- medium intensity in natural gamma ray
- low to medium resistivity
- medium porosity.

This series is crosscut by two dolerite intrusions at the depths of 500 -600m and 750-850m. These intrusions disturb somewhat the overall picture as shown in fig. 54. The intrusions have lower intensity of gamma ray than the host rock, whereas the resistivity is higher and porosity is lower than the values in the lavas of Series II.

Further implications within the depth interval covered by Series II is the zone of high porosity registered in the depth interval 1050-1150m. Some variations in gamma ray intensity are seen at this depth interval, but these variations are hardly sufficient to warrant a special geological unit to this interval.

Series III ranges from 1600m depth to the bottom of the hole. The characteristics of this series are;

- low intensity in gamma ray
- low resistivity
- medium porosity

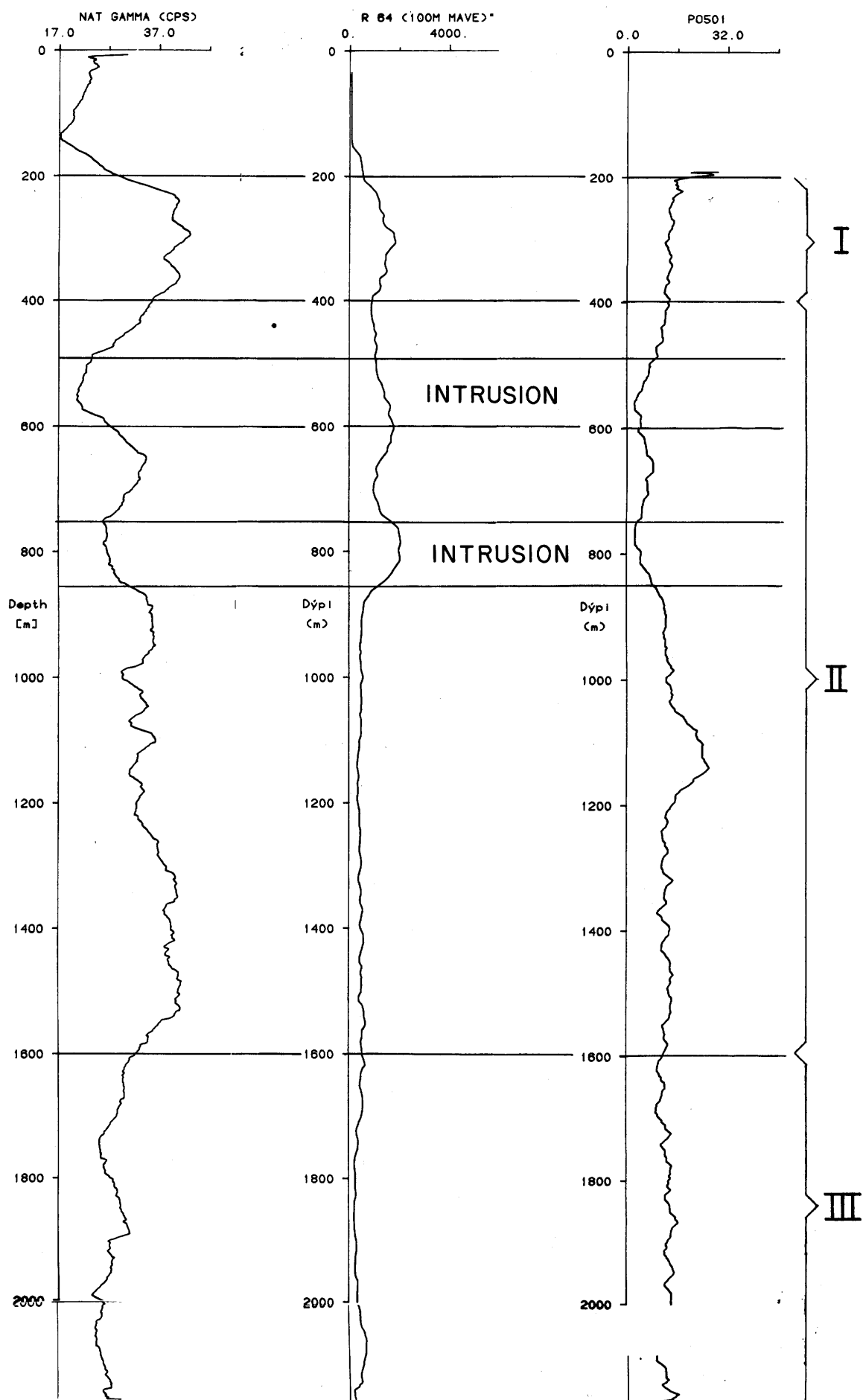


Figure 54. Long scale variation of natural gamma ray, resistivity and porosity in the Lopra-1 borehole, with the proposed division of the lava pile

It should be stressed that the above proposed division of the lava pile in Lopra-1 is only based on the large scale variations in the geophysical logs. This hypothesis can most likely be tested by an extensive study of trace elements in the rocks.

Chemical analyses of trace elements have been done on 41 samples from Lopra-1 (Waagstein et al. 1982). Figure 55 shows the results for Ba, Zr, V, and Cr. In the depth interval 200-400m high values of Ba and Zr are recorded, which is in agreement with the proposed division of the lava pile as presented in fig. 54.

The large scale variations of porosity and resistivity in Vestmanna-1 is shown on fig. 56. A running average of 50m is used in this figure. No pronounced changes with depth are seen in these parameters. The lava pile penetrated by Vestmanna-1 is assumed to be entirely within the middle stratigraphy basalt series of Rasmussen and Noe-Nygaard (1970) so relatively uniform characteristics of the formation are expected.

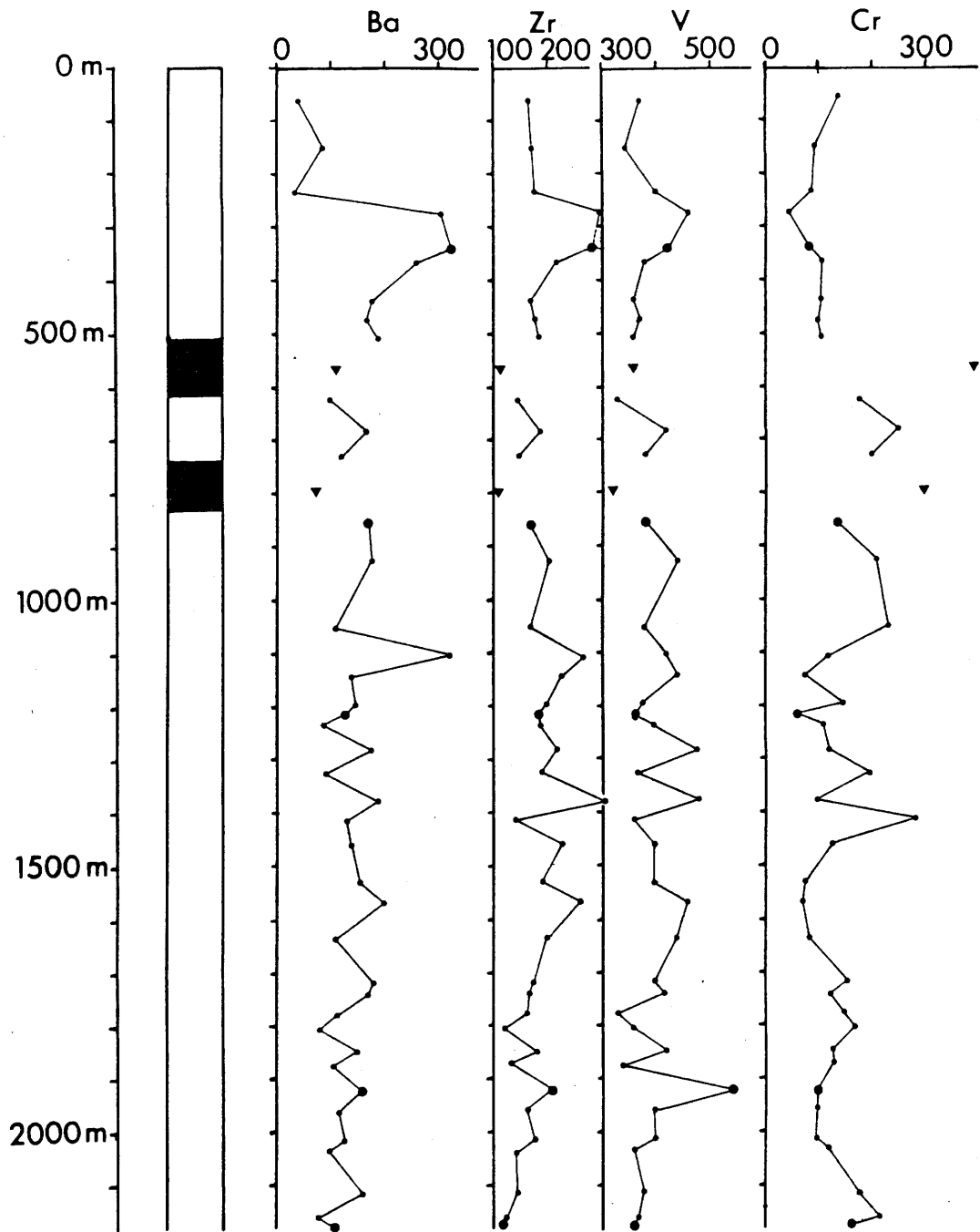


Figure 55. Lopra-1. Concentration of Ba, Zr, V, and Cr as a function of depth (Waagstein et al. 1982)

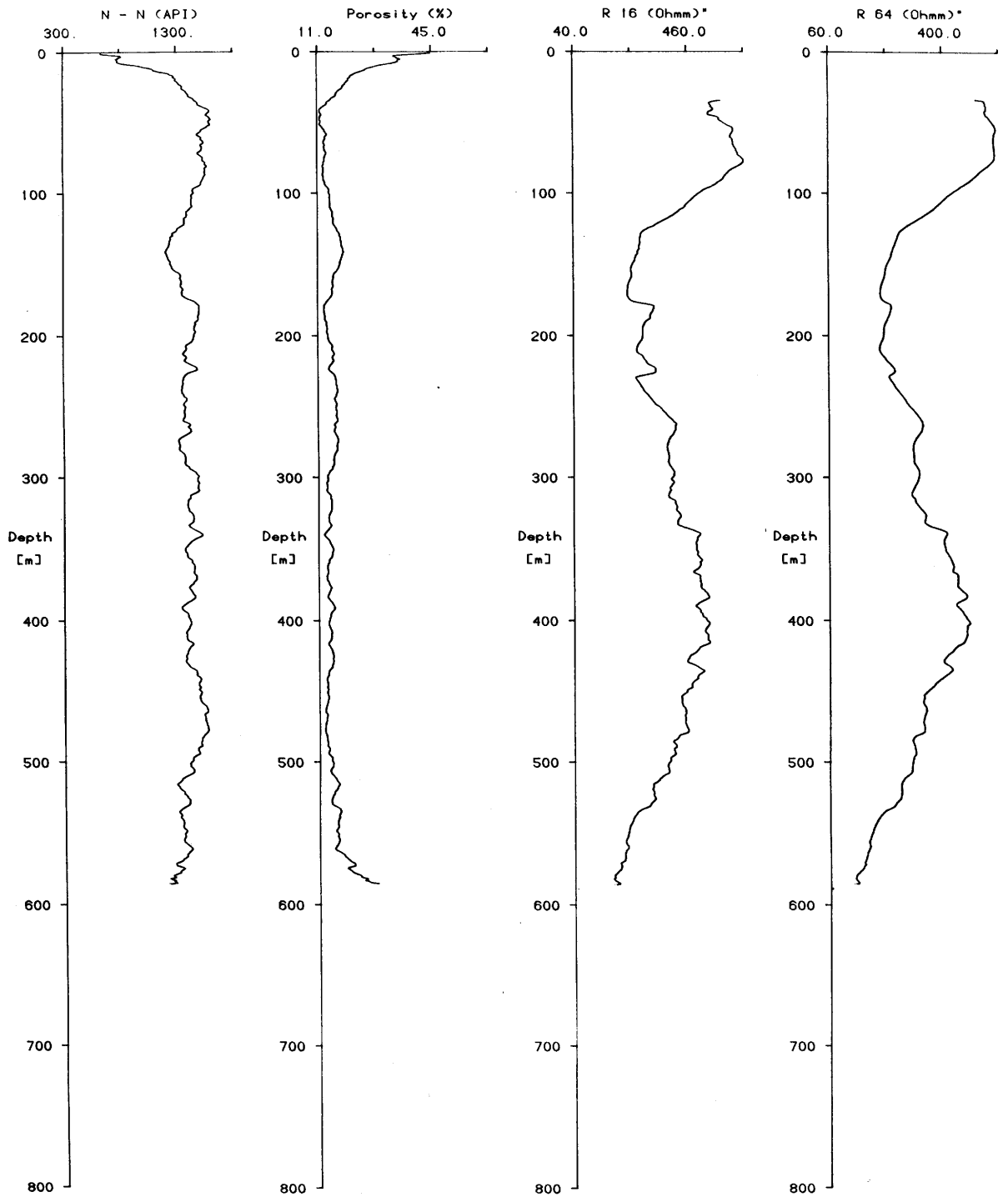


Figure 56. Vestmanna-1. Large scale variations of porosity and resistivity with depth.

REFERENCES

- Archie, G. E. 1942: The electrical resistivity log as an aid in determining some reservoir characteristics. Trans. AIME, 146, 54-67.
- Brace, W. F., and Orange, A. S. 1968: Electrical resistivity changes in saturated rocks during fracture and frictional sliding. J. Geophys. Res., 73, 1433-1445.
- Brace, W. F., Orange, A. S., and Madden, T. R. 1965: The effect of pressure on the electrical resistivity of water-saturated crystalline rocks. J. Geophys. Res., 70, 5669-5678.
- Czubek, J. A. 1981 a: Some Aspects of Nuclear Well Logging in Igneous Rock. OS81009/JHD05, Orkustofnun, Reykjavík.
- Czubek, J. A. 1981 b: Introduction to geostatistics - Lecture notes. OS81012/JHD08, Orkustofnun, Reykjavík.
- Gariépy, Cl., Ludden, J., and Brooks, Ch. 1983: Isotopic and trace element constraints on the genesis of the Faeroe lava pile. Earth Planet. Sci. Lett. 63, 257-272.
- GOI 1975: Formation Evaluation Data Handbook. Gearhart-Owen Industries. inc. Texas.
- Jonsson, G., and Stefánsson, V. 1982: Density and porosity logging in the IRDP-hole, Iceland. J. geophys. Res. 87, 6619-6630.
- Matheron, G. 1965: Les variables régionalisées et leur estimation. Editions Masson, Paris.

Rasmussen, J., and Noe-Nygaard, A. 1969: Beskrivelse til geologisk kort over Færøerne. Danm. geol. Unders., række 1, 24.

Rasmussen, J., and Noe-Nygaard, A. 1970: The geology of the Faeroe Islands (pre-Quaternary) Geol. Surv. Denmark I. Ser 25, 142.

Stefánsson, V. 1979: Geophysical logging in the IRDP hole in Reyðarfjörður, Iceland, Rep. OS79003-JHD02, Orkustofnun, Reykjavík, Jan.

Stefánsson, V., and Emmerman, R. 1980: Gamma ray activity in Icelandic rocks, paper presented at the IRDP Second Post-Drilling Science Review, Reykjavík, Iceland, May 13-15.

Stefánsson, V., Axelsson, G., and Sigurðsson, Ó. 1982: Resistivity logging of fractured basalt, Proc. Eight Workshop of Geothermal Reservoir Engineering, Stanford University Dec. 14-16.

Stefánsson, V., Guðmundsson, A., and Emmerman, R. 1982: Gamma ray logging in Icelandic rocks. The Log Analyst, XX111, No. 4, 11-16.

Stefánsson, V. 1982: Geofysiska borrhalsmatningar í Island, 16. Nordiske Geologiske Vintermode, Reykjavík 5-8 Jan.

Stefánsson, V., and Tulinius, H. 1983: Geophysical logs from Lopra-1 and Vestmanna-1. Progress report-1, OS83021/JHD-06 B, Orkustofnun, Reykjavík.

Stefánsson, V., Guðmundsson, A., Steingrímsson, B., Guðmundsson, G., Friðleifsson, G. Ó., Axelsson, G., Ármannsson, H., Sigvaldason, H., Benjamínsson, J., and Sigurðsson, Ó., 1983: Krafla, holur KJ 16, 17 og 18. Rannsóknir samhliða borun og vinnslueiginleikar. Orkustofnun, Reykjavík (in preparation).

Waagstein, R., Nielsen, P.H., Fine, S., and Hald, N. 1982: Lopra Well no 1, Suduroy, Faeroe Island, Geological Well Completion Report., Faeroe Department, Geological Survey of Denmark.